CELL CYCLE REGULATION IN RESPONSE TO DNA DAMAGING AGENTS AND TRANSCRIPT-PROFILING OF GENE SEQUENCES INVOLVED IN THE REGULATORY PATHWAY IN *PHYSARUM POLYCEPHALUM*

Thesis submitted to University of Calicut

in Partial fulfilment of the requirement for the award of

Doctor of Philosophy
In
Biotechnology

By

REMITHA RABINDRAN M.

DEPARTMENT OF BIOTECHNOLOGY

UNIVERSITY OF CALICUT

2012

CERTIFICATE

This is to certify that the thesis entitled "**Cell cycle regulation in response to DNA damaging agents and transcript-profiling of gene sequences involved in the regulatory pathway in *Physarum polycephalum***" submitted to the University of Calicut, as partial fulfilment of Integrated M.Phil. - Ph.D. programme for the award of the degree of Doctor of Philosophy in Biotechnology by **Remitha Rabindran M**., embodies the results of bonafide research work carried out by her under my supervision and guidance in the Department of Biotechnology, and the thesis has not previously formed the basis for the award of any degree, diploma, associateship, fellowship or other similar title or recognition. The candidate has passed the course work of the M.Phil. - Ph.D. programme in 2005-06.

DR. P. R. MANISH KUMAR
(Research Supervisor)
Associate Professor
Department of Biotechnology
University of Calicut

DECLARATION

I hereby declare that the work presented in this thesis entitled "**Cell cycle regulation in response to DNA damaging agents and transcript-profiling of gene sequences involved in the regulatory pathway in *Physarum polycephalum*"** submitted to the University of Calicut, as partial fulfilment of Integrated M.Phil. - Ph.D. programme for the award of the degree of Doctor of Philosophy in Biotechnology is original and carried out by me under the supervision of **Dr. P. R. Manish Kumar**, Department of Biotechnology, University of Calicut. This has not been submitted earlier either in part or in full for any degree or diploma of any university.

C.U.Campus

Date: ..... **Remitha Rabindran M.**

ACKNOWLEDGEMENTS

This thesis arose as a natural continuation of my research since I came to the Recombinant DNA laboratory for my M.Phil. degree. It is a pleasure to convey my heartfelt gratitude to my supervisor Dr. P. R. Manish Kumar for the opportunity to work in his laboratory and for his direction and guidance throughout my work. He provided me with unflinching encouragement, knowledge and support in various ways. I am profoundly indebted to him.

I gratefully thank my teacher Dr. Jayasree Manish for her encouragement and help all through my work. Her involvement and views have nourished my intellectual maturing from which I shall continue to benefit, for a long time to come.

I express my sincere gratitude to Dr. M.V. Joseph, Professor, Department of Biotechnology, for his encouragement and help when I first joined the lab and for his continued support during the tenure of my work.

I would like to thank Dr. K. K. Elyas for his helpful discussions and timely help. Thanks are also due to Sri. C. Gopinathan, H.O.D, Department of Biotechnology, for all help rendered. I would also like to thank Dr. Smitha Bava for her beneficial advice.

I thankfully acknowledge the help from Dr. K. G. Raghu, Scientist, NIIST (CSIR), Trivandrum, and Dr. T. R. Santhosh Kumar, Scientist, RGCB, Trivandrum for FACS analysis of my research samples at their instruments facility.

My special thanks belong to Rajan Iyappan for supporting me during labwork and rendering lots of technical help with the figures, schematic representations and listing of references required for this thesis.

My warmest thanks to Nithya N. for her emotional support and help during crucial times. I would also like to thank Rahul Raghavan and Sanith C. for their timely help and cooperation. I also wish to thank all the research scholars of Biotechnology Department, with whom I have had the pleasure to interact during my work.

I thank the Department Librarian Ms. Saraswathy T. for her assistance and cooperation. I thank the technical assistant Mrs. Thara for help rendered during the tenure of my research.

I wish to thank all the past and present members of the non-teaching staff of this Department for all the assistance provided and helps rendered.

The Kerala State Council for Science, Technology and Environment (KSCSTE) is gratefully acknowledged for the financial support.

It is a pleasure to pay tribute to my beloved parents, for their inalterable support and prayers.

I take this opportunity to express my profound gratitude to my husband Sri. Anlu M. S., for his moral support and patience during my research work.

Finally a warm thanks to my family for their support and encouragement.

Remitha R.

CONTENTS

List of Figures

List of Tables

ABBREVIATIONS

µg	:	Microgram
µL	:	Microliter
µm	:	Micrometer
$^1O_2$	:	Singlet oxygen
3meA	:	3-Methyl-Adenine
4E-BP1	:	Eukaryotic translation initiation factor 4E-binding protein 1
53BP1	:	p53-binding protein 1
6-4PPs	:	Pyrimidine 6-4 pyrimidone photoproducts
8oxoG	:	8-Oxo-Guanine
Abl	:	Abelson murine leukemia
AIP1/Alix	:	ALG-2-interacting-protein-1
AKT	:	Alpha serine/threonine-protein kinase
ALG-2	:	Alix/apoptosis-linked gene-2
AP	:	Anchored primer
AP	:	Oligo dT Anchored primer
AP-1	:	Activator protein 1
AP1	:	Oligo-dT(12)GG
AP2	:	Oligo-dT(12)GC
AP3	:	Oligo-dT(12)CC
AP4	:	Oligo-dT(12)CG
AP5	:	Oligo-dT(12)AG
AP6	:	Oligo-dT(12)AC
APC	:	Anaphase-promoting complex
APC/C	:	APC – cyclosome
APL	:	Acute promyelocytic leukemia
AR	:	Arsenic trioxide
ARF	:	Alternate reading frame
As [111]	:	Arsenic trioxide

ATM	:	Ataxia telangiectasia mutated
ATR	:	Ataxia telangiectasia and Rad3-related
ATRIP	:	ATR-interacting protein
BASC	:	BRCA 1-associated genome surveillance complex
Bax	:	Bcl-2–associated X protein
BCIP/NBT	:	5-bromo-4-chloro-3'-indolylphosphate /nitro-blue tetrazolium
Bcl-2	:	B-cell lymphoma 2
BER	:	Base excision repair
BLM	:	Bloom’s syndrome helicase
bp	:	Base pair
BRCA1	:	Breast cancer associated gene 1
BRCT	:	BRCA 1 C-terminal
C	:	Control
CAF	:	Caffeine
CAK	:	Cdk activating kinase
CDC	:	Cell division cycle
CDKs	:	Cyclin-dependent kinases
CHK	:	Checkpoint kinases
CHL	:	Chlorambucil
CHOP	:	CCAAT/enhancer binding protein (C/EBP)
Chy.try	:	Chymotrypsin
CIA	:	Chloroform/Isoamyl alcohol
Cip/Kip	:	CDK inhibitory Protein/Kinase Inhibitor protein
CK2	:	Casein kinase 2
CKIs	:	CDK-inhibitory proteins
CLC	:	Clamp loading complex
CNAs	:	Copy-number alterations
CP	:	Capsaicin
CPDs	:	Cyclobutane pyrimidine dimers
Crb2	:	Crumbs homolog 2

Crb2	:	Crumbs homolog 2 (Drosophila)
CSC	:	Checkpoint sliding clamp
CtBP	:	C-terminal binding protein
CtIP	:	CtBP-interacting protein
Daxx	:	Death-domain associated protein
DD - PCR	:	Differential display PCR
DDR	:	DNA damage response
DMSO	:	Dimethyl sulfoxide
DNA	:	Deoxyribonucleic acid
DNA-PK	:	DNA dependent protein kinase
DNase	:	Deoxyribonuclease
dNTP	:	Deoxy nucleoside triphosphate
DR	:	Downregulated
DSBs	:	Double-strand breaks
dsDNA	:	Double stranded DNA
EG2	:	Early G2 phase
EGFR	:	Epidermal growth factor receptor
ER	:	Endoplasmic reticulum
ERCC1	:	Excision repair cross-complementing rodent repair deficiency complementation group 1
ERK	:	Extracellular signal-regulated kinases
ES	:	Early S phase
ETC	:	Electron transport chain
FACS	:	Fluorescence-activated cell sorting
FAK	:	Focal Adhesion Kinase
FANCD2	:	Fanconi anaemia complementation group D2
FapyGua	:	2,6-diamino-4-hydroxy-5-formamidoguanine
FHA	:	Forkhead-associated domain
Flk1	:	Fetal Liver Kinase 1
FP	:	Fungal primer RFuB#1

GADD	:	Growth Arrest and DNA Damage
GCN2	:	General control non repressed 2
GPx	:	Glutathione peroxidase
GSH	:	Glutathione
GVBD	:	Germinal vesicle breaks down
h	:	Hour(s)
HAUSP	:	Herpes virus-associated ubiquitin-specific protease
HDACs	:	Histone deacetylases
HER2	:	Human Epidermal Growth Factor Receptor 2
hMDM2	:	Human homologue of mouse double minute 2 gene product homologous protein
HR	:	Homologous recombination
HSP	:	Heat shock protein
iAs	:	Inorganic arsenic
IN	:	Inhibited
IND	:	Induced
IR	:	Infra-Red
IRIF	:	Irradiation-induced foci
JNK	:	c-Jun N-terminal kinase
kDa	:	Kilodalton
KDR	:	Kinase insert domain receptor
L	:	Liter
LG2	:	Late G2 phase
Lig4	:	DNA-Ligase 4
LS	:	Late S phase
M	:	Molar
M	:	Molecular Weight marker in gel photographs
MAPK	:	Mitogen-activated protein kinases
MC7	:	Mammary cancer cell line7
MCM	:	Mini-chromosome maintenance proteins

MCPH1	:	Microcephalin
MDC1	:	Mediator of DNA damage checkpoint
MDM2	:	Murine double minute 2 - Negative regulator of p53
mg	:	Milligram
MG2	:	Middle G2 phase
min	:	Minutes
MK2	:	Mitogen-activated protein kinase–activated protein kinase 2
ml	:	Milliliter
MLH2	:	MutL protein homolog 2
mM	:	Millimolar
MMA[III]	:	Monomethylarsonous acid
MMA[V]	:	Monomethylarsonic acid
M-MLV	:	Moloney-Murine leukemia virus
MMS	:	Methyl methane sulphonate
MP	:	Middle pre prophase
MPF	:	Maturation promoting factor
MRE11	:	Meiotic recombination 11
MRN	:	MRE11-RAD50-NBS1 complex
MSH2	:	MutS homolog 2
MSK	:	Mitogen- and stress-activated protein kinase
MSS	:	Minimum salts solution
MTOCs	:	Microtubular organising centres
mTOR	:	Mammalian target of rapamycin
mtTFA	:	Mitochondrial transcription factor A
NAD	:	Nicotinamide adenine dinucleotide
Nbs	:	Nijmegen breakage syndrome
NER	:	Nucleotide excision repair
NF-kB	:	Nuclear factor-kappa β
NHEJ	:	Nonhomologous end-joining
NRF-1	:	Nuclear respiratory factor-1

OGG1	:	8-Oxoguanine glycosylase
ORF	:	Open reading frame
PAR	:	Poly (ADP) ribose
PARP	:	Poly (ADP) ribose polymerase.
PBD	:	Polo-box domain
PBS	:	Phosphate buffered saline
PC-3	:	Prostate cancer cell line 3
PCD	:	Programmed cell death
PCNA	:	Proliferating cell nuclear antigen
PCR	:	Polymerase chain reaction
PDK	:	PI 3K dependent protein kinases
PFM	:	Post-fusion mitosis
PI 3K	:	Phosphatidylinositol 3-kinase
PI	:	Propidium iodide
PIKKs	:	Phosphatidylinositol 3- kinase-like protein kinases
PKB	:	Protein kinase B
Plk	:	Polo-like kinase
Plx	:	*Xenopus* polo-like kinase
PML	:	Promyleocytic leukemia protein
PNK	:	Polynucleotide kinase
PP	:	Protein phosphatase
p-ser	:	Phosphoserine
PTIP	:	Pax Transactivation-Domain Interacting Protein
p-tyr	:	Phosphotyrosine
Rad	:	Radiation
Rb	:	Retinoblastoma
RFC	:	Replication factor C
RFuB#1	:	Oligonucleotide RAPD fungal primer
RFWD3	:	RING finger and WD repeat domain 3
RMI	:	RecQ-Mediated Genome Instability

RNA	:	Ribonucleic acid
RNase	:	Ribonuclease
RNasin	:	Ribonuclease inhibitor
ROS	:	Reactive oxygen species
RPA	:	Replication protein A
RSK	:	Ribosomal S6 kinase
RT	:	Reverse transcriptase
SAM	:	S-adenosylmethionine
SCF	:	Skp cullin- F-box containing complex
SDM	:	Semi- defined medium
SDS-PAGE	:	Sodium dodecyl sulfate polyacrylamide gel electrophoresis
sec	:	Seconds
Skp	:	S-phase kinase associated proteins
SMC	:	Structural Maintenance of Chromosomes
SOD	:	Super Oxide Dismutase
SPF	:	S-phase promoting factor
SqCC	:	Squamous cell carcinoma
SSBs	:	Single strand breaks
ssDNA	:	Single-stranded DNA
SSRP	:	Structure specific recognition protein
STAT	:	Signal transducer and activator of transcription
T	:	Treated
TBS	:	Tris-buffered saline
TCM	:	Traditional Chinese Medicine
TEL2	:	Telomere maintenance 2
Tip	:	Tat interacting protein
TNF	:	Tumor necrosis factor
TOP1	:	Nuclear topoisomerase I
TOPBP1	:	DNA topoisomerase II-binding protein 1
TP	:	Transition point

TRPV1	:	Transient receptor potential vanilloid 1
TTI	:	Tel two-interacting protein
TTI1	:	TEL2-interacting protein 1 homolog
TTI2	:	TEL2-interacting protein 2 homolog
UPS	:	Ubiquitin proteosome systems
UR	:	Upregulated
UVR	:	Ultra violet radiation
V	:	Volt
VEGF	:	Vascular endothelial growth factor
W	:	Watt
WAF1	:	Wild type p53 activated protein-1
Wip1	:	WPP domain interacting protein 1
WM	:	Wortmannin
WRN	:	Werner's syndrome helicase
XLF	:	XRCC4-like factor
XP	:	Xeroderma pigmentosum
XRCC4	:	X-ray repair complementing defective repair in Chinese hamster cells 4
βTrCP	:	β-Transducin Repeat-containing Protein

1. INTRODUCTION

1.1 The cell cycle

Cell cycle is a complex process that involves numerous regulatory proteins that direct the cell through a specific sequence of cell growth and division culminating in the production of two daughter cells. A typical eukaryotic cell cycle is divided into four different phases: gap phase - G1, synthesis phase - S, gap phase - G2 (collectively known as interphase) which lasts for at least 12-24h and mitotic phase - M lasting for 1-2h. DNA is replicated once per cell cycle in the S phase, duplicated chromosomes are separated and moved to two opposite poles of mitotic spindle in the M phase. S and M phases are separated in time by the gaps G1and G2. G1 precedes S phase and prepares cell for DNA replication; G2 precedes M phase and prepares cell for division.

Dependent on environmental and developmental signals, some cells in G1 phase may temporarily or permanently leave the cell cycle and enter a quiescent or arrested phase known as G0 phase. M phase consists of five sub phases: prophase - the extended duplicated genome condenses into chromosomes, which are highly ordered structures and metabolic activity is reduced; prometaphase - the nuclear envelope breaks and microtubules elongate from centromeres; metaphase - condensed chromosomes align properly in the metaphase plane; anaphase - the duplicated chromosomes are separated into two identical parts and move towards the opposite poles of the spindle; telophase - the chromosomes decondense, metabolic activity is restored, and the nuclear envelope is reconstructed. The cell cycle ends with cytokinesis where the cell divides into two each with same copies of genetic material.

External signals and intrinsic information together determine whether cell enters a division cycle. External signals affect this decision only until cells commit to

go through the entire cycle, at a time in G1, known as "START" in yeast and "Restriction point" in mammals. From there on, progression through the cell cycle is controlled intrinsically by the cell-cycle machinery. The basic components of this machinery are conserved in all eukaryotes.

1.2 Regulators of cell cycle

Progression through the cell-division cycle is driven by activation and inactivation of cyclin-dependent kinases (CDKs), which trigger the transition to subsequent phases of the cycle. CDKs are small serine/threonine protein kinases that require association with a cyclin subunit for their activation. Mammalian Cyclins include (i) G1 cyclin (cyclin D) (ii) S-phase cyclins (cyclins E and A) and (iii) Mitotic cyclins (cyclins B and A). Their levels in the cell rise and fall with the stages of the cell cycle. Cdks are G1-phase Cdk (Cdk4), S-phase Cdk (Cdk2) and M-phase Cdk (Cdk1). Their levels are relatively constant throughout the cell cycle.

Many levels of regulation impinge upon the CDKs to impose tight control over cell-cycle progression such as controlled expression and destruction of cyclins, activating and inhibitory phosphorylation and dephosphorylation of the CDKs, and expression and destruction of inhibitory proteins that associate with CDKs, or CDK/cyclin complexes. Inhibitory phosphorylations include Thr14 and Tyr15 phosphorylation by Wee1 and Myt1 kinases. Activating phosphorylation include Thr161 phosphorylation by CAK (Cdk activating kinase). Activating dephosphorylation by members of the Cdc25 family of dual-specificity phosphatases counteract Wee1/Myt1 phosphorylation and control the appropriate timing of CDK activation. Three different proteins, p21Cip1, p27Kip1 and p57Kip2, form the "CDK inhibitory Protein/Kinase Inhibitor protein" (Cip/Kip) family in mammals. An illustrative model for CDK regulation has been shown in Figure 1.1

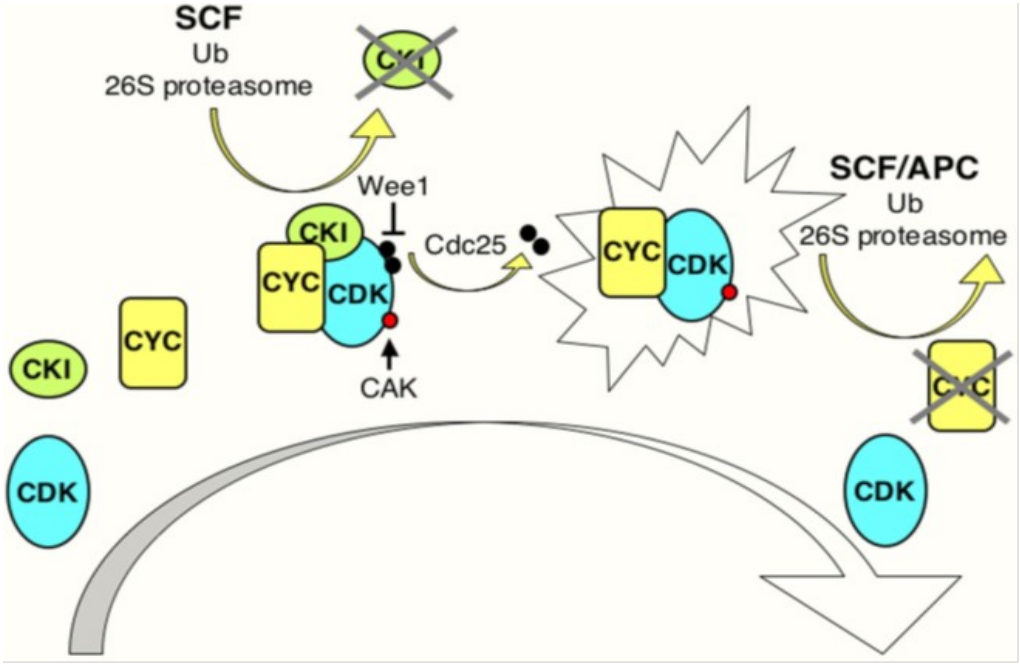

Fig. 1.1

Model illustrating general aspects of CDK regulation: CDK activation requires cyclin expression and association. Cyclin/CDK complexes are kept inactive through association with CDK-inhibitory proteins (CKIs) and inhibitory phosphorylation by Wee1/Myt1 kinases (black circles). Activation requires ubiquitin-dependent proteolysis of the CKI, phosphorylation of the CDK by a CDK-activating kinase (CAK; red circle), and removal of the inhibitory phosphates by a Cdc25 phosphatase. Cyclin destruction leads to inactivation. Ubiquitin-dependent proteolysis of cell cycle regulators in late G1 and S involves Skp cullin- F-box containing complex (SCF) based E3 ligases, while in M phase and early G1 the anaphase-promoting complex (APC) is active. The exclamation figure denotes the active kinase complex; the large arrow indicates time (*Van den Heuvel, 2005).*

Activated Cdk-cycln complexes add phosphate groups to a variety of protein substrates that control processes in the cell cycle.

1.3 Steps in the cell cycle

(i) A rising level of G1-cyclins binds to their Cdks and signal the cell to prepare the chromosomes for replication.

(ii) A rising level of S-phase promoting factor (SPF) - which includes cyclin A bound to Cdk2 - enters the nucleus and prepares the cell to duplicate its DNA (and its centrosomes).

(iii) As DNA replication continues, cyclin E is destroyed, and the level of mitotic cyclins begins to rise (in G2).

(iv) M-phase promoting factor (the complex of mitotic cyclins with the M-phase Cdk) initiates assembly of the mitotic spindle, breakdown of the nuclear envelope and condensation of the chromosomes. These events take the cell to metaphase of mitosis. At this point, the M-phase promoting factor activates the anaphase-promoting complex (APC/C) which allows the sister chromatids at the metaphase plate to separate and move to the poles (anaphase), completing mitosis. APC/C helps in destruction of cyclin B by attaching it to the protein ubiquitin which targets it for destruction by proteasomes, synthesis of G1 cyclin for the next turn of the cycle is turned on and degrades geminin, a protein that keeps the freshly synthesized DNA in S phase from being re-replicated before mitosis. This mechanism ensures that every portion of the cells genome is copied once - and only once - during S phase.

1.4 Cell cycle and surveillance mechanisms

The control of progression of cell through the four phases ensures that the crucial processes of replication and division are performed with high fidelity. These are called checkpoint controls which include both internal and external control mechanisms. The internal mechanisms monitor the timely completion of critical cell cycle events in proper order. External mechanisms control the progress of the cell cycle mainly in response to three important events – DNA damage, replication blocks and mitotic spindle damage.

DNA damage checkpoint - When cells have DNA damages that have to be repaired, cells activate this checkpoint that arrests cell cycle. According to the cell cycle stages, DNA damage checkpoints are classified into at least 3 checkpoints: G1/S (G1) checkpoint, intra-S phase checkpoint, and G2/M checkpoint. Upon perturbation

of DNA replication by drugs that interfere with DNA synthesis, DNA lesions, or obstacles on DNA, cells activate DNA replication checkpoint that arrests cell cycle at G2/M transition until DNA replication is complete.

Spindle checkpoint - The spindle checkpoint arrests cell cycle at M phase until all chromosomes are aligned on spindle. This checkpoint is very important for equal distribution of chromosomes.

Morphogenesis checkpoint - Morphogenesis checkpoint detects abnormality in cytoskeleton and arrests cell cycle at G2/M transition.

1.5 Main sources of DNA damage

These include environmental agents such as genotoxic chemicals, UV and ionizing radiation and damages from within the cell (intrinsic) such as highly reactive free radicals, by-products of cellular metabolism; cell physiological conditions that disintegrate the chemical bonds in DNA. These damages occur as single strand breaks (SSBs), double strand breaks (DSBs) and point mutations. Replication blocks occur during DNA synthesis due to insufficient nucleotides and proteins or lesions on the DNA templates halting synthesis of DNA strands. Inactivation or under-expression of the proteins involved in the spindle formation causing misalignment of chromosomes resulting in mitotic spindle defects.

1.6 DNA damage response

DNA damage signaling pathways (DNA damage checkpoint pathways) include, sensors which detect the presence of DNA damage, transducers which produce a DNA damage signal, and effectors which induce cell death or cell cycle arrest and repair (Fig. 1.2).

Phospho-inositide kinase-related kinases (PIKKs), ATM and ATM-Rad3-related (ATR) in mammals and their homologues in budding and fission yeast are

central to the entire DNA damage response. Downstream of these proteins are two families of checkpoint kinases (CHK), the Chk1 and Chk2 kinases, and their homologues. These kinases carry out subsets of the DNA damage response in mammals and are targets of regulation by ATM and ATR kinases. The fourth conserved family is the BRCT-repeat containing proteins. Below this level of signal transduction are the effectors that execute the functions of the DNA damage response. These include substrates of both PIKKs and CHK kinases and proteins involved in DNA repair, transcription regulation and cell-cycle control, such as BRCA1, Nbs1, p53 and Cdc25C.

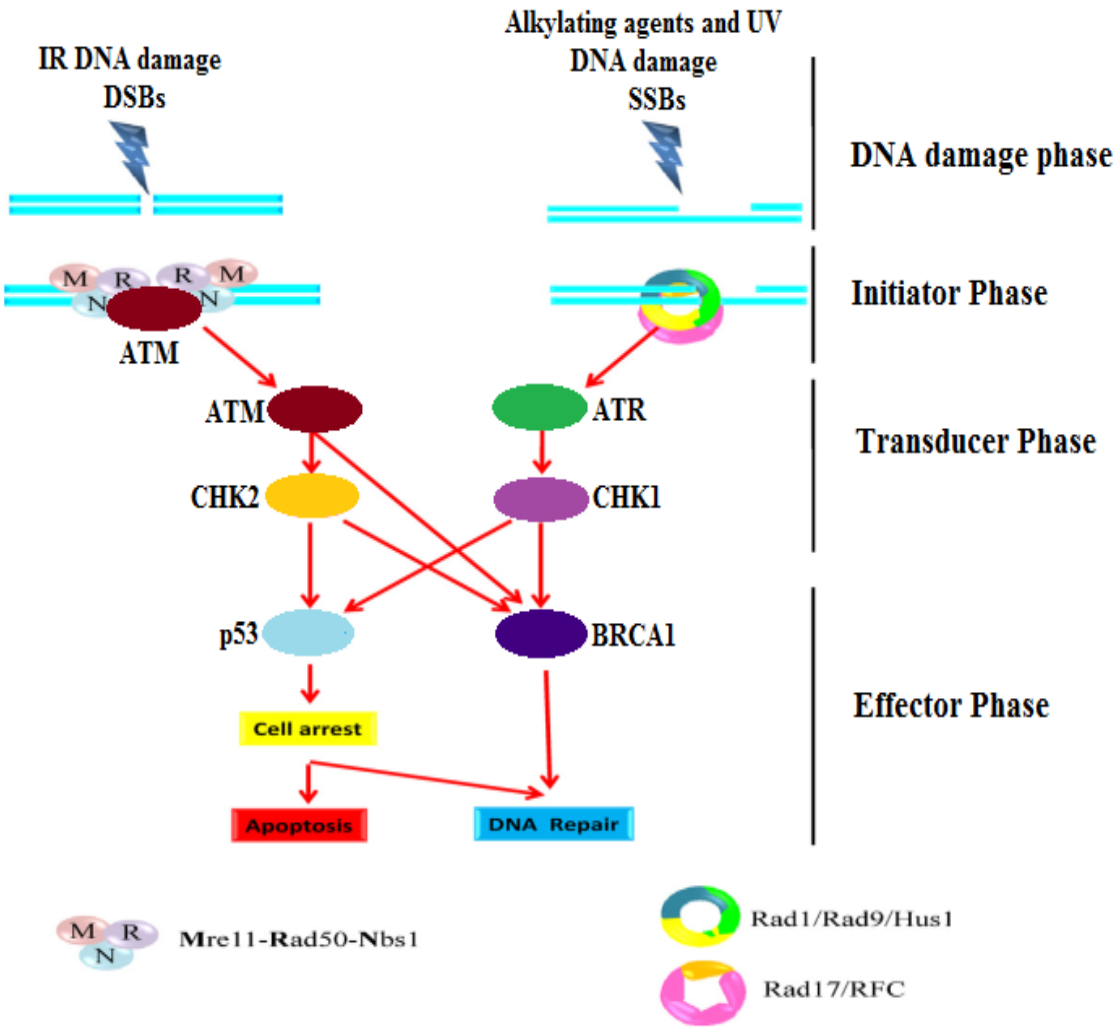

Fig. 1.2

DNA damage response: (A) Formation of a DSB leads to the recruitment of the MRN (meiotic recombination protein-11[Mre11]–Rad50–Nijmegen breakage syndrome protein-1 [Nbs1]) complex activating ataxia-telangiectasia mutated (ATM) by phosphorylation. The activated ATM phosphorylates downstream targets, including CHK2 and p53. (B) Formation of DNA SSBs activates two complexes: Rad9–Rad1–Hus1 (also known as 9–1–1) and one comprising the single-stranded DNA replication factor C (RFC), which binds to Rad17. Rad17–replication factor C (RFC) loads the 9–1–1 complex. Loading of the 9–1–1 complex brings the ATR to the damaged site leading to the phosphorylation of the downstream CHK1 and other ATR effectors that include breast cancer-1 (BRCA1). ATM- or ATR-induced phosphorylation of downstream targets leads to cell-cycle arrest, cell death pathways activation and DNA repair (Rodriguez-Rocha et al 2011).

1.6.A. DNA repair and Apoptosis

DNA repair is involved in processes that minimize cell killing, mutations, replication errors, persistence of DNA damage and genomic instability. Multiple systems for repairing damage to DNA have evolved, probably because of the importance of the DNA information content. They are direct DNA damage reversal, base excision repair, nucleotide excision repair, mismatch repair and double strand break repair. If the DNA damage is severe beyond repair, then those cells are eliminated by apoptosis. Apoptosis is a process of deliberate life relinquishment by a cell in a multicellular organism. It is one of the main types of programmed cell death (PCD), and involves an orchestrated series of biochemical events leading to a characteristic cell morphology and death. The apoptotic process is executed in such a way as to safely dispose of cell corpses and fragments. DNA damage from ionizing radiations or toxic chemicals can also induce apoptosis via the actions of the tumor-suppressing gene p53. Apoptosis also plays a role in preventing cancer; if a cell is unable to undergo apoptosis, due to mutation or biochemical inhibition, it can continue dividing and develop into a tumor.

1.7 Significance of DNA damaging agents in cell cycle and cancer research

Failure to repair DNA lesions may result in blockages of transcription and replication, mutagenesis, and/or cellular cytotoxicity. In humans, DNA damage has been shown to be involved in a variety of genetically inherited disorders, in aging, and in carcinogenesis. Hence, studying molecular pathways in DNA damage response gains a better understanding of the mechanisms underlying human disease, which could potentially provide a basis for the development of new therapies. Scientists are now focussing on targeted cancer therapies where drugs or other substances block the growth and spread of cancer by interfering with specific ‘molecular targets’ involved in tumor growth and progression. By focusing on molecular and cellular changes that are specific to cancer, targeted cancer therapies may be more effective than other

types of treatment, including chemotherapy and radiotherapy, and less harmful to normal cells. Targeted cancer therapies are being studied to be used alone, in combination with other targeted therapies and/or with other cancer treatments, such as chemotherapy. Targeted cancer therapies interfere with cancer cell division (proliferation) and its spread in different ways. Many of these therapies focus on proteins that are involved in cell signaling pathways, which form a complex communication system that governs basic cellular functions and activities, such as cell division, cell movement, cell responses to specific external stimuli, and even cell death. By blocking signals that tell cancer cells to grow and divide uncontrollably, targeted cancer therapies can help stop cancer progression and may induce cancer cell death through apoptosis. Other targeted therapies can cause cancer cell death directly, by specifically inducing apoptosis, or indirectly, by stimulating the immune system to recognize and destroy cancer cells and/or by delivering toxic substances directly to the cancer cells.

Several DNA damaging agents both physical (IR and UV- radiations) and chemical (MMS, paclitaxel, bleomycin, chlorambucil, heavy metals, doxorubicin, psoralen, cytarabine etc.) has been employed for studying the DNA damage response (DDR pathway).

Genetic studies regarding cell cycle progression in simple model organisms such as yeast have been extremely useful for understanding these processes in human cells - both in normal development and in cancer. G2 checkpoint is conserved in all eukaryotes. In human cells an additional, G1 checkpoint coordinates extracellular signals with cell cycle progression and directs alternate cell fates of senescence and apoptosis. Such controls are frequently mutated in tumor cells, which resemble the more primitive controls in yeast. G2 checkpoint genes are rarely if ever mutated in cancer cells, suggesting that these genes are essential for tumour viability. These checkpoint differences between somatic and tumor cell cycles may be exploited to

selectively kill tumour cells. Inhibition of G2 DNA damage checkpoint pathway accompanied by external DNA damaging agents has proven to be an effective *in vitro* therapy to kill tumor cells.

1.8 About this thesis

Aims: The present investigation was envisaged to determine the cell cycle modulating effects of select DNA damaging agents which are known to have a direct or indirect damaging effect on cellular DNA. DNA damaging agents chosen in this study – UV-C radiations, Capsaicin, Arsenic trioxide and Chlorambucil fall under various categories of physical and chemical agents. A compound known to interfere with checkpoint activation, Wortmannin, has also been used in this study to check for cell cycle modulations and deviations in macromolecular status with respect to DNA, RNA and proteins affected by the agent. Combination treatments using two agents have also been carried out to investigate whether the responses of the cell to the synergistic action of the two agents are differential, additive or overlapping.

Parameters evaluated: This evaluation comprises parameters such as changes in total nuclear DNA content, genotoxicity, variations of protein profiles in cellular and nuclear lysates and transcript profiling to enable a comprehensive understanding of the overall effects of these cell cycle perturbers at the cellular and molecular level.

Several model systems like yeast, frog embryos, *Drosophila* and cultured mammalian cells has been used for cell cycle studies. Despite the easy amenability to genetic manipulations, yeast as a system, lacks enough stockpiling of proteins needed for biochemical analysis. Giant fertilized eggs of many animals have thus become largely useful for such purposes. The need for achieving cell synchronisation by the use of physical/chemical agents for cell cycle studies also throws additional challenges.

Model system used for the study*:* A naturally synchronized cell cycle and the availability of large amounts of cell cycle phase specific macromolecules (DNA, RNA and protein) in the model system used for the study – synchronous surface cultures of the slime mould, *Physarum polycephalum* - addresses many of the above mentioned drawbacks. The vegetative phase of this acellular organism exhibits natural mitotic synchrony within the syncytium. This feature eliminates the need to induce synchrony using agents such as heat shocks or DNA synthesis blockers like aphidicolin which itself can affect cellular homeostasis and bring about artifacts affecting interpretation of results. The lack of G1 phase and G1 checkpoint in this organism mimics the status of a typical cancer cell where the only functional G2 checkpoint assumes critical importance. The ease of monitoring the cell cycle phases based on nuclear morphology and mitotic timings by phase-contrast microscopy of syncytial explants provides an easy handle to carry out treatments with agents confined to specific phases of the cell cycle. This eliminates the need for expensive equipment to assess or quantitate sub-populations of cells at various cell cycle phases. Moreover, the syncytium can be grown to a sufficiently large size to provide enough material for biochemical analysis. Lastly, the inexpensive method of culturing and maintenance makes this model system unusually attractive. However, the major limitation of this model system is lack of mutants for genetic studies.

Thesis layout: The thesis is divided into seven major chapters. The first chapter highlights the theme of the research work. The second chapter deals with review of literature, which includes a general account on DNA damage response, checkpoint pathways and the agents employed in this study. Third chapter gives a brief account on the model system. Fourth chapter deals with ‘materials and methods’ where all the methods employed in the investigation are described in detail. Fifth chapter furnishes a diagrammatic representation of the ‘experimental design’ followed to execute the study. Sixth chapter comprises of ‘results and discussion’. Results are presented in

tables and figures. The findings are discussed in detail. Finally, the highlights of the entire work have been included in the seventh chapter, 'Conclusion and future perspectives'. This is followed by a detailed bibliography of all citations made in this thesis. An appendix at the end of the thesis provides recipes for reagents, solutions excluded from chapter four. A list of abbreviations, figures and tables have been given in the *pre-pages*.

2. REVIEW OF LITERATURE

Cells are under constant threat of endogenous and exogenous DNA damaging agents which compromise genomic integrity. In response to this, cells initiate a coordinated programme of events termed DNA damage response (DDR) which is critical for maintenance of genomic integrity and prevention of many human diseases related to DNA damage such as ageing and cancer (Kastan, 2008; Polo et al., 2010 ; Deckbar et al., 2011). DNA damage checkpoint signaling pathways are evolutionarily conserved. They ensure the genomic stability by monitoring the structure of chromosomes and coordinating DNA replication, repair, cell cycle progression and programmed cell death (Giannattasio et al., 2004; Zhou and Elledge, 2000).

2.1 DDR pathway

DDR pathway is essentially a signal transduction pathway consisting of signals, sensors, mediators, transducers and effectors (Polo and Jackson, 2011; Su, 2006). However, a strict categorization of the various proteins under these heads is arduous, due to their overlapping functions.

Alteration in chromatin structure, for instance, acts as a signal leading to the activation of downstream events. Chromatin decondensation which is a likely outcome of DSBs (double strand breaks) signals the downstream events by exposing the modifications on histones such as methylation of Histone H3 –Lys79, which increase the affinity for 53 BPI mediator (Cann and Dellaire, 2011; Su, 2006). Sensor triggers the activation of transducing system. Candidates for DNA damage sensors are members of the Rad group of checkpoint proteins, which include Rad1, Rad9, Rad17, Rad26 and Hus1. Rad1, Rad9, and Hus1 together form the 9-1-1 complex which exhibits structural similarity to the proliferating cell nuclear antigen (PCNA) and form a checkpoint sliding clamp (CSC), which serves as a nucleus for the

recruitment of the checkpoint signalling machinery. Rad17 (homologous to the replication factor C (RFC) associates with RFC subunits 2-5 to form a putative checkpoint clamp-loading complex (CLC) that governs the interaction of CSC with damaged DNA (Green et al., 2000; Luncsford et al., 2010; O'Connell et al., 2000). In response to DNA double strand breaks, the MRN (MRE11- RAD50- Nbs1) complex serves as the sensor of DNA breakage, and recruits and helps to activate the key signal transducer of the DDR machinery (Bartkova et al., 2008; Hu and Gatti, 2011). Breast cancer protein BRCA1, another candidate sensor is part of large complex named BASC (BRCA1-associated genome surveillance complex) comprising of ATM, MRN complex, mismatch proteins (MSH2/6 and MLH2), Fanconi anaemia complementation group D2 (FANCD2), RFC, PCNA and the Bloom's helicase (BLM). It is impossible to distinguish between a sensory role and an effector role for any of these proteins, and it is plausible that the activity of an entire complex must be intact to properly sense and respond to damage (Bhattacharyya et al., 2010; Zhou and Elledge, 2000).

BRCA1, MDC1, 53 BPI, MCPH1, PTIP, TOPBP1 and claspin have been grouped as ‘mediators’ / ‘adaptors’ which lack catalytic activity but facilitate signaling by promoting physical interaction between other proteins (Polo and Jackson, 2011; Su, 2006; Yan et al., 2011).

Transducers include Phospho-inositide kinase related proteins (PIKKs), such as ATM and ATR in mammals and their homologues in budding and fission yeast. Two families of checkpoint kinases (CHK), Chk1 and Chk2 kinases, and their homologues act downstream of the above proteins. These kinases are targets of regulation by ATM and ATR kinases. BRCT-repeat containing conserved family proteins, which include budding yeast Rad9 and fission yeast Crb2 also act as transducers.

Effectors are the executors of DDR, which include substrates of both PIKK and CHK kinases, proteins involved in DNA repair, transcription regulation and cell-cycle control such as BRCA1, Nbs1, p53 and Cdc25 (Hu and Gatti, 2011; Zhou and Elledge, 2000).

2.1.A. DNA repair checkpoints

Mammalian cells have three major DNA repair checkpoints: G1/S, intra-S and G2/M, whereas in fission yeast there is only intra-S and G2/M checkpoint (Langerak and Russell, 2011). In response to DNA damage, cells activate the checkpoint pathways to arrest the cell cycle for repair of the damaged DNA. Apoptosis is triggered if the damage is beyond repair (Yang et al., 2010). The DDR is primarily mediated by proteins of the PIKKs family ATM, ATR and DNA-PK and by members of PARP family. DNA-PK primarily regulates a smaller group of proteins involved in DSB end joining. PARP1 and PARP2 activated by SSBs and DSBs and catalyze the addition of poly(ADP-ribose) chains on proteins to recruit DDR factors to chromatin at breaks (Ciccia and Elledge, 2010). Much of the current understanding of the DDR is based on the study of two major DNA damage signalling pathways: The ATM -Chk2 pathway and the ATR -Chk1 pathway (Yang et al., 2010). The final targets of these pathways are Cyclin/Cdk complexes that promote cell cycle progression (Deckbar et al., 2011). Although these two pathways functionally overlap in response to DNA damage and share most downstream effectors, the DSBs primarily activates the ATM-Chk2 pathway, ATR is activated mainly by ssDNA ends that are generated following the induction of DNA adducts or during the processing of DSBs or collapsed replication forks. Their length as well as ssDNA–dsDNA junctions are key factors in ATR's activation (Bensimon et al., 2011; Yang et al., 2010). There is potential crosstalk between the activities of these two kinases. In response to UV or replication stress, ATR mediates downstream activation of ATM. On the other hand, during the S and G2 phases of the cell cycle, the response of ATR to DSBs that are

not part of the replication process is ATM - dependent which is mediated by the generation of RPA coated ssDNA by the endonuclease or exonuclease activity of Mre11/CtIP complexes and also through phosphorylation of the ATR activator, TopBP1 which directly binds and activates ATR (Bensimon et al., 2011; Rai et al., 2007; Reinhardt and Yaffe, 2009).

The earliest event in the DDR signalling pathway involves alteration in chromatin structure the details of which are poorly understood (Reinhardt and Yaffe, 2009). DNA lesions are recognised by the sensor proteins and are recruited to the DNA damage sites independently of the ATM and ATR. This promotes DDR by enhancing the activity of the PIKK proteins and/or by recruiting PIKK substrates to the vicinity of DNA damage, thus facilitating their phosphorylation. With the help of mediator proteins such as MDC1, 53BP1 and BRCA1 for ATM, and TopBP1 and Claspin for ATR, transducer kinases activate the effector kinases Chk1 and Chk2, which then spread the signal throughout the nucleus (Polo and Jackson, 2011). Finally effector proteins of the DNA damage response are either directly phosphorylated by ATM/ATR or by the CHK1 and CHK2 kinases, as well as other kinases such as CK2, p38 and MK2 (Harper and Elledge, 2007). The stability of ATM and ATR and other PIKKs is dependent on the TEL2-TTI 1-TTI 2 (Triple T) complex, which has been reported to associate with the heat shock protein HSP90 and possibly promote the maturation of newly synthesized PIKKs (Ciccia and Elledge, 2010). In the case of DSBs, MRN complex serves as the main sensor, as it recognizes and locates to the DSB during all stages of the cell cycle (Langerak and Russell, 2011). ATM is activated when it is recruited to sites of DNA damage by the MRN complex through binding to the Nbs1 subunit of MRN. ATM activation involves its autophoshorylation and monomerisation following DNA damage and also its acetylation by Tip60 acetyl transferase. But no such mechanism is known to exist for ATR activation (Reinhardt and Yaffe, 2009; Vaissière and Herceg, 2010).

DSBs provoke the formation of defined nuclear structures called irradiation induced foci (IRIF), which are believed to originate by chromatin modification, such as, at the site of DSBs followed by the recruitment of signaling and repair factors. MRN localization to DSBs independently of H2AX phosphorylation is critical for the formation of IRIF and the consequent response to DNA damage (Costanzo et al., 2004). ATR is recruited to sites of damage by binding of its interaction partner ATRIP (ATR-interacting protein) to RPA-coated ssDNA (Langerak and Russell, 2011). The initial sensor of RPA- coated ssDNA is 9-1-1 complex which forms a heterotrimeric sliding clamp that is loaded on to RPA-coated ssDNA by RFC (Kuntz and O'Connell, 2009). Once activated, ATM and ATR phosphorylate an array of proteins essential for DDR. Substrates of activated ATM include p53, the kinases Chk1 and Chk2, FANCD2, the DNA helicase BLM1, BRCA1, histone H2AX, the replication fork-associated MCM proteins, and the MRN complex itself. Similarly, ATR phosphorylates Chk1, BRCA1, and BLM, 9-1-1 complex. These proteins function as transducers, affecting apoptosis (p53 and Chk2), DNA repair (BLM, BRCA1, H2AX, MRN, and SMC1) and cell cycle arrest (p53, FANCD2, SMC1, Chk1, and Chk2). The binding of MDC1 to chromatin requires phosphorylation of histone H2AX (H2AXϒ) and 53BP1. MDC1 is required for sustained binding of MRN and 53BP1 to the damaged chromatin (Rai et al., 2007). As a substrate for both ATM and ATR, Chk1 is a key player in the DNA damage response pathway, the major function of which is to arrest cell cycle at the G2/M and S phase checkpoints. ATR/ATM mediated phosphorylation of TOPBP1 leads to the binding of this protein to Rad9 subunit of 9-1-1 complex, 53BP1 binds to this phosphorylated TOPBP1 and in turn get phosphorylated by ATM. This enables the recruitment of Chk1 kinase to the damaged site. Claspin binds to Chk1 and is necessary for the activation of Chk1 by ATR. After activation by phosphorylation at Ser345 and Ser317 in the C-terminal residue, Chk1 is able to phosphorylate the CDC25 phosphatases. Phosphorylation of

CDC25A results in its ubiquitination and subsequent degradation. In its non-ubiquitinated state, CDC25A would otherwise dephosphorylate and activate the cyclin dependent kinases CDK1 and CDK2 which would allow progression through the S and G2 phase checkpoints causing catastrophic consequences in a cell harboring DNA damage. Chk1 also phosphorylates CDC25C at Ser 216, leading to its cytoplasmic sequestration by the 14-3-3 proteins and preventing it from acting on CDK1, resulting in cell cycle arrest at the G2/M checkpoint. Chk1 is essential for the maintenance of stalled replication forks. Chk2 is a multifunctional serine/threonine kinase, which is activated in response DNA damage.

ATM phosphorylates Thr68 on Chk2 after sensing DSBs in cells, which leads to the oligomerization of Chk2 monomers and the transphosphorylation at Thr383 and Thr387, resulting in its kinase activity. Once activated, Chk2 can phosphorylate several key substrates, including Cdc25C, Cdc25A, p53, Brca1, the promyleocytic leukemia protein (PML), and E2F-1, which is required to mediate cell cycle arrest, DNA repair, and apoptosis (Boutros et al., 2007; Rai et al., 2007).

The G1/S checkpoint inactivates Cyclin D/ Cdk4/6 and CyclinE/ Cdk2 complexes that regulate S-Phase entry. Two distinct pathways have been described - slow and rapid. Slow pathway involves the tumor suppressor, p53 which lies at the heart of the G1 checkpoint. Ser15 phosphorylation of p53 by ATM stimulates the transactivating function of p53 by enhancing the binding of this protein to the transcriptional coactivator, p300. Ser15 phosphorylation greatly enhances the subsequent phosphorylation of p53 at Ser18 by casein kinase I. The presence of phosphates at Ser15 and Ser18 reduces the avidity of full-length p53 for E3 ubiquitin ligase, MDM2, a protein that targets p53 for ubiquitination, nuclear export, and proteasome degradation by approximately threefold. Once stabilized and transciptionally activated, p53 induces the activation of the G1/S checkpoint.

ATM dependent pathways may instigate the onset of apoptosis when excessive DNA damage occurs. Chk2 mediated phosphorylation of p53 at Ser20 also leads to the stabilization of p53 protein levels by disrupting interactions between p53 and hMdm2 (Abraham, 2001). MDM2 phosphorylation has also been implicated in mediating p53 activation. DNA damage induces MDM2 phosphorylation on Ser395 by ATM, on Ser407 by ATR. These phosphorylations favor stabilization of p53 by interfering with the shuttling activity of MDM2. Interaction of MDM2 with the scaffold protein Daxx and de-ubiquitinating enzyme HAUSP is stimulated by DNA damage, which promote p53 de-ubiquitination. DNA damage induces MDM2 degradation in a phosphorylation-dependent fashion, suggesting that elimination of MDM2 leads to p53 stabilization (Cheng and Chen, 2010). p53 stabilization in the late phase after ionizing radiation correlates with active ubiquitination. E3 ubiquitin ligase RFWD3 (RNF201/FLJ10520) forms a complex with Mdm2 and p53 to synergistically ubiquitinate p53 and is required to stabilize p53 in the late response to DNA damage. RFWD3 (RING finger and WD repeat domain 3) is phosphorylated and activated by ATM/ATR kinases. RFWD3–Mdm2 complex restricts the polyubiquitination of p53 by Mdm2 (Fu et al., 2010). The potential role of ATR in the activation of the G1 checkpoint by any form of genotoxic stress remains relatively obscure. It is conceivable that a parallel ATR–Chk1 pathway also drives p53 accumulation in cells that have incurred IR or UV light-induced DNA damage by continued maintenance of phosphorylation at Ser15. The real action with respect to ATR begins with the entry of cells into S phase (Goodarzi et al., 2003). ATM also induces the accumulation of the E2F1 transcription factor in response to DNA damage, by phosphorylating E2F1 at Ser31 (Lin et al., 2001). E2F1 may contribute to stabilization of p53 protein by up-regulating p19ARF, an inhibitor of hMdm2 (Foster and Lozano, 2002). ATM phosphorylates c-Abl at Ser446 leading to the induction of cell cycle arrest in a p53- dependent manner, with the possible involvement of Rb.

With respect to the G1 checkpoint, a key target for transcriptional activation by p53 is the cyclin-dependent kinase inhibitor, p21 (also termed WAF1 or CIP1). The p53-dependent increase in p21 expression suppresses cyclin E and cyclin A - associated Cdk2 activities, and thereby prevents G1 to S phase progression. As p53 dependent pathway involves transcriptional activation following posttranslational modifications, its full activation requires several hours and is important in maintaining G1 arrest by inhibiting Rb phosphorylation (Deckbar et al., 2011).

Rapid response of G1 checkpoint operates through ATM dependent phosphorylation of CHK2 and subsequent phosphorylation at Ser123 of CDC25A tyrosine phosphatases, promoting its degradation. CDC25A dephosphorylates the inhibitory phosphorylation of CDK. Destruction of CDC25A, therefore, inhibits the activation of Cyclin-Cdk complex (Deckbar et al., 2011; Niida and Nakanishi, 2006). Initial rapid response also requires UPS which are known to contain potential SQ phosphorylation sites for ATM/ATR. Protein degradation is an important mechanism for the rapid G1 arrest. UPS proteins are also required for sustained G1 arrest. It is conceivable that the UPS may regulate the sustained G1 arrest through p53-dependent transcriptional program as transcription co-regulators or through other novel pathways yet to be discovered (Mu et al., 2007).

2.1.B. DNA repair

SSB repair **-** SSBs generated by IR, ROS or arising indirectly during BER of abasic sites and altered DNA bases, such as 8oxoG and 3meA, activate PARP family members (Caldecott, 2008). PARP1 and PARP2 both of which act as molecular sensors of SSBs and DSBs, are recognized by two PARP1 zinc finger motifs. PARP1 and PARP2 activation and subsequent synthesis of PAR chains occurs within seconds at damage sites and is one of the earliest events of the DNA damage response. PAR chains are rapidly disassembled by the PAR hydrolyzing enzyme PARG to provide a quick transient response lasting minutes. Upon DNA binding, PARP1/2 assembles

PAR moieties from NAD^+ on target proteins including histones H1 and H2B, and PARP1 itself. Histone PARylation is thought to contribute to chromatin reorganization and recruitment of DNA repair and chromatin modifying complexes, such as polycomb and HDACs complexes, at DNA damage sites (Ciccia and Elledge, 2010; Polo et al., 2010; Schreiber et al., 2006)

DSB repair mechanism - Two main mechanisms for DSB repair in eukaryotic cells are NHEJ and HR. NHEJ is active throughout the cell cycle and relies on rejoining free DNA ends without the need for sequence homology. HR involves the use of a homologous DNA sequence as a template for resynthesis. In yeast, the homologous chromosome can be used allowing HR to operate in all cell cycle phases but in mammalian cells, HR only uses the sister chromatid restricting HR to the post replicational cell cycle phase. However, even in G2, the majority of DSB repair occurs via NHEJ with HR being restricted to the repair of a subset of DSBs locating to heterochromatic regions (Beucher et al., 2009). HR plays a major role during S phase, both in repairing replication-associated DSBs and in promoting replication fork restart. During NHEJ, the free DSB ends recognized and bound with high affinity by the Ku70/Ku80 heterodimer, forms a ring-like structure enabling it to thread onto a DNA end, thereby protecting the ends from diffusing apart and undergoing nucleolytic degradation. Binding of Ku70/Ku80 to the damage ends stimulates the binding of the catalytic subunit of the DNA-dependent protein kinase (DNAPKcs) to the outer end of the DNA which, together with Ku70/Ku80, constitutes the active DNA-PK holoenzyme. The subsequent trans-autophosphorylation of DNA-PK results in a conformational change and exposure of the DSB ends promoting recruitment of the Lig4/XRCC4/XLF complex and finally ligation. IR induced complex DSBs that possess additional lesions such as SSBs, base damages, abasic sites or phosphoglycosylates in close proximity to the DSB and chemical (such as topoisomerase II inhibitors and other drugs used for tumor treatment) induced DSBs

with covalently bound proteins or with single-stranded overhangs needs further processing prior to ligation. Such processing involves nucleases, such as Artemis, as well as additional enzymes that include polynucleotide kinase (PNK), DNA polymerases μ and λ and WRN (Mahaney et al., 2009), interacts in concert with DNA-PK to remove these "bulky" lesions.

HR is initiated by the binding of MRN complex to the free DSB ends. CtIP and the MRN promotes subsequent resection which is extended by Exo1 and Dna2 supported by the BLM (Mimitou and Symington, 2009; Mazón et al., 2010; Symington and Gautier, 2011). The resulting 3'-overhangs, which extend over several hundred bases, are stabilized RPA, which is subsequently replaced by the recombinase Rad51. After homology searching, this nucleoprotein filament invades into the double-helix of the homologous sister chromatid. Using the free 3'-OH as a primer, DNA synthesis is performed by DNA-polymerase δ and η and ligation by DNA-Ligase I. The resulting Holliday Junctions are finally resolved by the helicase BLM in complex with TopIIIα / RMI1 (Cheok et al., 2005; Chu and Hickson, 2009). Recent studies have further identified Mus81-Eme1 GEN1 and SLX1 as potential Holliday Junction resolvases (Fekairi et al., 2009; Ip et al., 2008; Muñoz et al., 2009; Svendsen and Harper, 2010).

2.1.C. Checkpoint termination

The process of termination is not well understood. Protein phosphatases such as Wip1, PP2A, PP4 or PP6 counteract the activity of the checkpoint activating kinases, ATM and ATR, by removing phosphates from Chk1, Chk2, p53 and the damage signal amplifying histone variant H2AX (Deckbar et al., 2011; Nakada et al., 2008; Shreeram et al., 2006). In the course of repair, the checkpoint activating signal decreases shifting the balance between activating and inactivating signals toward inactivation. Once the cell has repaired below a certain DSB level, phosphatase activities dominate over the kinase activities and boost the process of checkpoint

termination. The adaptation process which counteracts the checkpoint activation pathways requires Plk1/Plx1 and claspin. ATR-dependent phosphorylation of claspin at Thr906 creates a docking site for Plx1 enabling Plx1 to phosphorylate Claspin on Ser934. In the course of checkpoint adaptation, despite the persisting replicational stress, Claspin is progressively phosphorylated in a Plx1-dependent manner, resulting in the release of Claspin from the chromatin and finally the inactivation of Chk1. Ubiquitin ligase SCF-βTrCP ubiquitinylates Claspin resulting in its degradation and thus Chk1 inactivation (Deckbar et al., 2011; Mailand et al., 2006). Plk1 phosphorylates the N-terminus of Claspin promoting its SCF-βTrCP-dependent ubiquitinylation and degradation. Plk1 also triggers βTrCP-dependent ubiquitinylation and degradation of the Cdk1-inhibiting kinase Wee1. It has been demonstrated that Cdk dependent phoshphorylation of 53BP1 at PBD binding site serves as a platform for Chk2 binding and subsequent phosphorylation by Plk1 at FHA domain of Chk2 results in its inactivation (Deckbar et al., 2011). CDC25B is also required for recovery from G2/M arrest (Boutros et al., 2007).

2.2 G2 abrogation – an anticancer strategy

Checkpoint inhibition has become an area of novel drug development. Cancer cells are dependent on the S and G2 checkpoints for repair of DNA damage, due to the presence of defective G1 checkpoint mechanisms. Because the S-phase checkpoint facilitates slowing, rather than arrest, of the cell cycle, a cancer cell harbouring DNA damage may progress through the S checkpoint, only to halt at the G2 checkpoint. Thus, the G2 checkpoint, a key guardian of the cancer cell genome, has emerged as an attractive therapeutic target for anticancer therapy. G2 abrogation prevents cancer cells from repairing DNA damage, forcing them into M phase leading to ‘mitotic catastrophe’ and apoptosis. The ideal G2 checkpoint abrogator would be selective, targeting a molecule not involved in G1 checkpoint or S-phase checkpoint

or, if involved, in a nonredundant fashion (Kawabe, 2004). The molecules which are targeted for G2 abrogation include ATM/ATR kinases (caffeine, pentoxifylline), MK2, WEE1 kinase (PD0166285), Chk1 kinase (UCN-01,XL-844) and HSP90 (17-AAG) (Bucher and Britten, 2008).

2.3 Classification of programmed cell death

The various types of programmed cell death (PCD) have in common that they are executed by active cellular processes that can be intercepted by interfering with intracellular signaling. This distinguishes them from accidental necrosis. One model involves autophagy, which is also called type II cell death to distinguish it from apoptosis or type I cell death. This process is characterized by sequestration of bulk cytoplasm and organelles in double or multimembrane autophagic vesicles and their delivery to and subsequent degradation by the cells own lysosomal system. It serves to eliminate long-lived proteins and organelle components and has an important function in cellular remodeling due to differentiation, stress, or damage induced by cytokines. Cells that undergo excessive autophagy are triggered to die in a nonapoptotic manner, without activation of caspases. Autophagy may factor into both the promotion and prevention of cancer, and its role may be altered during tumor progression. Reports on the autophagy gene Beclin 1, showed that heterogeneous disruption of this gene leads to increased tumorigenesis in mice. However, cancer cells may need autophagy to survive nutrient-limiting and low-oxygen conditions and autophagy may protect cancer cells against ionizing radiation by removing damaged elements. The precise role of cell death by autophagy in mammals is not fully understood (Bröker et al., 2005; Qu et al., 2007).

Paraptosis has recently been characterized by cytoplasmatic vacuolation that begins with progressive swelling of mitochondria and the endoplasmic reticulum (ER). It typically does not respond to caspase inhibitors nor does it involve activation of caspases, the formation of apoptotic bodies, or other characteristics of apoptotic

morphology. Paraptosis has been described to be mediated by mitogen-activated protein kinases and can be triggered by the TNF receptor family member TAJ/TROY and the insulin-like growth factor I receptor. Paraptosis has been shown to be inhibited by AIP1/Alix, a protein interacting with the cell calcium-binding death-related protein ALG-2, suggesting that this type of cell death is fundamentally different from apoptosis.

Mitotic catastrophe is another cell death pathway, which is not typical for apoptosis. It is triggered by mitotic failure caused by defective cell cycle checkpoints and the threatening development of aneuploid cells that are doomed to die. Mitotic catastrophe can, in particular, be triggered by microtubule stabilizing or destabilizing agents and DNA damage. This death pathway kills the cell during or close to the metaphase in a p53-independent manner, or occurs partially dependent of p53 after failed mitosis by activation of a polyploidy checkpoint. Mitotic catastrophe has been reported to be accompanied by mitochondrial membrane permeabilization and caspase activation, but others have argued that it is fundamentally different from apoptosis, as caspase inhibition or Bcl-2 overexpression fails to prevent catastrophic mitosis or the development of giant multinucleated cells (Bröker et al., 2005).

Leist and Jaattela (2001) classified cell death into four subclasses, according to their nuclear morphology. Apoptosis is defined by stage II chromatin condensation into compact figures, which are often globular or crescent shaped. Slightly different is apoptosis-like PCD, which is characterized by less-compact chromatin condensation, so-called stage I chromatin condensation. In contrast, in necrosis-like PCD no chromatin condensation is observed, but at best, chromatin clustering to loose speckles, whereas necrosis is characterized by cytoplasmatic swelling and cell membrane rupture leading to release of cellular components and inflammatory tissue response. The dominant cell death phenotype is determined by the relative speed of

the available death programs; although characteristics of several death pathways can be displayed, only the fastest and most effective death pathway is usually evident.

2.4 Agents used for treatment

2.4.A. Arsenic trioxide (AR)

Arsenic, one of the most abundant element in Earth's crust is chemically classified as metalloid, exhibiting organic (linked with carbon and hydrogen) and inorganic (linked with oxygen, chlorine and sulphur, among other elements) forms. Inorganic arsenic (iAs) is present naturally in soil, and in atmosphere as airborne dust. iAs is found in several oxidation states, more frequently as trivalent (iAs[III], also known as arsenite) and pentavalent (iAs[V] or arsenate) species. These forms are differently metabolized by mammals and exhibit distinct grades of toxicity. Exposure to iAs leads to several health effects with the majority of harmful exposure coming from ingestion through drinking water. Malignancies associated with iAs include skin lesions, hypertension, ischemia, some endemic peripheral vascular disorders, severe arteriosclerosis, neuropathies and different types of cancer. Studies have established significant associations between iAs dose in drinking water and occurrence of tumors of the skin, bladder, kidney, liver, prostate, and lungs (Marshall et al., 2007; Martinez et al., 2011). iAs [III] exhibits a significantly higher biological activity than As[V]. However, effects observed in mammals could be similar, since absorbed iAs[V] is mostly reduced to iAs[III] on the initial steps of AR metabolism in mammals. The biotransformation process of iAs occurs via methylation through alternating reduction of iAs[V] to iAs[III], and subsequent addition of methyl groups. This methylation processes is catalysed by SAM-dependant iAs[III]-methyltransferase using SAM as a methyl group donor producing methylated and dimethylated arsenic compounds.

Despite evidence of biotransformation in AR carcinogenicity, it has been demonstrated that AR can induce malignant transformation in cell lines with deficient

AR-methylation capacity in RWPE-1 human prostate epithelial cells (Kojima et al., 2009). This alternative mechanism of AR-induced malignant transformation might be associated with mitochondrial dysfunction specifically through transcription and replication of the mitochondrial genome, in which the mitochondrial transcription factor A (mtTFA) and its regulators, such the nuclear respiratory factor-1 (NRF-1), play key roles (Ekstrand et al., 2004; Kanki et al., 2004; Singh et al., 2011). It has been demonstrated that mtTFA and NRF-1 expressions levels are increased in cells exposed to iAs[III] in a concentration-dependent manner, suggesting that AR regulates mitochondrial activity through an NRF-1-dependent pathway (Singh et al., 2011).

The exact mechanism of iAs induced carcinogenesis is still unknown. There is evidence supporting low level mutagenic activity of iAs and also it has also been shown that iAs can induce transformation in several cell types (Rossman, 2003). Since the AR biotransformation pathway uses SAM as a methyl group donor, iAs can interfere with a number of biological processes, including DNA methylation. Therefore, epigenetic mechanisms have also been proposed to participate in iAs-induced carcinogenesis (Simeonova and Luster, 2000). Oxidative stress has been proposed as a general mode of action for iAs carcinogenesis. iAs exposure results in the generation of ROS such as superoxide anion (O_2^-), H_2O_2 and •OH in various cellular systems, and its production has been proposed as one of the early biological events on iAs-related carcinogenic process (Kitchin and Conolly, 2010, Martinez, 2011). iAs exposure can affect expression of genes associated with stress-related components, DNA damage and repair-responsive genes, activation of transcription factors such as the AP-1 complex, and increases in proinflammatory cytokines, which could influence response to acute AR toxicity (Liu et al., 2001). Genotoxic mechanisms associated with AR carcinogenicity remain controversial. Rossman (2003) proposed that arsenite does not react directly with DNA. On the other hand, it

has been proposed that iAs[III] is a significant mutagen that induces mainly large chromosomal mutations (Hei et al., 1998). AR can also induce mutations as well as methylation changes in the mouse testicular Leydig cell genome. Comet assay performed on human prostate epithelial cells exposed to 100 pg/ml of AR exhibited tail-like structures, suggesting induction of nuclear DNA damage (Singh and Dumond, 2007; Singh et al., 2011). iAs is known to induce chromosomal damage.

Much of the DNA damage observed during iAs exposure is indirect, occurring mainly as a result of ROS induction which generates DNA adducts, DNA strand breaks, cross links, and chromosomal aberrations (Halliwell, 2007; Kitchin and Wallace, 2008). Depending on which cell cycle phase exposure occurs, as a consequence of DNA oxidation, iAs can result in gross chromosomal aberrations including DNA strand breaks (Liu et al., 2001; Shi et al., 2004). iAs can induce DNA strand breaks even at low concentrations. ssDNA breaks are the most common lesions induced by exogenous genotoxins. ROS derived from iAs biotransformation can act as cocarcinogens, for example, increasing damage potential of ultraviolet (UV) light. All these events could be associated, in part, to iAs-related carcinogenic mechanism. iAs was found to increase UVR-mediated DNA strand breaks by interfering with PARP-1 activity, which plays an important role in the ssDNA or dsDNA breaks repair process (Helleday et al., 2007; Qin et al., 2008; Ying et al., 2009). MMA[III] was found to be a potent clastogen in late G1- or S-phase-treated cells. However, lesions induced by MMA[III] are quickly repaired through BER mechanisms when they are induced in G0- or G1-phase of the cell cycle. Trivalent arsenicals might induce either chromatid- or chromosome-type aberrations during treatment in G0 or G1. If ssDNA or dsDNA breaks produced by iAs-induced ROS pass the S-Phase (DNA synthesis), replication occurs and chromatid and chromosome-type aberrations can be produced (Kligerman and Tennant, 2007; Kligerman et al., 2010).

iAs can also induce DNA damage by interfering with the DNA repair processes. Inhibition or impairment of the DNA repair processes, principally the repair of DNA strand breaks, is considered one of the main mechanisms of iAs carcinogenesis (Fisher et al., 2007; Qin et al., 2008). iAs was shown to alter BER mechanisms in GM847 lung fibroblasts and HaCaT keratinocytes, increasing levels of BER-related enzymes and repair capacity. Several enzymes participating in the BER mechanism are known to be modulated by iAs. Among them, DNA polymerase β (Polβ) and DNA ligase I (LIG1) have been described as affected by As[III] (Martinez et al., 2011). Interestingly, DNA copy-number alterations (CNAs) in lung squamous cell carcinoma (SqCC) from iAs-exposed patients from northern Chile contain the Polδ 1 (DNA polymerase δ 1, catalytic subunit), which codes for the proofreading domain of the DNA polymerase δ complex and also participates in ssDNA breaks repair process (Parsons et al., 2007; Venkatesan et al., 2007; Martinez et al., 2011). It has been proposed that iAs[III] works at transcriptional level to repress a group of genes encoding for DNA repair enzymes participating in BER and NER mechanisms, mainly through its downregulation. This, in combination with other events, contributes to toxicity or cancer. Exposure to AR in drinking water was correlated to decreased expression of ERCC1, XPB, and XPF in lymphocytes from exposed individuals.

iAs can specifically inhibit DNA. It has been shown that the mRNA, protein and activity levels of both DNA ligase I and ligase III are significantly reduced in mammalian cells in response to As[III]. As[III] retards DNA break rejoining by interacting with the vicinal dithiols and thus inhibiting DNA ligation. Mammalian cells have been shown to exhibit a dose-dependent decrease in ligase activity with exposure to As[III], corresponding to a decrease in mRNA levels of this enzyme (Martinez et al., 2011; Sykora and Snow, 2008).

AR is one of the oldest drugs in both Western and traditional Chinese (TCM) medicines. It was first used to treat various diseases from syphilis to cancer. Because it is both a therapeutic agent and a poison, AR was used only to treat severe diseases with the principle of "taming an evil with a toxic agent" in TCM. In recent years, the clinical efficacy of AR has been well characterized in the treatment of newly diagnosed and relapsed acute promyelocytic leukemia (APL). In addition, *in vitro* studies showed that AR apparently affected numerous intracellular signal transduction pathways to alter cellular functions. Therapeutic benefits of AR treatment involve antiproliferation, antiangiogenesis, promotion of differentiation, and induction of apoptosis in a wide variety of malignancies, including both hematologic cancer and solid tumors. However, clinical trials indicate that AR as a single agent has not demonstrated significant benefit in a variety of non-APL hematological malignancies (Lu et al., 2012).

2.4.B. Capsaicin (CP)

CP is an active and spicy component and primary capsaicinoid of hot chili pepper. It has been used as food additive for a long time. CP and dihydrocapsiacin accounts for approximately 90% of capsaicinoids in chilli pepper and are the two most potent capsaicinoids. CP, a homovanillic acid (trans-8-methyl-N-vanillyl-6-nonenamide) is a crystalline, lipophilic, colorless and odourless alkaloid with the molecular formula $C_{18}H_{27}NO_3$. CP was first crystallized in 1876 by Tresh, who named it, 'capsaicin' (Oyagbemi et al., 2010; Pramanik et al., 2011; Reyes-Escogido et al., 2011).

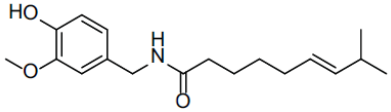

Capsaicin

CP has been used to treat pain and inflammation, associated with a variety of diseases such as rheumatoid arthritis, diabetic neuropathy, cluster headaches,

vasomotor rhinitis, herpes zoster etc (Derry et al., 2009; Frucht Pery et al., 1997; Greiner and Meltzer, 2011; Maity et al., 2010; Richards et al., 2012). Three major metabolites have been identified for CP: 16-hydroxycapsaicin, 17-hydroxycapsaicin and 16,17-dihydrocapsaicin (Chanda et al., 2008). *In vitro* studies in human skin, CP biotransformation was found to be slow and most CP remained unchanged while a small fraction was metabolized to vanillylamine and vanillyl acid suggesting that cytochrome P450 enzymes participate minimally in CP transformation in skin in comparison to their role in hepatic metabolism. CP is mainly eliminated by the kidneys with a small untransformed proportion excreted in the faeces and urine (Suresh and Srinivasan, 2010). Antioxidant property has been attributed to CP due to its phenolic moiety in the molecule (Meghvansi et al., 2010). Extracts of capsicum have been extensively used to study their genotoxicity and mutagenicity effects both *in vivo* and *in vitro*. Conflicting results on tumor initiating/promoting and chemopreventive effects were observed depending upon the cell types used for the study. CP is found to have gastroprotective effect against experimental gastric injury when given intragastrically. Increased gastric mucus production, reduction in mucosal mucus depletion and stimulation of afferent neurons by intragastric CP was suggested to offer protection against gastric mucosal damage (Ito et al., 2004; Oyagbemi et al., 2010). Several studies have demonstrated antiproliferative activity of CP in hepatic, gastric, prostate, colon, leukemic cells (Thoennissen et al., 2009) and human small cell lung cancer. CP suppresses the growth of cancer cells by inactivation of NF-kB and AP-1, ROS generations, activating JNK, ceramide accumulation, cell-cycle arrest, modulating EGFR/HER-2 pathways, dissipation of the mitochondrial inner transmembrane potential DeltaPsi (m), and activation of caspase 3 (Kang et al., 2003; Lee et al., 2004; Min et al., 2004; Oyagbemi et al., 2010; Sánchez et al., 2007; Sánchez et al., 2008; Surh, 2002; Thoennissen et al., 2009). In human prostate PC-3 cancer cells, CP induced upregulation of GADD153 / CHOP, an

endoplasmic reticulum stress-regulated gene has been detected suggesting that CP exerts the antiproliferative effect through a mechanism facilitated by endoplasmic reticulum (ER) stress in these cells (Sánchez et al., 2008).

CP generally exerts its physiologic response by stimulating TRPV1 receptor, previously known as the vanilloid receptor, which is mainly expressed in the sensory neurons. However, receptor independent effects of CP have been observed in cancer (Pramanik et al., 2011; Reyes-Escogido et al., 2011). The exact mechanism by which CP causes ROS generation and cell death is not clear. CP induced apoptosis in humn pancreatic cell lines BxPC-3 and AsPC-1 was associated with ROS generation due to marked inhibition of mitochondrial ETC complexes-I and III and downregulation of antioxidants such as GSH, catalase, SOD and GPx indicating the involvement of mitochondria (Pramanik et al., 2011).

CP was found to decrease the percentage of viable cells of human esophagus epidermoid carcinoma cells CE 81T/VGH, via induction of G0–G1 phase cell cycle arrest and apoptosis. CP induced G0–G1 phase arrest underwent the promotion of p53 and p21, which is an inhibitor of Cdk2 and cyclin E complex. CP induced DNA damage in these cells. Levels of Cdk4, Cdk6, and cyclin E were decreased and the levels of p53 and that of p21 were increased by CP treatment in these cells leading to G2/M arrests. CP increased the expressions of p53, p21, Bax, and caspase-3, and decreased the expression of Bcl-2, and released cytochrome c from mitochondria led to apoptosis in these cells (Wu et al., 2006).

CP induced apoptosis has been demonstrated in numerous cancer cell lines (Chang et al., 2011; Huang et al., 2009; Huh et al., 2011; Ip et al., 2010; Moon et al., 2011). CP caused G1 arrest of endothelial cell through downregulation of cyclin D1 and VEGF-induced angiogenic signaling pathways (Jang et al., 1989). CP was reported to block the downstream event of VEGF-induced KDR / FIK-1 signaling such as, the activation of p38 mitogen-activated protein kinase and p125 FAK

tyrosine phosphorylation that are required for the mitogenic activity of VEGF in endothelial cells (Bradbury et al., 2003; Mifflin et al., 2002; Yang et al., 2002). STAT3 phosphorylation plays a critical role in the transformation and proliferation of tumour cells. It has been found that CP could specifically suppress both constitutive and inducible STAT3 activation. Similarly, it has been observed that CP suppressed nuclear translocation and the DNA-binding activity of STAT3 in several cancer cells. CP suppresses the expression of several STAT3-regulated proteins, including proliferative (cyclin D1), antiapoptotic (survivin, Bcl-2, and Bcl-xL), and angiogenic (VEGF) gene products (Bai et al., 2011; Bhutani et al., 2007; Song and Grandis, 2000). The downregulation of cyclin D1 expression by CP correlates with suppression of proliferation and accumulation of cells in G1 phase of the cell cycle (Min et al., 2004).

2.4.C. Chlorambucil (CHL)

Chlorambucil is a bifunctional alkylating agent used extensively in the treatment of autoimmune and neoplastic disease. Alkylating agents are derivatives of mustard gas (nitrogen mustards), which were extensively used as chemical warfare agents in both World War I and II. CHL was developed in 1953 by Everett et al, with the addition of an aryl group to the nitrogen mustard molecule known as bis-(2-chloroethyl) amine (Bateman, 2010). Alkylation agents exert their effect directly on DNA, RNA and proteins, usually by nonspecific means. The chlorine groups on the nitrogen mustard facilitate nucleophilic attack of nitrogen to form an imminium ion (R_3N). This highly reactive ion undergoes alkylation at N7 of guanine to form a monoalkylated product on the DNA strand. Repetition of this cycle causes cross-linking of DNA. In the case of CHL, two complementary strands of DNA are cross-linked. Cross-linking of DNA prevents separation of DNA strands for transcription and subsequent failure of transcription leads to apoptosis. CHL can also covalently

bond to RNA and proteins through a similar mechanism. CHL is considered to be cell cycle non-specific (Bateman, 2010).

CHL treatment in HeLa cells inhibited the rate of DNA synthesis within 1h of treatment. Synchronous populations of HeLa cells treated prior to DNA synthesis, in the G1 phase of the cell cycle, were not delayed in their progression into the S phase where they exhibited a marked dose-dependent inhibition of the rate of DNA synthesis. Cells in which DNA synthesis had been depressed showed a prolongation of the S phase and this was accompanied by a corresponding dose-dependent mitotic delay. Treatment during the G2 phase of the cell cycle did not induce any delay or block in the next mitosis, but did inhibit the rate of DNA synthesis in the following cell cycle in a dose dependent manner; this depression of DNA synthesis was followed by a delay in the next mitosis (Roberts, 1975). Treatment of A2780 cells with CHL resulted in a cell cycle arrest in S phase followed by apoptosis, while A2780/100 cells demonstrated a transitional G2/M arrest and survived drug treatment (Boldogh et al., 2001; Boldogh et al., 2003). *In vitro* CHL treatment induces Rad51 expression, which could be the reason for resistance to this drug in chemotherapy (Christodoulopoulos et al., 1999).

2.4.D. UV- radiations

There is increased incidence of UV radiation (UVR) on the Earth's surface due to depletion of stratosphere ozone layer caused by environmental pollutants (Lubin and Jensen, 1995). UVR is one of the most effective and carcinogenic exogenous agents that can interact with DNA and alter the genome integrity and may affect the normal life processes of all organisms ranging from prokaryotes to mammals (Solomon, 2008; Zeeshan and Prasad, 2009; Llabres et al., 2010). Among all the groups of UVR (UVA: 315-400 nm; UVB: 280-315 nm; UVC: <280 nm), UVB radiation produces adverse effects on diverse habitats, even though most of the extra-terrestrial UVB is absorbed by the stratospheric ozone (McKenzie et al., 2003).

UVA radiation has a poor efficiency in inducing DNA damage, because it is not absorbed by native DNA. UVA is able to generate singlet oxygen ($^1O_2$) that can damage DNA via indirect photosensitizing reactions (Alscher et al., 1997). Harmful effects of UVC radiation on biota is comparatively less since it is quantitatively absorbed by oxygen and ozone in the Earth's atmosphere. UV radiation is absorbed by nucleic acids and proteins, which can cause photo-damage and conformational changes, and subsequently disturb vital metabolic functions such as transcription, DNA replication, and translation (Llabres et al., 2010; Sinha et al., 2008). One of the most prominent targets of UV-radiation is cellular DNA, which absorbs UVB radiation and causes adverse effects on living systems (de Lima-Bessa et al., 2008). Two adjacent cytosines are considered as mutation hotspots of UVB and UVC radiations (Ravanat et al., 2001). It has been found that T-T and T-C sequences are more photoreactive than C-T and C-C sequences (Courdavault et al., 2005). It has been demonstrated that the main photoproducts are cis-syn-configured cyclobutane pyrimidine dimers (CPD) lesions, while trans-syn-configured CPD lesions are formed in much less quantity. The base damage by UVR is determined by the flexibility of the DNA strand as well as nature and position of the base. The heterogeneous distribution of the UV-induced photolesions in the DNA depends on the sequences that facilitate DNA bending as well as the chromatin modulation through the binding of specific protein (Balajee and Bohr, 2000).

UV-induced ROS acts as a powerful oxidant that may cause oxidative DNA damage. A number of oxidation products of purine bases such as 8-oxo-7,8-dihydroguanyl (8-oxoGua), 8-oxo-Ade, 2,6-diamino-4-hydroxy-5-formamidoguanine (FapyGua), FapyAde, and oxazolone have been reported to form upon exposure of DNA to UV radiation (Rastogi et al., 2010). Longer wavelength UV (UVB and UVA) induce oxidative stress and protein denaturation, while short wavelength UV radiation (UVC) causes predominantly DNA damage to cells in the form of

pyrimidine dimers and 6-4 photoproducts . Several DNA damage-induced signaling cascades such as ATR/Chk1, AKT, jun N-terminal kinase and p38 MAPK/ ERK, pathways are activated following UVC radiation, leading to activation of NER and recovery mechanisms via transcription factors such as p53, NF-κB and AP-1 leading to transcriptional response resulting in regulation of DNA damage repair, cell cycle progression and apoptosis. However, the molecular mechanisms underlying the cellular UV response remains to be elucidated. Depending on the dose of irradiation, UV induced cell cycle arrest in the G1 phase may or may not be p53 dependent. p53 dependent pathway which is the most important regulators of UV-induced cellular reponse, upregulates p21 and GADD45α to mediate G1/S arrest and DNA repair. ERK activation is responsible for p53 independent cell cycle arrest and apoptosis following UV irradiation (Xia et al., 2011; Aleem, 2012). Zhong et al (2011) showed induction pattern of different response signaling pathways of MAPKs and PI 3 kinases leading to eIF2α phosphorylation depends on the wavelengths of UV exposures. ERKs were found to be activated strongly by UVA in a dose dependent manner, whereas a relative moderate or weaker activation level is induced in the UVB or UVC responses, respectively.Conversely, UVC can cause a significant increase in activation of JNKs, but a moderate or weaker level of JNKs activation was stimulated by exposure to either UVB or UVA. However, no difference was observed between UVA, UVB and UVC in their ability to activate p38 kinase.

PIKK family members ATM, ATR and DNA-PK can differentially sense wavelength-specific DNA damage stresses and secondary oxidative stresses, and also transduce multiple response signals toward eIF2α phosphorylation. ATM is involved in modulating UVA-induced apoptosis through JNKs and p53, and also participated in the regulation of STAT3 signaling through RSK and its upstream kinases ERKs and JNKs rather than p38 kinase. However, ATM kinase is not required in the activation of UVC-triggered signaling, whereas the UVC response is activated through ATR

(Zhang et al., 2002; Zhang et al., 2003). UVB-induced phosphorylation of 4E-BP1 occurs through a mechanism involving the p38 and its downstream kinase MSK1 (Liu et al., 2002). DNA-PKcs is required for UVB induction of the elF2α kinase GCN2 and consequent translation reprogramming (Powley et al., 2009).

The effect of UV irradiation has been studied extensively in *Physarum polycephalum*. Irradiation of plasmodia with UV radiation alters the timing of one or more mitoses. The number of nuclei destroyed by UV and the timing of their degradation appears to be the function of dose. If plasmodia are irradiated in early G2 the next mitosis is delayed. However, after division only a fraction of nuclei are able to complete their DNA synthesis, rest are broken down. Thus, the nucleo-cytoplasmic ratio is abnormally small at the start of first complete cycle after UV irradiation. This cycle is short, as expected. On the other hand, the second and third post irradiation cycles are of normal duration.

It has been reported that UV irradiation (200-500 Jm^{-2}) of plasmodia at any time between early S and mid G2 caused a 2-4h delay at the onset of next nuclear division. Irradiation with UV light during S phase has been reported to reduce the rate of DNA synthesis, as measured by incorporation of radioactive thymidine into DNA. Mitotic delay is not due to the inhibition of DNA synthesis *per se* because; UV sensitivity extends into G2 period. Indeed, UV irradiation applied in the mid to late interphase reduces the rate DNA synthesis in the following S phase but the subsequent mitosis is advanced, not delayed. Due to the destruction of nuclei, the overall DNA content relative to the total protein content in the irradiated plasmodia is drastically changed. The DNA : mass ratio has been proposed as a critical parameter in various models of mitotic mechanism (Nair, 1995). Measuring [^{3}H] thymidine incorporation, Sachsenmaier et al (1970) showed that there was a substantial shortening of S period in response to UV exposure in G2 of the previous interphase. Further, during this shortened S phase, the increase in total DNA content was limited

presumably due to large fraction of pycnotic nuclei. It seems likely that UV treatment cause nuclear : cytoplasmic imbalance that results in an increased availability of enzymes and other components of the DNA replication machinery that are normally rate limiting (Nair, 1995). Jayasree and Nair (1993) have carried out BUdR substituted plasmodia showing the UV sensitivity of G2 phase *Physarum* macroplsmodia.

The response to UV (700 and 1400 Jm^{-2}) in *Physarum* is biphasic (Kumari and Nair 1984). The S-phase comprising the early one third of the cycle (Gl being absent) and the late G2-phase, including the UV-reversible, early part of prophase, forming the last 0.1 part of the cycle are the two phases with extra sensitivity. Between these two, the S-phase is the more sensitive, as indicated by the duration of the UV induced mitotic delay. However, the extra sensitivity seen during G2 is most relevant from the point of view of the mitotic process itself. In eukaryotes, entry into mitosis is controlled by MPF (Lorca et al., 2010), the activity of which has been reported in *Physarum* about 20 min prior to mitosis (Adlakha et al., 1988) which is the most UV sensitive time in G2 in *Physarum*. The UV-induced mitotic delay in *Physarum* is reported to be due to repair replication (Mccormick et al., 1972). The UV-induced G2 arrest thus could be by interfering with the activity of MPF.

2.4.E. Wortmannin (WM)

Wortmannin, an antifungal agent, is an effective radiosensitizer that irreversibly inhibits certain members of PIKK family. WM was isolated in 1957 by Brian and co-workers from the broth of *Penicillium wortmanni*. WM is a member of the structurally closely related class of steroidal furanoids, which include viridin, viridiol, demethoxyviridin, demethoxyviridiol and wortmannolone.

The structural origin of WM's biological activity, and quite likely of other members of the viridin class of steroidal furans, arises at least in part from the electrophilic character of the strained tricyclic furan moiety. The naphtho[1,8-

bc]furan subunit is generally flanked by electron-withdrawing carbonyl groups that increase the electrophilicity of the α-carbon of the furan ring, and the strained nature of the tricycle further enhances furan reactivity (Wipf and Halter, 2005)

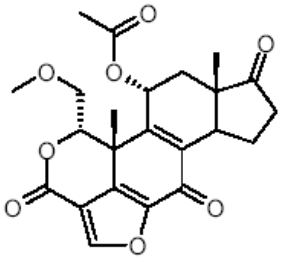

Wortmannin

WM has been widely used as a popular and powerful research tool to identify some of the physiological roles of the cellular signaling pathways. WM is a non-competitive inhibitor of ATP which binds irreversibly to the ATP-binding site of most serine/threonine protein kinases and alkylates a specific lysine in the catalytic site. Because of the unique geometry at the active site of the PI 3K and PIKK protein kinases, WM inhibits these enzymes at lower concentrations than those required to inhibit most other protein kinases. The concentration of WM required for 50% inhibition of the protein kinase activity (IC50) for Class I PI 3K is 2-5 nM; the IC50 for DNA-PK activity has been reported to be between 16 nM and 120-150 nM, while that for ATM and ATR occurs at 150 nM and 1800 nM, respectively. Thus, WM has the potential to distinguish between ATR and ATM-mediated substrate phosphorylation in cell extracts or *in vitro*. However, at higher concentrations (mM), WM inhibits other protein kinases such as myosin light chain kinase. Micromolar concentrations of WM are required to inhibit DNA-PK *in vivo*. These high concentrations of WM radiosensitize cells and inhibit DNA double-strand break repair in vivo. However, these concentrations of WM also inhibit PI 3K, ATM, ATR, and, indirectly, other PI 3K-dependent protein kinases such as PKB/Akt and PDK1. Thus WM, is not a specific protein kinase inhibitor (Goodarzi et al., 2003).

WM and its 11-desacetoxy analog were subsequently identified as potent anti-inflammatory agents (Wipf and Halter, 2005). WM was also found to be a potent inhibitor of mammalian Polo-like kinases (PLK1 and PLK3). This enzyme is involved in cell cycle progression of rapidly proliferating, nontransformed cells as well as tumor cells. In cancer, overexpression of PLK1 contributes to the malignant state by aberrant cell cycle regulation at the G2/M phase (Liu et al., 2007; Didier et al., 2008). Proteolysis and mutagenesis studies of PI 3K revealed that Lys802 was the target for a covalent attachment of WM. This lysine residue resides in the ATP binding site of the p110 catalytic subunit and thus has a crucial role in the phosphotransfer reaction. Specifically, the irreversible inhibition of PI 3K involves the formation of a vinylogous carbamate by an attack of the lysine side chain amino group onto the furan ring. WM is a bimodal inhibitor of PI 3Ks. The inherent affinity of the natural product to the ATP-pocket would in itself be sufficient to inhibit the kinase domain, but the process then proceeds toward covalent modification of the lysine residue and formation of the irreversible adduct. Accordingly, the non-covalent binding interaction is sufficient to inhibit the enzyme, and Lys modification only makes it irreversible.

Aside from selectivity and toxicity issues, another obstacle to the use of WM and other viridins as clinical candidates is their instability and poor solubility. Both WM and demethoxyviridin, when stored as aqueous solutions at either 37 or 0°C at neutral pH (Tris–HCl buffer, pH 7.4), are subject to decomposition by hydrolytic opening of the furan ring. This chemical instability is much more pronounced in demethoxyviridin than WM, mirroring their relative potency. Furthermore, lactone hydrolysis in WM followed by elimination of methoxyacetaldehyde leads to aromatization of the B-ring and loss of PI 3K inhibition (Isosaki et al., 2011; Wipf and Halter, 2005).

WM, a known radiation sensitizer, has been used in experiments with synchronized cells to compare its effect on radiation survival and mutation induction within the cell cycle. WM significantly potentiates the induction of p21WAF1, a p53 regulated gene that encodes for a key mediator of cell cycle / growth arrest, when determined at late times after irradiation. This late WM dependent potentiation of p21WAF1 induction following radiation exposure is observed in normal human fibroblasts and in p53 wild type tumor cell lines but not in p53 deficient tumor cell lines, concluding that radiosensitization of p53 proficient human cells by WM may in part be associated with delayed induction of p21WAF1, which can lead to a sustained growth-arrested phenotype resembling senescence (Chernikova et al., 2001; Mirzayans et al., 2004).

Hyperthermia has cell killing effect either by itself or synergistically with radiation, and is used to treat cancer mostly combined with radiation. WM enhanced heat-induced cell death in cultured Chinese Hamster V79 cells accompanying cleavage of poly(ADP-ribose) polymerases (PARP). Additionally, the induction of heat shock protein HSP70 was suppressed and delayed in WM treated cells. Heat sensitizing effect of WM was obvious at more than 5 or 10 μM of final concentrations, while radiosensitization was apparent at 5 μM. Requirement for high concentration of WM (μM), suggests a possible role of certain protein kinases, such as DNA-PK and/or ATM among PI3-kinase family. The sensitization was minimal when WM was added at the end of heat treatment. Since heat-induced cell death and PARP cleavage preceded HSP70 induction phenomenon, the sensitization to the hyperthermic treatment was considered mainly caused by enhanced apoptotic cell death rather than secondary to suppression or delay by WM of HSP70 induction. Further, the radiosensitization by WM was also at least partly mediated through enhancement of apoptotic cell death (Tomita et al., 2000). The relative broad range of potencies with which WM inhibits different members of the extended PI 3K family suggests that chemical modification of sterol like nucleus of WM might yield

compounds with more selective inhibitory effect (Sarkaria et al., 1998). One obstacle to evaluating the *in vivo* pharmacology of WM has been the lack of any assay suitable for quantitation of WM in biological matrices. The *in vitro* metabolism studies showed that carbonyl reductase enzyme is responsible for WM metabolism to 17-OH WM, which is 10 fold more potent than WM in its ability to inhibit PI3-kinase, and is more toxic than WM (Holleran et al., 2004).

DNA damage dependent, PIKK induced reduction in the H3K9Ac and H3K56Ac levels were found to be inhibited by WM (Tjeertes et al., 2009). WM has been used to inhibit ATR kinase to check for the ATR dependent activation of p53 following UV irradiation in MC7 cells (Batchelor et al., 2011). Cisplatin-induced loss of nucleolar SSRP1 and DNA-PK activation are suppressed by pretreatment of the cells with WM (Dejmek et al., 2009). Recent works show the renoprotective effect and protection against high fat diet induced obesity following treatment with WM. This protective effect of WM is explained by WM induced inhibition of PI3 kinase and mTOR (Kim et al., 2012).

2.5 Differential display polymerase chain reaction

Differential display reverse transcription PCR (DDRT-PCR) is a procedure used to identify the induction or repression of gene expression (Luehrsen et al., 1997). Differential display has been developed as a tool to detect and characterize altered gene expression in eukaryotic cells. In this technique, total RNA isolated from cell types or tissues are reverse transcribed (RT), using an oligo-dT primer (the anchor primer) that has a specific dinucleotide at its 3'. This anchored primer and a random 10-mer (arbitrary primer) are then used to amplify, by polymerase chain reaction (PCR), cDNAs to which the 3'-anchor and 5'-arbitrary primers both hybridize. A radioactive nucleotide is included in the PCR reactions so that the PCR products can be run side-by-side on a 5% polyacrylamide gel and visualized by autoradiography. However, non-isotopic methods for DD-PCR on ethidium bromide stained agarose gels have also been reported (Boschi and Vergara, 1998). Bands that appear on the

display of RNA from one cell type but not the other correspond to differentially expressed mRNAs. These bands are excised from the gel and reamplified with the same primers used for the original display. The resulting PCR product can then be cloned and sequenced or used directly to probe Northern blots. Once confirmation of differential expression is obtained, the PCR products can be used to isolate full-length cDNAs from appropriate cDNA libraries (Whitelaw et al., 2002).

Advantages of DD-PCR over alternative approaches are: quantitative identification of differences in gene expression, simultaneous detection of upregulation and downregulation of genes, requirement of only small amounts of mRNA and reduced time of analysis (Bosch and Lohmann, 2002). DD-PCR has been employed to identify differentially expressed genes in dorsal and ventral chick midbrain (Chittka et al., 2009), endometrial and cervical tissues and tumors (Hebbar et al., 2005), smooth muscle cells and human coronary atherectomy tissues (Blaes et al., 2007) hepatoma cells (Charlton et al., 1999), cerebellar granule cells (Roschier et al., 2000), *Meningococcus* during the early stages of an infection (Talà et al., 2008) and in plant cells (Selvam et al., 2009; Whitelaw et al., 2002).

3. MODEL SYSTEM

3.1 *Physarum* as a model system

Although modern *Physarum research* was initiated to address biological questions of general importance, such as motility or growth and differentiation, the scientific community has been slow to accept this organism as a universal model of a eukaryotic cell. At that time other simple eukaryotic systems such as *Saccharomyces, Tetrahymena, and Dictyostelium* were already well established in the laboratory. Later on, due to its unique life history it was accepted as model system for various research activities including cancer.

The NIH (U.S.A) announced that Physarum polycephalum was one of the 18 new model organisms whose genomes will be sequenced as part of Comparative Genome Evolution project of the National Human Genome Research Institute (NHGRI) (NIH news release, 2004). The anticipated end product of this whole genome shotgun-sequencing project is an assembled genome sequence with approximate 6X coverage.

Physarum has recently come into limelight. Hailed as an 'intelligent' cell, the organism also called '*Physarum machine*' has now become the delight of researchers studying complex oscillatory behaviours (Bonner, 2010; Marwan, 2010; Tsuda and Jones, 2011), adaptive memory, computational and learning ability and networking (Jones and Adamatzky, 2010; Shirakawa et al., 2011). Based on the organism's ability to solve a maze and find the shortest path interconnecting multiple food sites during an adaptation process, Watanabe et al (2011) has recently proposed traffic optimization of railroad networks inspired by an algorithm mimicking this amoeba-like cell. In addition, it has recently been used for RNAi study (Haindl and Holler, 2005), RNA editing (Bundschuh et al., 2011) and for fishing out novel genes (Itoh et al., 2011).

Physarum polycephalum displays a large number of interesting biological phenomena, which attracts researchers from various fields. This includes:

***i) The synchronous mitosis in the plasmodium (Guttes et al., 1961)*:** Synchronous mitosis is perhaps the most spectacular event in plasmodium of *Physarum.* Harold P. Rusch rediscovered this in 1950s in his search for a model system to study cancer. He realized that its unique life strategy provided a good opportunity to investigate, independently, events associated with either growth of differentiation. Each microplasmodium is synchronous with respect to nuclear division but there is no synchrony among microplasmodia. But by fusion of a large number of microplasmodia on the surface of a filter paper a single giant 'cell'- macroplasmodium - is formed. Macroplasmodium with a diameter of 5-10 cm has more than 10^8 nuclei in which vigorous cytoplasmic streaming maintains a high degree of homogeneity. Being a common cytoplasm all nuclei of macroplasmodia undergo synchronous mitosis every 8-10h at 26^0C. The degree of synchrony within the plasmodium has been estimated by flow cytometry (Kubbies and Pierron, 1983). At least 99 % of 10^8 nuclei of the plasmodium are cycling. They divide in synchrony as evidenced by a shift of DNA fluorescence from 4C to 2C, which takes place in less than 5 min.

***ii) The high degree of synchrony is maintained throughout S phase*:** All the nuclei initiate DNA replication within minutes after telophase. The rate of DNA synthesis is high in the first 90 min of the S phase at which time more than 75 % of the genome has been replicated which then decreases from 5,000 kb / min to about 1,200 kb / min so that it takes another 90 min to replicate the last quarter of the genome (Kubbies and Pierron, 1983). This is not true for ribosomal DNA genes of *Physarum*, which are replicated throughout the cycle except for perhaps the first hour of the S phase. Autoradiographic and cytological studies have demonstrated a tight coupling between mitosis and S phase in the plasmodium of *Physarum.* S phase is one third of

interphase while G2 comprises 2/3rd of the interphase. The onset of DNA replication in *Physarum* is morphologically defined by the observation of telophase.

iii) Process of development and differentiation such as amoebal-plasmodial transition of the colonial strain, spherulation (Huttermann et al., 1970) and light-induced sporulation of plasmodium (Suaer, 1982).

Differentiation of *Physarum* plasmodia is controlled by environmental conditions, UV or blue or red light induces the highly synchronous irreversible differentiation into fruiting bodies, when applied to competent plasmodia at a sufficient dose. In the dark, macroplasmodia convert into sclerotia consisting of spherule clusters. Spherulation is investigated mainly in suspension of microplasmodia. It is induced by starvation alone or by various kinds of environmental stress. Like sporulation spherulation in *Physarum* plasmodia is a reversible encystment and not a terminal differentiation process. The plasmodia spherule transition is inhibited by continuous illumination with blue light (Aldrich and Daniel, 1982).

***iv) Motile and contractile phenomenon in both amoebae and plasmodia (Jacobson et al, 1976)*:**

The ability of the living cytoplasm to contract at all cellular sites is based on the ubiquitous cytoplasmic actomyosin. Its special arrangement in plasmodial strand resembles the location of muscle actomyosin in muscle tubes. The isotonically contracting fibrils in the ectoplasmic tube exert pressure on the interior or endoplasmic channel thus inducing a translocation of endoplasm in the direction of lower pressure. This is the normal mode of endoplasmic mass transport in macroplasmodia. Owing to this well-established mechanism and to the ability to follow the contractile process by measurement of several microscopic and

tensiometric parameters on plasmodial strands, these objects are of special value in creating clear-cut experimental conditions to analyze the physiology of cytoplasmic actomyosin. This is a central problem in current research on cytoskeleton. Macroplasmodium represents a most favourable material because its size allows the application of techniques such as tensiometry.

3.1.A. Life cycle of *Physarum*

Physarum polycephalum is a member of the class/superclass Myxogastridae (or myxomycetes) commonly referred to as plasmodial or true slime molds. Although historically classified as fungi, molecular data now clearly show that they are most closely related to the cellular slime molds (Dictyostelidae). Together they form the supergroup Amoebozoa

P. polycephalum belongs to the family Physaraceae (Alexopoulos, 1982) and is often referred to as the "many-headed slime". It inhabits shady, cool, moist areas, such as decaying leaves and logs. A typical life cycle of *Physarum polycephalum* is illustrated in Fig.3.1.A.

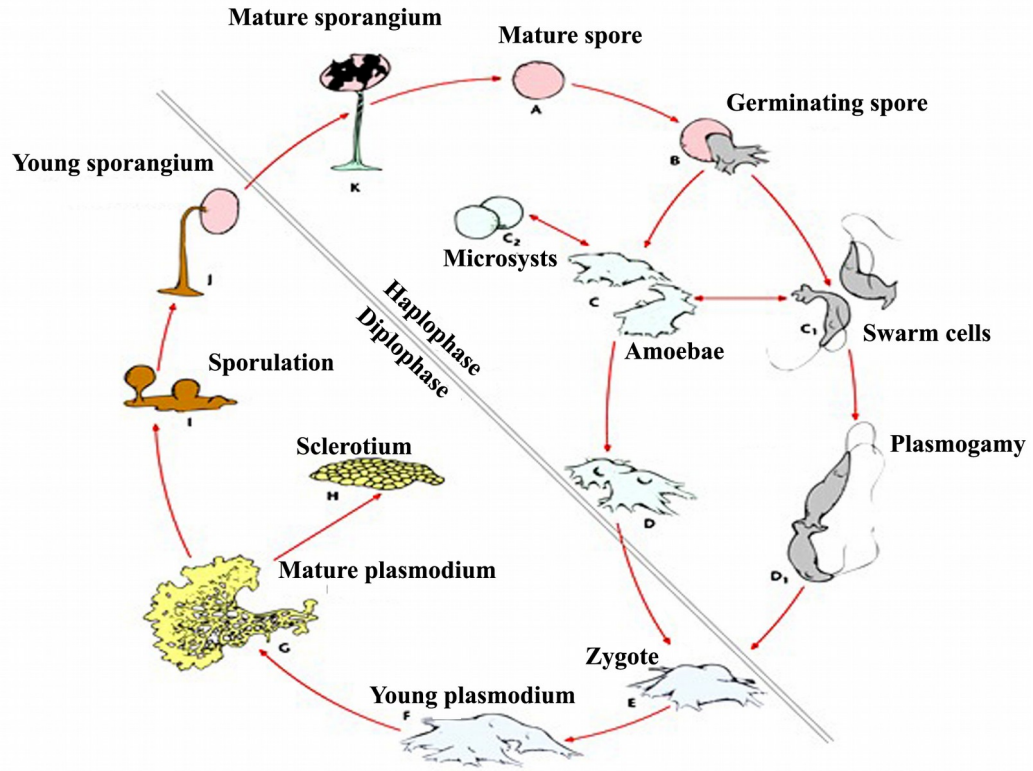

Fig. 3.1.A

Physarum exist in at least three distinct forms. The essential stages in the life cycle are shownabove: The main macroscopic vegetative phase of P. polycephalum is the plasmodium (the active, streaming form of slime molds). Plasmodium of P. polycephalum is a bright yellow glistening mass that can grow to 30 cms across under the right conditions (Martin and Alexopoulos, 1969), comprising of intricate network of protoplasmic veins, and many nuclei. It is during this stage that the organism searches for food. Plasmodia phagocytose bacteria, myxomycete amoebae and other microbes. The plasmodium surrounds its food and secretes enzymes to digest it. Locomotion of this giant multi-nucleate cell occurs as a result of protoplasmic streaming of the cell contents within the veins, the direction of streaming, reverses every 30-60 sec. Plasmodia can be grown in the laboratory on surface or in shaken cultures. On surface the multinucleate plasmodium is yellow, flat, disc like and consists of protoplasm which shows rapid to and fro movements. Fusion of the large number of genetically similar microplasmodia on filter paper gives rise to a giant cell, macroplasmodium, in which all nuclei undergo synchronous mitosis every 8-10 h at 26^0C (Guttes and Guttes, 1964). If environmental conditions cause the plasmodium to desiccate during feeding or migration, Physarum will form a sclerotium. The sclerotium is basically hardened multinucleated tissue that serves as a dormant stage, protecting Physarum for long periods of time. Once favourable conditions resume, the plasmodium reappears to continue its quest for food. As the food supply runs out, the plasmodium stops feeding and begins its reproductive phase. Stalks of sporangia arise from the plasmodium; it is within these structures that meiosis occurs and spores are formed. Sporangia are usually formed in the open so that the spores they release will be spread by wind currents. Spores can remain dormant for years if need be. However, when environmental conditions are favorable for growth, the spores germinate and release either flagellated or amoeboid swarm cells (motile stage); the swarm cells then fuse together to form a new plasmodium (The figure given above has been taken from the article of Kohama and Nakamura, 2001)

3.1.B. Major limitation

At present major limitation in using *Physarum* as a model organism for cell cycle studies is due to lack of mutants defective in cell cycle functions, analogous to *cdc* and *wee* mutations in yeast cells. Several succeeded in isolating plasmodial cell cycle mutants (Burland and Dee, 1980), but none of them were studied in detail. (Laffler and Tyson, 1986).

3.1.C. Periodic events and cell cycle regulation in the plasmodia of *Physarum polycephalum*

The findings that mitosis is driven by a factor with homologous properties in cells from fungi to man (Draetta et al., 1988; Murray and Kirschner, 1989; Murray and Hunt 1993) has made it quite evident that the basic control mechanisms operating on the cell cycle and mitosis are about the same in all eukaryotes.

Adlakha et al., 1988, demonstrated the homology of plasmodial MPF to that of other organisms by inducing germinal vesicle breakdown (GVBD) in *Xenopus* oocytes. With the help of an antibody directed against a conserved sequence of Cdc2 protein (the catalytic subunit of MPF), a homolog of this cell cycle regulatory gene product has been identified in the plasmodia. The following periodic events or processes in the cell cycle of the plasmodia of the *P. polycephalum* have been studied:

1. Thymidine kinase synthesis and its overall activities.
2. The organization and duplication of Microtubular Organzing Centers (MTOCs) of the mitotic spindle
3. The co-triggring of tubulin and histone genes and translation of their mRNA's
4. Triggering of Cdc2 kinase activity.

These events have been shown to serve as good markers to monitor the progress of the plasmodial cell cycle in an unperturbed system; they are also amenable to specific perturbations and this may yield valuable information on some of cell cycle control mechanisms operating in this organism. Moreover they are representative of the three major cell cycle regulatory pathways in the plasmodia.

5. Chromosomal DNA synthesis and repair pathway.
6. Microtubule associated pathways involving MTOC organisation and duplication and regulation of tubulin synthesis, and
7. A pathway which links microtubular and DNA synthesis pathways (Nair, 1995).

In eukaryotic cells, the DNA synthesis and/or repair pathway and the microtubular pathway appear to be coordinated at a point very close to metaphase, i.e. during the transition period between early prophase and metaphase by Cdc2 kinase (Lewin, 2004).

3.1.D. Cell cycle Perturbation studies using *Physarum*

The studies carried on the plasmodia employing microtubular poisons and DNA synthesis inhibitors showed that the full activation of mitotic kinase here requires at least two successive triggering signals, one involving microtubular components and the other involving DNA synthesis, showing thereby the coordinating nature of this enzymatic activity. The kinase activity is maximal in early metaphase and then declines when nuclei are still in metaphase (Ducommun et al., 1990). An earlier study had shown that the kinase activity stays high in cycloheximide-treated, metaphase-blocked plasmodia (Ducommun and Wright, 1989) indicating that the inactivation of kinase requires protein synthesis. It is not surprising that in the case of the plasmodia of *Physarum,* the transition point (TP) *w*ith respect to a large number of perturbers is located around the time in the cell cycle, where the activity of the Cdc 2 kinase reaches a maximum.

Earlier studies on the effect of UV-radiation on *Physarum* cell cycle has been already reviewed extensively chapter 2. The effect of Caffeine in reducing UV-induced mitotic delay was found to be maximum in plasmodia irradiated about 20 min prior to metaphase (Jayasree and Nair, 1991; Jayasree and Nair, 1993). Caffeine was also found to reverse G2 arrest in the plasmodia following X-ray irradiation (Deinl et al., 1990). The above noted effect of Caffeine on the irradiated plasmodia appears to be due to an action of the drug, albeit indirect, at the level of the mitogenic factor.

Strong evidence for size control in *Physarum* has been obtained from UV-irradiated, heat shocked, cycloheximide treated and X-ray irradiated plasmodia (Nair, 1995). Among the above the UV - irradiated system has been the most ideal for these kind of studies. The post - irradiation short cycles developed significant resistance to high concentration of actinomycin-D. The resistance is complete with respect to the process of mitosis, including cycle duration, and partial with respect to transcription. The reduced sensitivity of the post irradiated system to actinomycin appears to be

specific for this drug, since it is susceptible to Cordycepin, another inhibitor of transcription whose mode of action is different from that of former (Nair, 1995).

Work by researchers on the effect of UV alone or in combinations with other compounds, antimicrotubular drugs and heat-shocks affecting cell cycle (Kumari and Nair,1981,1983,1984; Kumar and Nair, 1990, 1991, 1992, 1993; Indirabai and Nair,1991; Jayasree and Nair,1991,1993; Aravindan,1992) have all been reviewed by Nair (1995).

Enhancement of UV-induced mitotic delay in G2 phase plasmodia that were labeled with 5-Bromo-2[1]-deoxyuridine in the S phase, highlights the importance of genomic integrity in traversing the G2/M checkpoint of the cell cycle (Jayasree et al., 2000). On the contrary, shortening of the cell cycle duration by *Brahmi* (*Bacopa monnieri*) extracts have also been reported (Venu et al.,2003).

4. MATERIALS AND METHODS

4.1 Culturing of *Physarum polycephalum*

P. polycephalum (McArdle Strain, M3C, McArdle Cancer Laboratory, Univ. of Wisconsin, Madison,U.S.A) microplasmodia were cultured in semi-defined medium (SDM) (Daniel and Baldwin,1964) as shake cultures. To 45ml of medium in a 500ml flask, about 1-2ml inoculum was added. The flasks were then kept on a shaker in the dark, at 24-26^{0}C.

4.1.A. Starting of the culture

Preparation of Strips **-** The spherules of an overgrown (>72h) culture were spun down at 1000 rpm for 2 min. The pellet washed in 8 volumes of 1:1 diluted minimum salt solution (MSS) was resuspended in equal volume of 1:1 diluted salt solution. The suspension was then spotted on the autoclaved filter papers strips which were then dried and stored in culture tubes along with silica bags for desiccation.

Surface Culture - The spotted strips (one or two) per plate were placed on 2% SDM-agar plates, incubated at 24^{0}C for 48h till a yellow fan shaped structure (the macroplasmodium) germinated from the spherules and spread over the agar surface.

Starting of liquid culture **-** A portion of the agar with the moving front of the fan was scooped out and put into 45ml of SDM in a 500ml conical flask. It was kept at 24^{0}C without shaking for 24h in dark in an inclined position to prevent the agar from being submerged in the medium.

4.1.B. Preparation of macroplasmodia

Mitotically synchronous plasmodia were prepared by fusion of actively growing microplasmodia (Kumar and Nair, 1990; Jayasree and Nair, 1991). Microplasmodia were allowed to sediment for sometime and supernatant was discarded. Sediment was centrifuged at 2000 rpm for 90sec. The supernatant was discarded, after noting the packed volume of microplasmodia. Microplasmodia were

washed with five volumes of sterile water after resuspension and then centrifuged at 1500 rpm for 1 min to remove slime and pigments. Once again supernatant was discarded and an equal volume of sterile water was added. 400µl of the suspension was placed on sterile Whatman No. 40 filter paper supported by glass beads in a sterile plate. The Petri plates were kept in dark for about 2h to allow fusion of the microplasmodial population. SDM was then added underneath the filter papers for the growth of the macroplasmodium (Fig. 4.1.A).

4.1. C. Determination of mitotic stages

At intervals after fusion, synchronous Post-fusion mitosis (PFM) were observed and ethanol-fixed smears prepared from macroplasmodial explants were used to determine the mitotic stages using phase contrast microscopy (Fig. 4.1.B).

4.2 Treatment with various agents

The agents used in the present study were purchased from Sigma-Aldrich, U.S.A. The details of the preparation of stock solutions, working concentrations and treatment schedule are given in chapter 5 (experimental design). Following each drug treatment for 3h, macroplasmodia was given three 10 min washes in three aliquots of fresh SDM (without drug) to eliminate any carryover of drug.

4.3 UV-C Irradiation

For combination treatments with WM, a total UV dose of 1400 $J.m^{-2}s^{-1}$ and with CP, a dose of 243 $J.m^{-2}s^{-1}$ was delivered respectively, using a Philips germicidal lamp (30W), which emits approximately 90 % of its energy at 2537^{0}A. The dose rate was 5.1 $J.m^{-2}s^{-1}$ as determined by Potassium Ferri-oxalate Actinometry (Jagger, 1967).

4.4 Monitoring cell cycle related modulations

4.4.A. Cell cycle progression

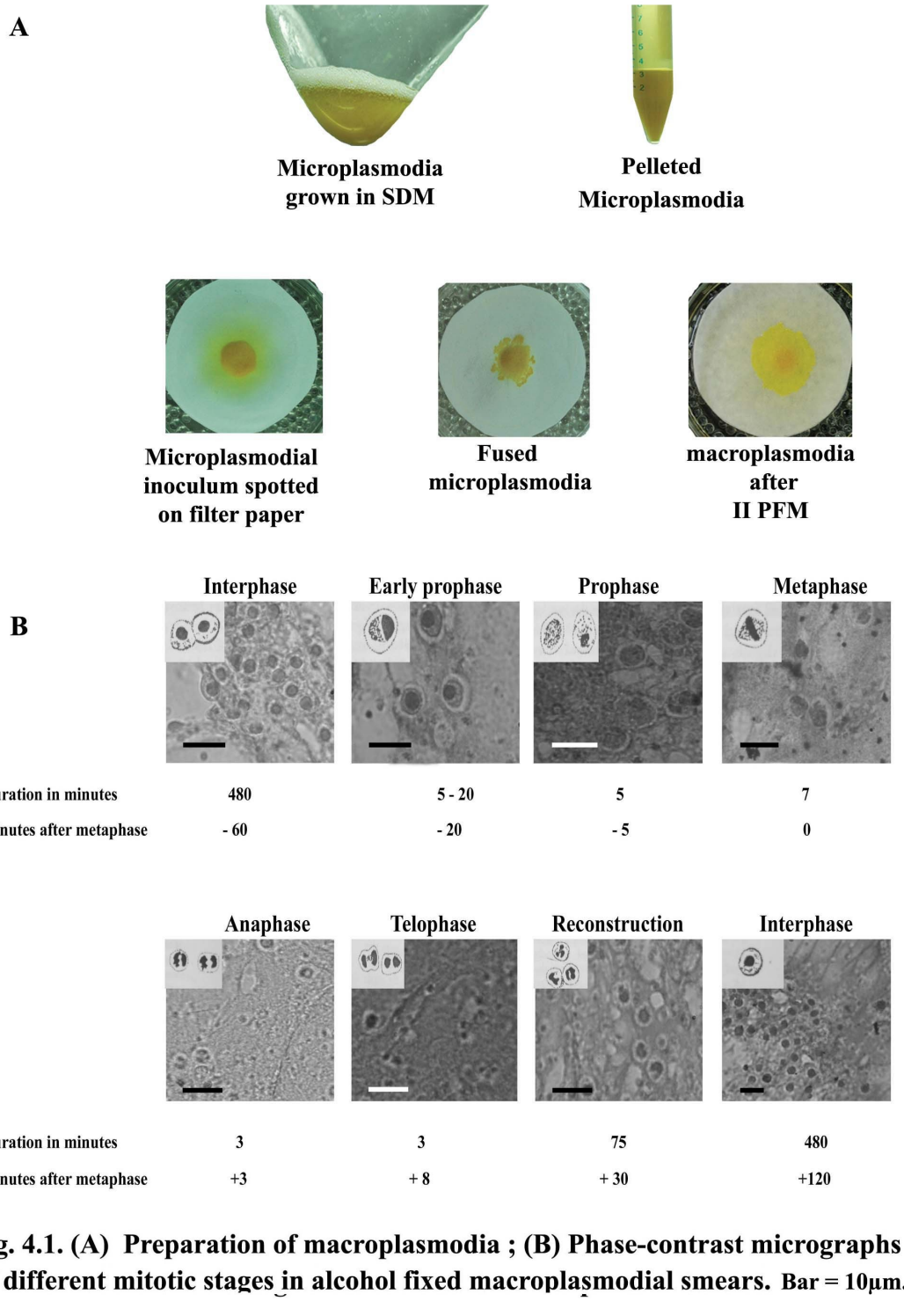

Fig. 4.1. (A) Preparation of macroplasmodia ; (B) Phase-contrast micrographs of different mitotic stages in alcohol fixed macroplasmodial smears. Bar = 10µm.

Cell cycle delays were monitored by observing the G2 - M transition. For this the mitotic timings after various drug treatments were noted with respect to the controls. The mitotic cycle between the second and the third PFM which had duration of 8 - 9h was used for various experiments described here because by then the plasmodia would be large enough to cut into the required number of sectors needed for the various treatments. This way a strict comparison of the mitotic timings in the various treated sectors of a single macroplasmodium can be made with its own control sectors.

For each experiment, a set of sister plasmodia were made from pooled microplasmodial suspension. On citing the metaphase of the second PFM, each plasmodium in a set of sisters was cut into a few equal sized sectors. One sector from each plasmodium served as untreated control and the others were transferred into appropriate drug containing medium. Following drug treatment, and the subsequent washes by serial changes in drug-free normal SDM, they were grown in fresh SDM till the third PFM was observed in them. Mitotic timings in the different treated sectors of a plasmodium were compared with that of the control sector of that plasmodium to see the effect of drugs on the progression of cell cycle.

4.4.B. FACS Analysis

Physarum being a syncytium, nuclear suspensions were used for FACS analysis instead of cell suspension. Nuclear pellets were isolated from treated and control sectors. The method used for isolation (Thiriet and Hayes, 2001) and staining of nuclei (Fry and Matthews, 1987) is outlined below.

A quarter sector of plasmodium was cut out and placed on sterile Petri dishes kept on crushed ice. The culture was then scrapped off with sterile scalpel leaving the inoculum. The scraped sample was collected in 500µl of Buffer A and homogenized thoroughly in a Potter-Elvejhem homogenizer. The homogenate was spun down at

2000 rpm for 10 min at 4^0C. The supernatant was discarded and the pellet was resuspended in 500µl of Buffer A, overlaid on 1ml of Buffer B (sucrose cushion) and centrifuged at 2000 rpm for 20 min at 4^0C. Supernatant was discarded and the creamy nuclear pellet was suspended in 1ml of 'washing solution' followed by centrifugation at 2000 rpm for 10 min. at 4^0C. The pellets were washed with ice cold PBS, fixed in 70 % ice-cold ethanol and finally resuspended in 500µl PI / Triton X100 staining solution (To 10-ml of 0.1 % (v/v) Triton X100 in PBS added 2 mg DNAse free RNAse A and 0.4 ml of 500 µg/ml PI). Following Incubation at 37^0C for 15 min, DNA content analysis was done according to manufacturer's protocol on BD FACS Aria™ using BD FACS Diva software version 5.0.2.

4.5 Genomic DNA integrity check

DNA integrity check was carried out to detect DNA laddering due to internucleosmal fragmentation in the G2 abrogated sample. For this, DNA was isolated from nuclei prepared as described above from the control and the treated plasmodia. 500µl of nuclear lysis buffer containing $1/20^{th}$ the volume of 2mg/ml proteinase K was added to the nuclear pellet and incubated at 70^0C for 15 min. After cooling to 37^0C, another $1/20^{th}$ volume of 2mg/ml proteinase K was added and incubated overnight at 37^0C. 1mg/ml RNAse ($1/10^{th}$ volume) was added and incubated at 37^0C for 2 h. Organic extractions were performed with equal volumes of tris buffer-equilibrated phenol (pH 8) followed by 1:1 mix of equilibrated phenol: chloroform/isoamyl alcohol (24:1) and finally with chloroform/isoamyl alcohol (24:1). DNA was then precipitated by adding $1/15^{th}$ volume of 3M-sodium acetate followed by 2 volumes of 100 % ethanol and mixed gently for the appearance of precipitate. The precipitate formed was then spooled out and washed with 70 % ethanol. Drained off the ethanol, air dried the precipitate and dissolved in 50ml of TE

(pH 8) (Burland, 1993). Solubilized nuclear DNA was then subjected to 1.2 % agarose gel electrophoresis at a constant voltage of 100 V.

4.6 Genotoxicity evaluation by comet assay

Comet assay was carried out to check the genotoxicity of various agents used for the study. The comet assay was performed essentially as described by (Singh et al., 1988) except for a slight modification in that instead of cell suspension a nuclear suspension was used. Briefly, nuclei isolated from the control and treated macroplasmodia as described above were subjected to alkaline gel electrophoresis followed by silver staining (Nadin et al., 2001). The slides were observed on a Leitz microscope (Dialux 20) and photographed using a Nikon D 60 SLR camera. Nuclei isolated from 5mM H_2O_2 treated macroplasmodia were taken as the positive control.

4.7 Protein profiling by SDS-PAGE

For the preparation of whole cell lysates, 7mm discs were punched out of the synchronous macroplasmodial surface cultures along with the supporting Whatman filter papers followed by rapid treatment with five volumes of ice cold acetone, incubated at -20^{0}C for 10 min and centrifuged at 12000 g for 5 min. The dried pellets were then directly solubilized in sample buffer, incubated in boiling water bath for 90 sec. For nuclear lysates, nuclei were isolated using the above mentioned procedure and were processed as described for cellular lysates. The samples were then analysed by SDS-PAGE (Laemmli, 1970) followed by monochromatic silver staining as described by Hames (1990).

4.8 Peptide - mapping

The bands of interest were excised from the silver stained gels with a sharp razor blade. The gel slices were destained with 1:1 solution of 30mM potassium ferricyanide and 100mM sodium thiosulphate briefly, rinsed with cold water, trimmed to 5 mm in size, and then soaked for 30 min in 10 ml of equilibration buffer (0.125M Tris-HCl, pH 6.8, 0.1 % SDS, and 1mM EDTA) with occasional swirling. The processed gel slices were finally placed in the sample wells of another gel (12.5 %) with a slightly longer than usual stacking gel. The sample wells were filled with the same buffer mentioned above and each gel slice was pushed to the bottom of a well with a spatula. Spaces around the slices were filled by overlaying each slice with 10µ1 of this buffer containing 20 % glycerol. Finally, 10µ1 of this buffer containing 10 % glycerol and a given amount of protease [Trypsin 10µg/ml, Chymotrypsin 100µg/ml (Sigma, U.S.A.)] was overlaid into each slot. Electrophoresis was performed normally except that the power was turned off for 40 min when bromophenol blue reached the bottom of the stacking gel to allow further digestion. Current was then turned on to complete the run (Rosenberg, 1996).

4.9 Western blot analysis

Following SDS-PAGE of *Physarum* protein samples, the gels were subjected to immunoblotting onto positively charged nylon membrane with a tank blotting unit (BioRad). After blocking with 10 % skimmed milk in Tris-buffered saline (100mM Tris-HCl, pH 7.5, 0.9 % NaCl), the membranes were incubated separately in monoclonal primary antibodies [mouse anti-p53(Zymed), anti p-Ser and anti p-Tyr (Sigma)] diluted with blocking buffer [1:200 for anti-p53 ; 1:700 for anti p-Tyr and 1:1000 for anti p-Ser] for Ih at room temperature. Following 5 washes with TBS (Tris-buffered saline) for 15 min, the membranes were incubated for 1h in secondary antibody (Goat anti-mouse IgG-ALP conjugate, Genei, Bangalore for anti-p53 and anti p-Ser, and rabbit anti-mouse IgG-ALP, Genei, Bangalore for anti p-Tyr) diluted

with blocking buffer (1:2000). Colour visualization following a repeat of TBS washes was carried out using the chromogenic substrate BCIP/NBT (Ausubel, 1995). Lysates from human lymphocytes cultured as described by Verma and Babu (1994) treated for 24h with 200µM H_2O_2 were used as positive control for immunostaining with anti-p53. Immunoblot of the *Physarum* proteins with anti-*Physarum* actin polyclonal antibody (1:5000 dilution) was carried out to stain actin, a standard house-keeping protein control.

4.10 Transcript profiling by differential display PCR

4.10.A. Isolation of total RNA using Tri® reagent

Macroplasmodial surface culture scraped out using sterile scalpel was homogenized thoroughly in 1ml of Tri reagent using a Potter-Elvejhem homogenizer. The homogenate was stored for 5 min at room temperature. Added 0.2ml of chloroform, mixed vigorously for 15 sec and stored at room temperature for 15 min. Following centrifugation at 12000g for 5 min at 4^0C, the aqueous phase was transferred to a fresh tube and RNA was precipitated by mixing with 0.5ml isopropanol. Stored the samples at room temperature for 5-10 min and centrifuged at 12,000 g for 8 min at 4^0C. Washed the pellet with 80 % ethanol, spun at 7,500 g for 5 min at 4^0C, briefly air-dried the RNA pellet for 3 - 5 min and dissolved in sterile double distilled water for subsequent analysis. RNA quantitation was done by spectrophotometry.

4.10.B. DNase I treatment

To a 1.5 ml microcentrifuge tube, added 60µg total RNA, 5µl 2.5X of DNase I buffer, 2.5µl RNasin of 40U/µl, 20.3µl of RNase free DNase I (1000U/ml), and 12µl of 25mM $MgCl_2$. Brought to 50µl with nuclease-free sterile water and mixed gently. The reaction mixture was incubated for 30 min in a 37^0C dry-bath and the RNA was

purified by two extractions with Phenol:CIA and CIA. Added 1/15th volume of 3M sodium acetate and mixed well. RNA was precipitated by adding 3 volumes of cold ethanol. Stored at -20^{0}C and centrifuged at 20,000 g for 30 min at 4^{0}C. Ethanol was discarded and the pellet was washed twice with 300 µl of cold 70 % ethanol solution. Following centrifugation at 20,000 g for 15 min at 4^{0}C, ethanol was discarded and the pellet was dried. The RNA was resuspended in nuclease-free sterile water to give a final concentration of 0.5µg/µl.

4.10.C. First strand cDNA synthesis

To each 0.2ml microcentrifuge tube, added 1µl 10mM dNTP mix, 1µl of respective oligo-dT anchored primers (oligo-dT(12)AC, oligo-dT(12)CG, oligo-dT(12)GG , oligo-dT(12)GC, oligo-dT(12)AG , oligo-dT(12)CC) of 25mM, 1µl of 0.5µg/µl DNase treated RNA template and made upto 10µl with nuclease free sterile water. Mixed gently and briefly centrifuged. The reaction mixture was incubated at 70^{0}C for 10 min and placed on ice. Added 2µl 10X M-MLV reverse transcriptase buffer (Sigma, U.S.A.), 1µl M-MLV reverse transcriptase, 0.5µl RNasin and made upto 20µl with sterile nuclease free water. After incubation at 37^{0}C for 50 min, the reaction mixture was heated to 94^{0}C for 10 min. The reaction was stored on ice for subsequent PCR reaction.

4.10.D. DD-PCR Amplification

To a 0.2µl microcentrifuge tube, added 1.25µl of cDNA synthesis reaction, 2µl 2.5 mM mixed dNTPs, 2.5µl 10X Taq DNA Polymerase buffer, 2.5µl 25mM (250 ng/reaction) anchored oligodT primer, 4µl 6.25mM (100 ng/reaction) 10-mer arbitrary primer (RFuB#1), 0.3µl Taq DNA Polymerase (3U/µl) and brought to 25µl with nuclease-free sterile water, mixed and briefly centrifuged. PCR reaction was performed as follows: 94^{0}C for 5 min, 30^{0}C for 2min, 72^{0}C for 2 min (1 cycle); 94^{0}C for 1 min, 30^{0}C for 2min, 72^{0}C for 1 min (45 cycles); 94^{0}C for 1 min, 30^{0}C for 2min, 72^{0}C for 10 min (1 cycle). PCR reactions were run on 1.2% agarose gel with

ethidium bromide as stain (Boschi and Vergara, 1998). The bands of interest were excised using a clean razor blade and eluted for reamplication using Fermentas (Genetix Biotech Asia) gel extraction kit. The reamplified PCR products were checked on agarose gels once again to confirm their molecular weights and a select few of these validated products were sequenced (SciGenom Labs Pvt.Ltd., Kochi).

5. EXPERIMENTAL DESIGN

5.1 Treatment with various DNA damaging agents

The design of the various experiments carried out in the study has been given in Fig. 5.1. Mitotically synchronous plasmodium (circular representation) was cut into sectors that were subjected to various DNA damaging agents treatments (agents/irradiation) denoted by the colour code on the right. The horizontal bar represents cell cycle duration in hours between II PFM (post fusion mitosis) and III PFM (post fusion mitosis) with subdivisions denoting 1h duration. In combination treatments with UV (pretreatment - UV irradiation followed by treatment with the agent or post treatment - treatment with the agent followed by UV irradiation), a two color code has been employed. Arrows indicate time of treatment with the DNA damaging agents and sample collection.

Table 5.1. Concentration of DNA damaging agents used in the study.

Agents used	Working concentration	Stock concentration	Solvent used
Arsenic trioxide	5-500µM	100mM	1N NaOH
Capsaicin	25-500µM	20mM	DMAO
Chlorambucil	10-500µM	100mM	DMSO
Wortmannin	10µM	1mM	DMSO

The schematic representations show the treatment schedule with respect to the various agents - AR (Fig. 5.1.A), CP / UV (Fig. 5.1.B & C), CHL (Fig. 5.1.D) and WM / UV (Fig. 5.1.E & F). Illustration of differential display polymerase chain reaction (DD - PCR) to identify differentially - expressed genes has been given in Fig. 5.1.G.

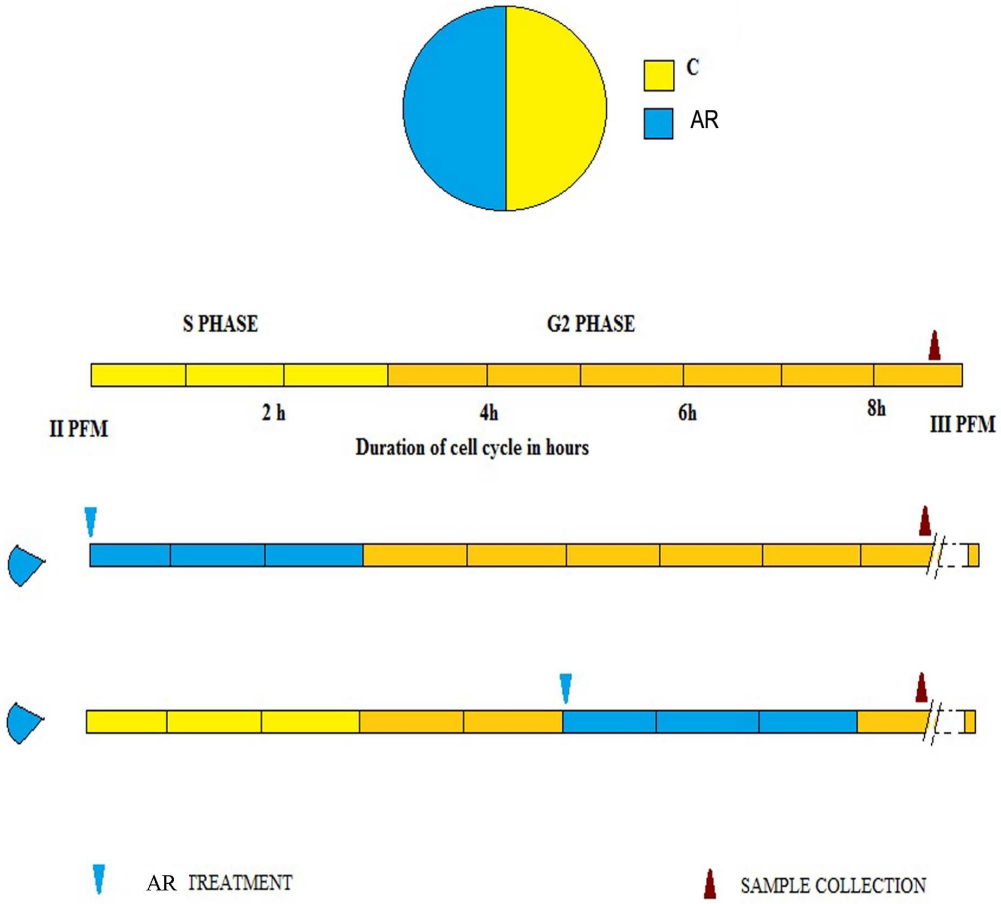

Fig. 5.1. A. Treatment schedule for Asenic trioxide

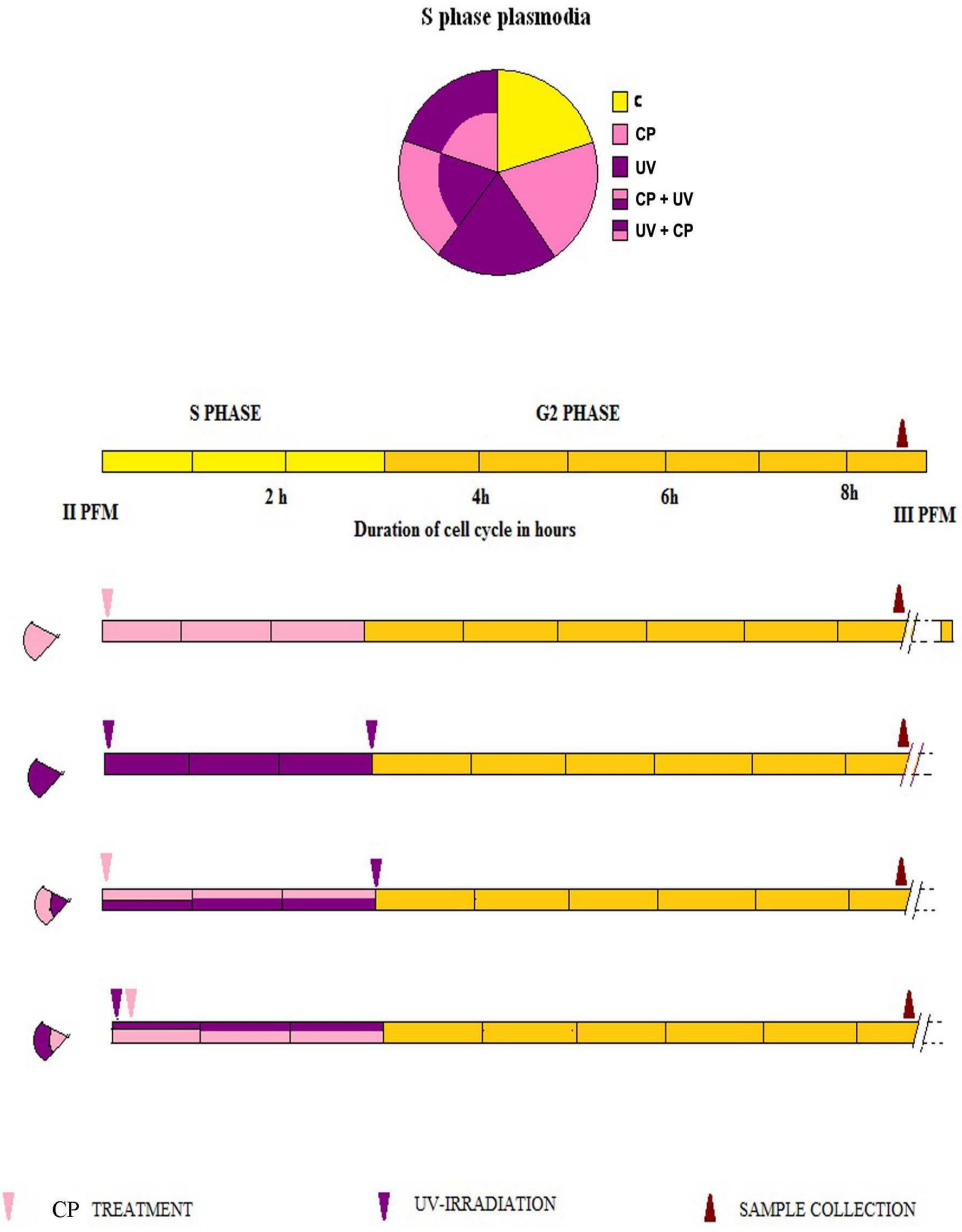

Fig. 5.1. B. Treatment schedule for Capsaicin and / or UV (S phase)

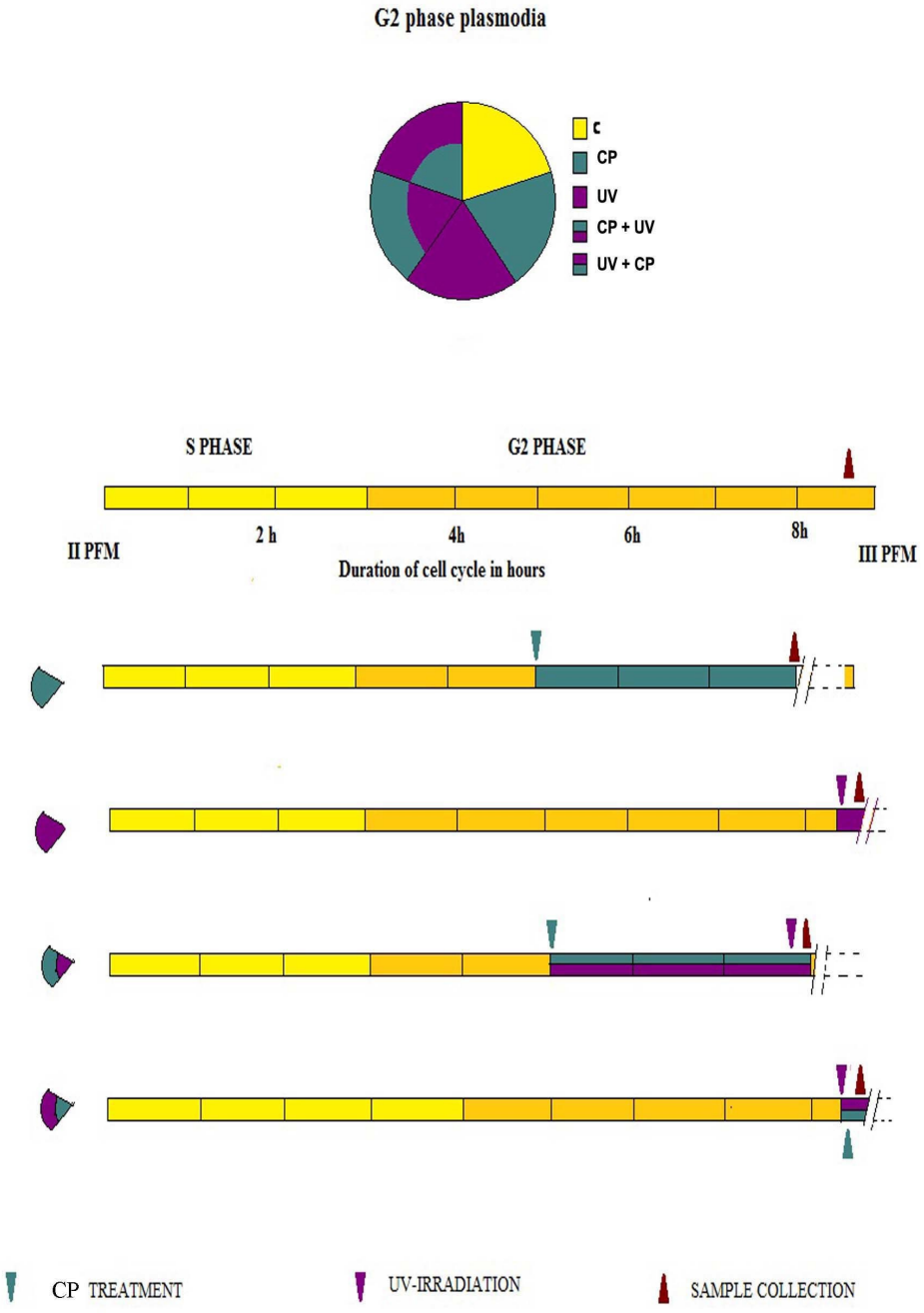

Fig. 5.1. C. Treatment schedule for Capsaicin and / or UV (G2 phase)

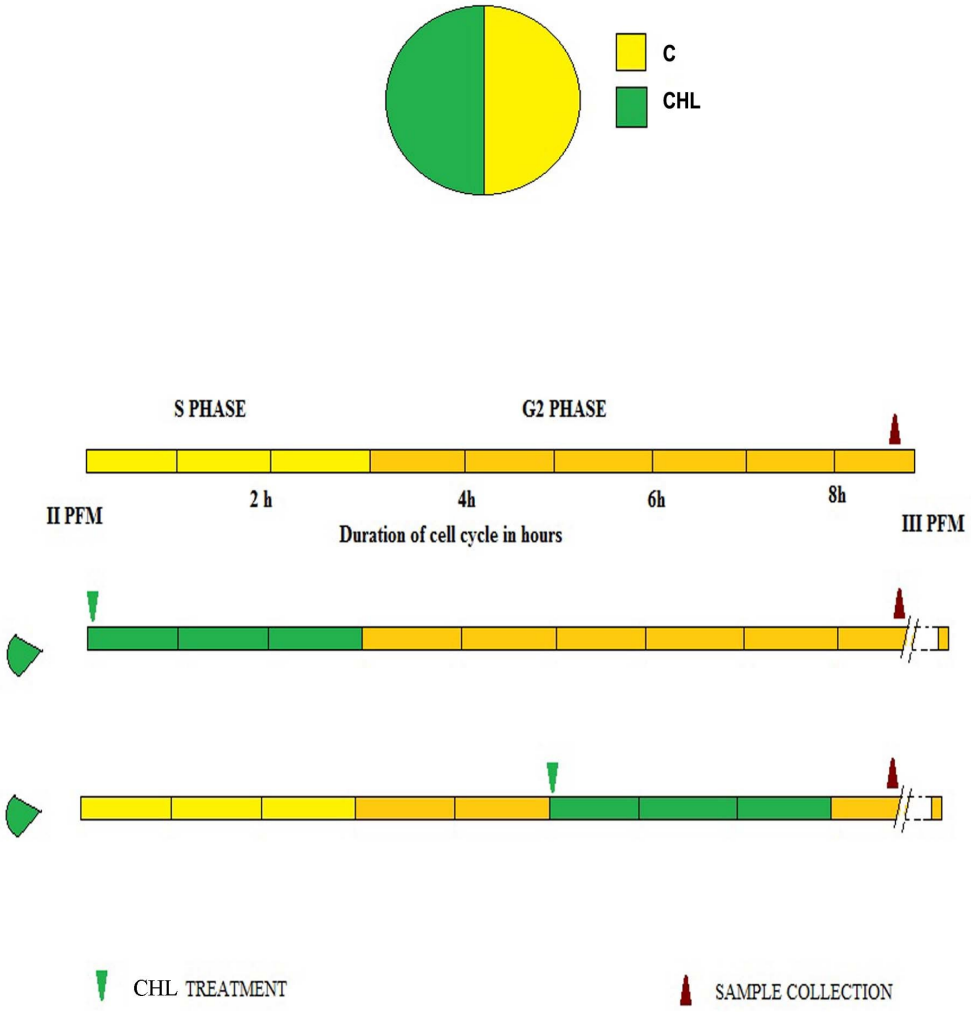

Fig. 5.1. D. Treatment schedule for Chlorambucil

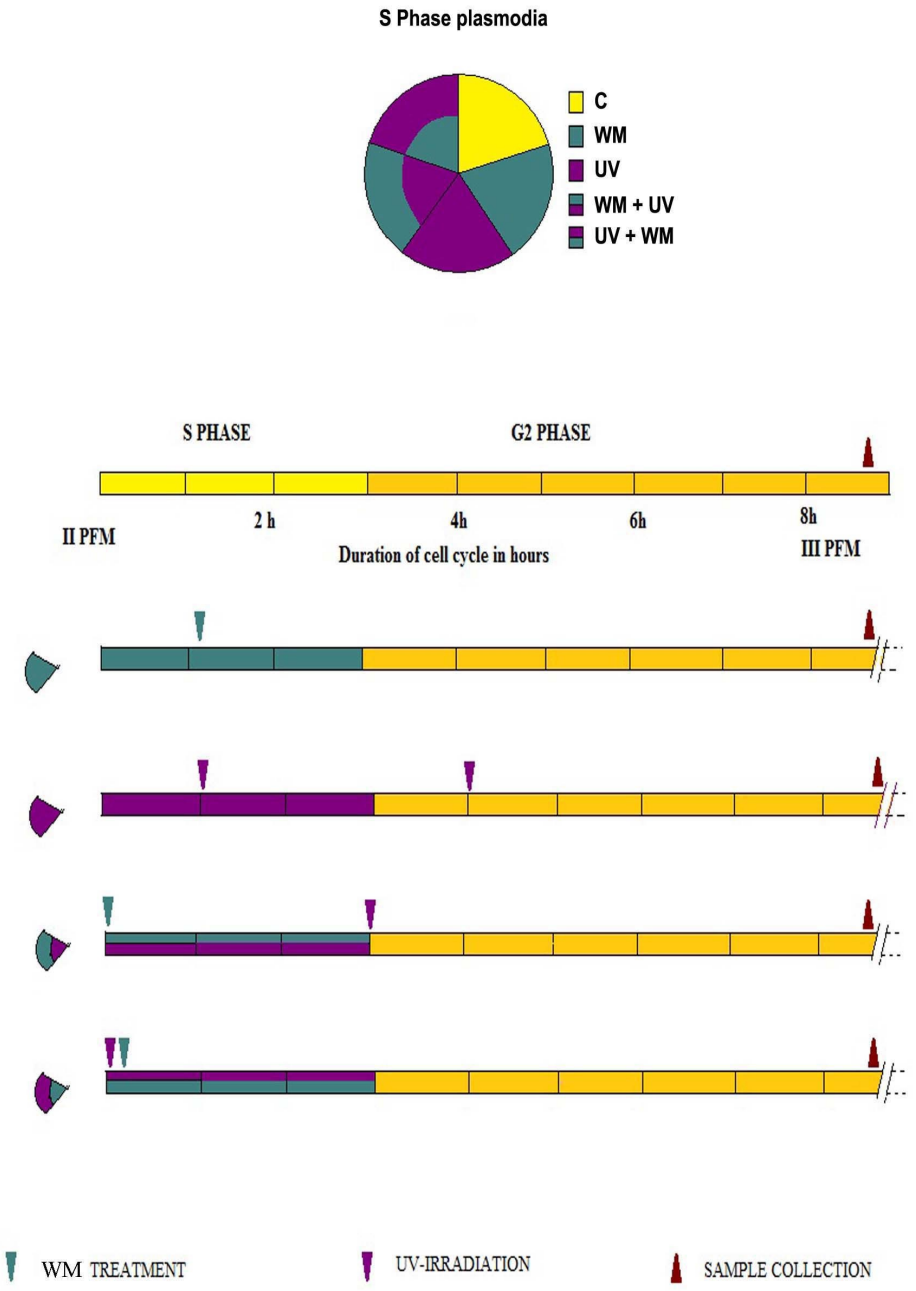

Fig. 5.1. E. Treatment schedule for Wortmannin and / or UV (S phase)

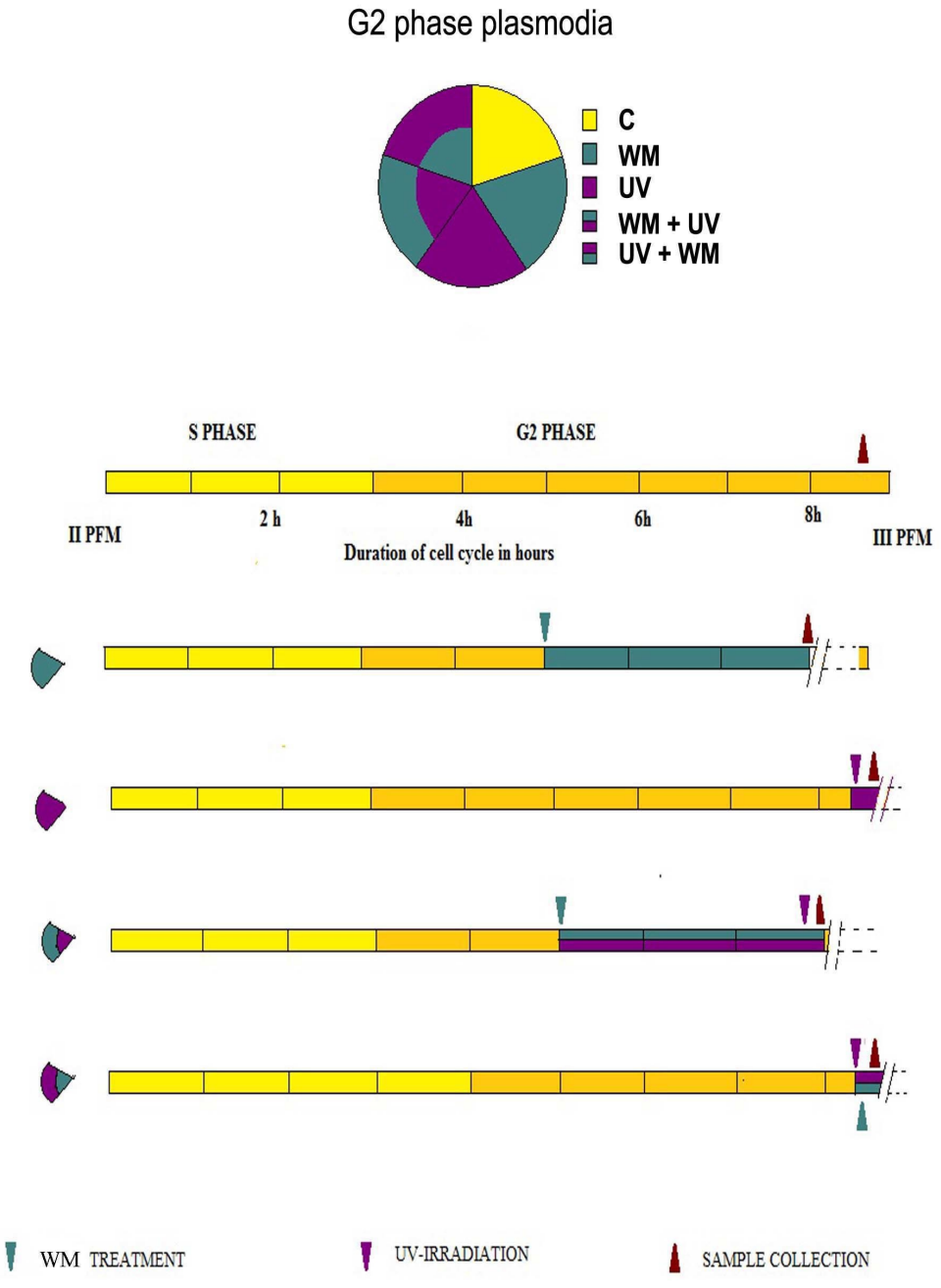

Fig. 5.1. F. Treatment schedule for Wortmannin and / or UV (G2 phase)

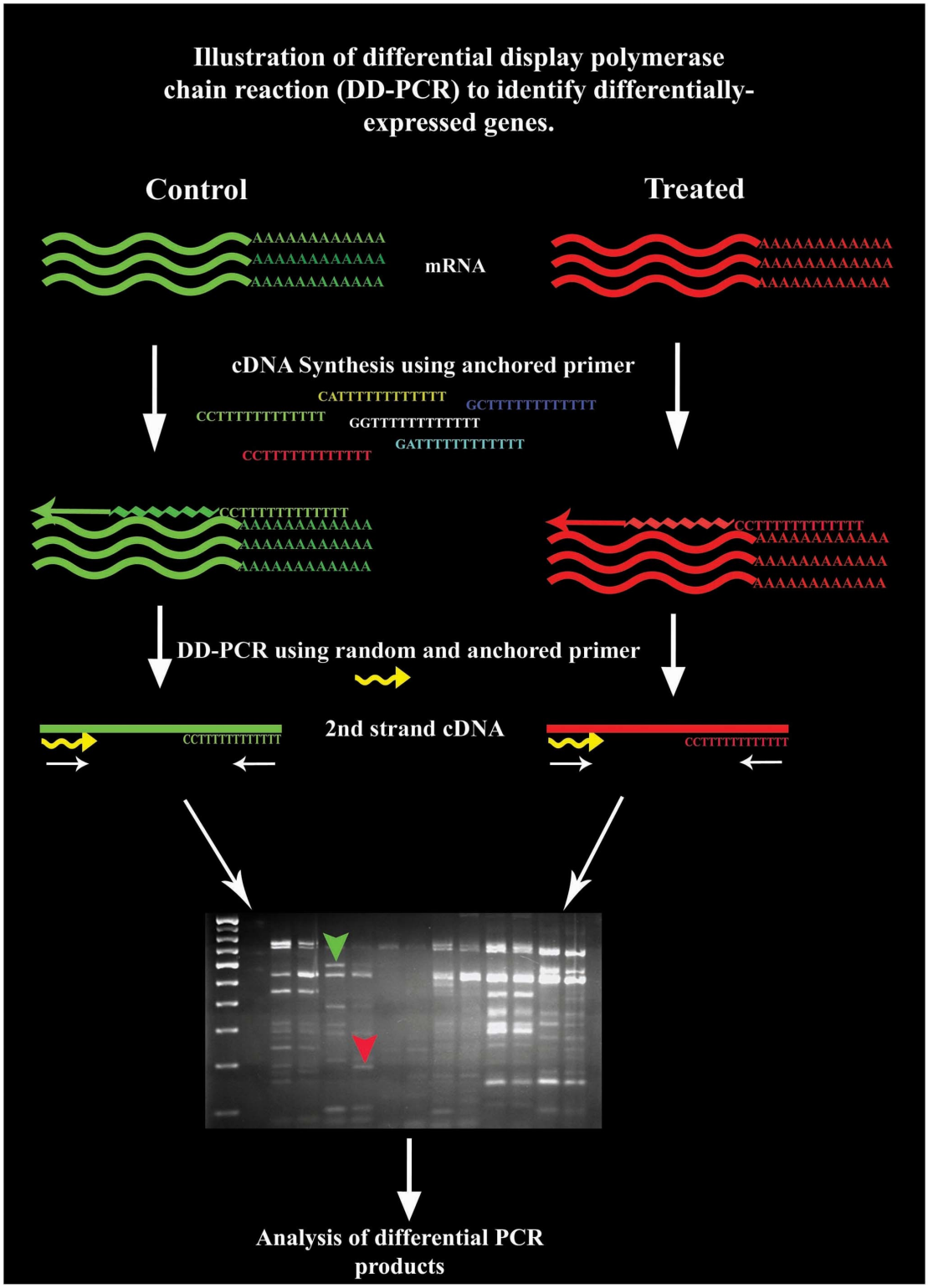

Fig. 5.1. G. Schematic representation of DD - PCR

6. RESULTS AND DISCUSSION

The results have been categorised to enable a comparison of the effects of the various agents, namely, AR, CP, and CHL. The effect of WM on cell cycle modulations were also investigated since it potentiates DNA damage by abolishing checkpoint activation. Therefore, experiments with WM were carried out using UV-C radiations to induce DNA damage and G2 arrest. In the case of CP, the modulatory effects obtained were suggestive of only minimal damage. Hence, combination treatments with low dose UV-C radiation were also employed to better dissect out the action of this agent.

The cell cycle modulatory effects of the above mentioned agents, in terms of cell cycle progression have been presented and discussed. In the cellular level study, the delay (G2 arrest) / advancement in G2-M transition was monitored by phase - microscopy. This was followed by the analysis of total nuclear DNA content by FACS as well as comet assays to assess the genotoxicity of the agent.

Molecular studies carried out at the level of DNA included checking the integrity of genomic DNA by agarose gel electrophoresis and protein level studies such as protein profiling by SDS-PAGE, peptide mapping and immunostaining of western blots. These studies were finally extended to the level of RNA, where analysis by transcript profiling - as evidenced by DD-PCR - following treatment with various agents was also carried out.

6.1 Cell cycle modulatory effects of DNA damaging agents

The results of the cell cycle modulatory effects of the DNA damaging agents - AR, CP and CHL discussed below have been shown in Figure 6.1.A – C. The experimental details have been described in 'Materials and Methods' (Chapter 4) and the treatment schedule has been depicted in 'Experimental Design' (Chapter 5).

6.1.A. Arsenic trioxide

The concentration range tested was from 5- 500µM. Low doses upto 50µM at S phase had little or no effect on cell cycle progression. From a marginal sensitivity to the compound at 100µM eliciting a mitotic delay of about 30 min (~ 6 % of cycle duration), a 6-fold increase (~33 %) in delay was observed at 200µM. At 500µM another 2.4 fold increase in delay was observed which amounted to about 80 % of total cell cycle duration (Fig.6.1.A). Lehmann and McCabe (2007) have demonstrated that the slow S phase progression in U937 cells is due to arsenite-dependent inhibition of Cdc25A. It has also been shown that AR treatment at 1µM concentration, substantially inhibits Cdc25A gene transcription inducing S phase arrest in AS4.1 cells (Han et al., 2007). Hence, the enormous delay observed by us in *Physarum* is attributable to the inactivation of Cdc25A homologue which normally activates the CDKs in S and G2 phases.

The threshold for AR sensitivity in G2 phase was found to be about 20-folds lower compared to that of S phase. At 5µM, 30 min delay (6 % of cycle duration) elicited remained unaffected up to a concentration of 50µM. At 100µM, a 2-fold increase (~13 %) and at 200µM a further 3-fold increment in delay was obtained. However, at 500µM, higher delay amounting to ~ 61 % of cell cycle duration was observed. In other words, sensitivity to AR in G2 was found to be greater at lower concentrations compared to that in S phase. On the other hand, in terms of magnitude, however, mitotic delays were maximal during S phase at higher concentrations. *In vitro* studies in human cancer cells such as pulmonary adenocarcinoma-Calu-6 and lung cancer-A549 cells showed arsenite-induced

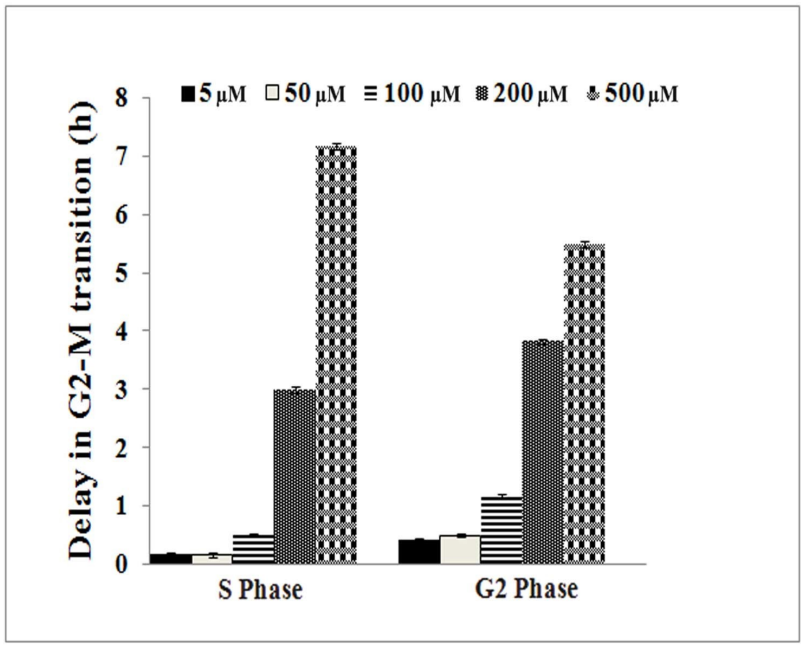

Fig. 6.1. A. Cell cycle modulatory effects of Arsenic trioxide

inhibition of CDK-cyclin complexes resulting in G1 and G2-M arrest. Although evidence indicates a potential role of p53 in AR-induced cell cycle arrest, results have been shown to be rather variable. A new GADD45α isoform, GADD45α1, known to be expressed under stressful growth conditions and in response to DNA damaging agents, was reported recently in response to AR treatment (Flora, 2011).

AR induced DNA damage has been proposed to occur mainly as a result of oxidative damage due to ROS production such as $O_2^{\cdot-}$, H_2O_2 and $^{\cdot}OH$ which can lead to both ssDNA and dsDNA breaks, cross-links, DNA adducts and chromosomal aberrations (Halliwell, 2007; Kitchin and Wallace, 2008). The extent and nature of damage is also dependent on the cell cycle phases (Liu et al., 2001; Shi et al., 2004). McCollum et al (2005) has reported that arsenite treatment in U937 myeloid leukemia cells increases the time spent in each phase of the cell cycle in addition to slowing down transit through traditional checkpoints. Sidhu et al (2006) have also demonstrated a dose-responsive delay in cell cycle progression in all cell cycle phases induced by AR in primary embryonic neuroepithelial cells.

6.1.B. Capsaicin

CP was found to exert distinctive cell cycle modulatory effects that were observed to be phase-specific and concentration-dependent [Fig.6.1.B(i)]. The concentrations tested ranged from 25-500µM. Early S-phase treatment elicited a shortening effect on the total cell cycle duration which peaked at 250µM with advancement in the G2-M transition 1h (9.3 % of cell cycle duration) earlier than in the respective control. At 500µM, however, this effect was found to be reversed resulting in a marginal delay of about 40 min. Treatments given at G2, evoked increasing delays with a maximum of 2.5h (28 %) obtained at 500µM.

There have been previous reports on shortened cell cycles. In *Physarum*, treatment with ethanolic extract of *Bacopa monniera* (Brahmi) resulted in a shortened cell cycle (Venu et al., 2003). Shorter than normal mitotic cycles have been observed

in *Physarum* plasmodia after the first UV-induced delayed mitosis, as a response to balance the disturbed nucleo-cytoplasmic ratio due to the breakdown of nuclei induced by radiation (Sachsenmaier et al., 1970). Over-expression of mitotic cyclins has also been shown to bring about advancements in the timing of mitosis in yeast (Alberts, 2002).

In this context, it is pertinent to note that although there are reports on CP induced G0/G1 arrest in various cell lines which finally lead to delayed G2-M transition (Chen et al., 2012; Ip et al., 2010; Tsou et al., 2006), the lack of G1 phase in *Physarum* cell cycle obviates discussion on these lines. However, in human esophagus epidermoid carcinoma CE 81T/VGH cells, CP treatment decreased the levels of cdk4, cdk6, and cyclin E and increased the levels of p53 and that of p21 leading to G2/M arrests (Wu et al., 2006).

To further explore the cell cycle shortening effect of CP during S phase, combination treatments with a physical agent - UV-C radiations at low dose - was employed [Fig.6.1.B(ii)]. UV-C pretreatment and post treatments in S-phase with 250µM CP showed a slight advancement of 20 min and a slight delay of 10 min in cell cycle respectively, when compared to UV-C irradiated control. But with 500µM concentration, pre/post-treatments resulted in approximately 1h 20 min delay compared to that in UV-control. However combination treatment in G2 phase resulted in delay with both concentrations compared to UV-C control. Pretreatment and post treatment with 250µM CP resulted in approximately 3h and 40 min delay respectively, whereas pre and post treatments at 500µM concentration resulted in approximately 4h and 2h delay. A critical analysis of this data leads to the inference that the cell cycle shortening effect of CP at 250µM is confined only to S phase. This effect is retained even in combination treatment, when CP is given prior to UV-irradiation. In G2, on the other hand, CP, given alone or in combination elicits only cell cycle delays which were found to be concentration dependent.

(i)

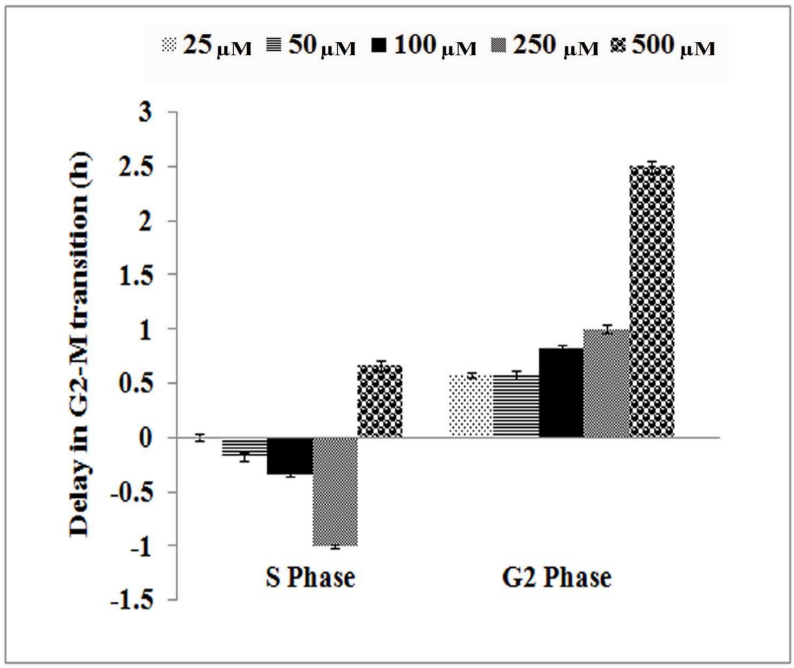

(ii)

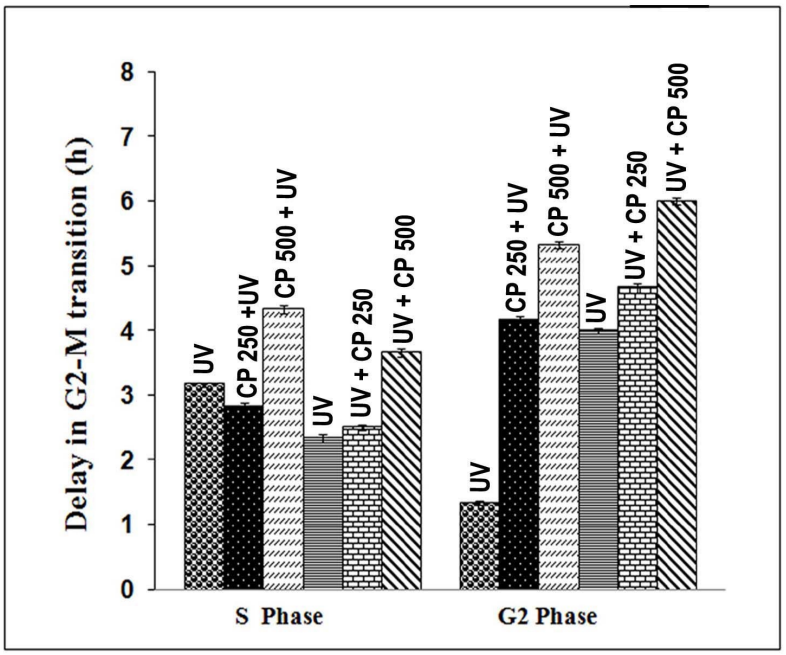

Fig. 6.1. B. Cell cycle modulatory effects of (i) Capsaicin and (ii) UV + / - Capsaicin

6.1.C. Chlorambucil

In the concentration range tested from 10-500µM, CHL treatment elicited phase-specific and concentration-dependent effects (Fig.6.1.C). Significant delays were obtained in S phase from 100µM onwards eliciting 1h delay (11 % of total cell cycle duration) upto more than 7h (81 %) at 500µM. This is in agreement with the few reports available on the cellular effects of CHL. Treatment of HeLa cells in G1 have not been shown to affect progression into S phase. However, upon entry into S phase, a marked dose-dependent inhibition of the rate of DNA synthesis was observed which was accompanied by prolongation of the S phase and a corresponding dose-dependent mitotic delay (Roberts, 1975). CHL treatment of A2780 cells further was shown to bring about cell cycle arrest in S phase followed by apoptosis (Boldogh et al., 2001).

CHL treatment in G2 phase of *Physarum* led to a tapering of cell cycle delay to about 50 % of that observed in S phase. This observation is in partial agreement with an earlier report, where HeLa cell treated with CHL during G2 phase of the cell cycle did not induce any delay or block in the next mitosis, but did inhibit the rate of DNA synthesis in the following cell cycle in a dose-dependent manner. This depression of DNA synthesis was followed by a delay in the next mitosis (Roberts, 1975). A2780/100 cells have also been employed to demonstrate a transitional G2/M arrest and survival following CHL treatment (Boldogh et al., 2001).

6.1.D. Wortmannin

In addition to the above mentioned DNA damaging agents, the cell cycle modulatory effect of a DNA damage potentiator, WM was also investigated. The dose of 10µM was employed as reported in earlier work with this fungal metabolite radiosensitizer known to act by targeting checkpoint pathways. In this case, a high dose of UV-C radiations were used to induce DNA damage and G2 arrest.

WM treatment elicited cell cycle phase specific effects (Fig. 6.1.D) in S and G2 phase where cell cycle delays of 2.5h and 45 min were observed respectively in comparison with untreated controls. Human colorectal adenocarcinoma cells (SW480 ACC) exposed to WM have been reported to be blocked mainly in G1 as a consequence of inhibition of p110α subunit of PI 3 kinase known to be involved in progression through G1 to S (Rosenzweig et al., 1997). At the concentration used (10μM) for the study, WM is known to non-specifically inhibit PI 3 kinase, which has been shown to induce S phase entry (Stein, 2001). Since *Physarum* cell cycle lacks G1, the treatment given at the end of mitosis coincides with S phase entry. Inhibition of PI 3 kinase pathway during S phase leading to G2 arrest (Shtivelman et al., 2002) and reduction in DNA synthesis in mesangial cells following PI 3 kinase inhibition (Mahimainathan et al., 2005) has been reported earlier. Hence the 2.5h cell cycle delay observed by us might be a consequence of either or both of the above-mentioned possibilities. This also offers a logical explanation to the shorter delay of 45 min observed in G2 treatment with WM as the process of DNA synthesis is over prior to treatment. However, G2-M transitory period within 20 min of metaphase was found to be refractory to WM. WM treatment in G2-M transitory period (within 20 min of metaphase) did not elicit any mitotic delay. This result is in agreement with earlier work on *Physarum* that has established that the transition point (TP) beyond which mitosis cannot be blocked by several cell cycle perturbing agents lies at 20 min before metaphase (Nair, 1995).

The UV-sensitizing effect of WM was clearly evident in S phase eliciting an additional delay of 1h 20 min and 30 min for pre-treated and post-treated categories respectively over the 9h delay observed in UV treated controls. In glioblastoma cells pre-treatment with WM has been reported to reverse UV-induced S phase arrest through inhibition of DNA-PK (Park et al., 1999). In such a situation, failure of DNA repair in S phase should lead to G2 checkpoint activation and G2 arrest to facilitate

repair. Hence, increased delays observed by us in UV-irradiated plasmodia pre/post-treated with WM during S phase is indeed the expected outcome. However, such treatments in G2 phase did not elicit any additional delay other than the 9h G2-arrest observed in control samples treated with UV radiations alone. The modulatory effect of WM was strikingly evident at the G2-M transition period in the post-treated category, when UV-irradiation was carried out 20 min prior to metaphase. The phenomenon of 'G2 checkpoint abrogation' was clearly evident in that the 9h UV-induced delay was drastically reduced to a mere 38 min. WM and caffeine are well known inhibitors of PIKK family including ATM, ATR and DNA-PK (Hanasoge and Ljungman, 2007; Kawabe, 2004). ATM and ATR are proximal kinases of DNA damage signaling pathways that link DNA damage repair, arrest of cell cycle progression and triggering of apoptosis. Inhibitions of ATM and ATR are known to contribute significantly to checkpoint inhibition and/or G2 abrogation (Abraham, 2001; Anderson et al., 2003). Our results clearly show that WM-induced overriding or abrogation of G2 checkpoint in *Physarum* only occurred in the post-treated category when UV-irradiation was carried out during a narrow time period of about 5 - 10 min prior to TP (Fig. 6.1.D, G2 phase). Interestingly, a similar effect by caffeine, the first G2 abrogator to be identified, has already been reported earlier in this organism (Jayasree and Nair, 1991). Putting forth an explanation as to why the 'G2 abrogating effect' in *Physarum*, is confined to this narrow time zone, in post-treated samples and its complete absence in the pre-treated category would require additional data on the different molecular events occurring at this time point. A detailed probing to dissect out this subphase of G2 should be rewarding.

6.2 Nuclear DNA estimation by flow cytometry

The effect of the various agents used in the study on total nuclear DNA content was analysed using flow cytometry of nuclei isolated from the control and

treated macroplasmodial cultures. The treatment schedule and the method of isolating synchronous nuclei and staining with propidium iodide have been given in Chapter 4 & 5 respectively. In the case of treated samples, only those which elicited maximal mitotic delays were processed for flow cytometry.

Nuclear samples from untreated control plasmodial cell cultures collected at different time points - early S, late S, early G2, mid-G2 and late G2 - have been employed to ensure precision in DNA estimations with respect to the treated samples. Figure 6.2 shows the results of DNA content analysis by flow cytometry. The main peak with its mode in fluorescence 50 representing the majority (>70%) of the synchronous nuclei was employed for computing nuclear DNA content of the treated samples with respect to controls. The minor second and third peaks with modes around channel 100 and 150 values corresponding to higher 'mixoploidies' is in line with the pattern reported earlier for the *Physarum* strain used in this study (Kubbies and Pierron, 1983).

Expectedly, the DNA content in controls increase in samples collected at early through late S. It may be pertinent to mention here that the replication of ribosomal DNA genes of *Physarum*, which exist as large palindromic extrachromosomal elements, is confined to the last two-thirds of S phase and all of the G2 phase. About 150 rDNA molecules, each 60 kb in size, are known to be present in each nucleus. Hence the increase in nuclear DNA continues into G2. This is in agreement with earlier work reported in *Physarum* (Hardman, 1986). A small decrement of about 5 % in nuclear DNA in control samples collected at very late G2 close to G2-M transition was observed. This is attributable to the reduced PI uptake due to commencement of chromatin condensation at this time in cell cycle as reported earlier (Freeman and Rayburn, 2004; Mazzini et al., 1983) (Fig. 6.2.A).

In S phase, all samples, excepting WM and CP-treated, showed a decrease in their nuclear DNA content when compared to their respective controls (Fig. 6.2.B).

UV-treated samples showed the lowest DNA content (42 %) followed by that observed in CHL (48 %) and AR (49 %) treated samples. DNA content of WM (55 %) and CP (57 %) treated samples were found to be comparable to that found in late G2 controls (57 %). Interestingly, the magnitude of delay induced by the agents exhibits a strong correlation with the reduction in nuclear DNA content. Taken together, these results indirectly demonstrate the usefulness of DNA content estimation by flow cytometry to infer the phase of cell cycle affected by respective treatments obviating the need for isotopic or non-isotopic labelling of DNA for estimation purposes.

In G2 phase treated samples, DNA content comparison with that of controls also aids to infer the cell cycle phase affected by various treatments (Fig.6.2.C). Unlike that possible with respect to S phase treatment, the magnitude of delay obtained in G2 phase treatments was not found to be proportional with reduction in nuclear DNA content since at this phase the mitotic delays induced may be due to reasons other than DNA synthesis *per se*, such as DNA repair, inhibition of transcription, translation and post translational modifications.

6.3 Comet assay

For comet assay, nuclear pellets were isolated from samples collected immediately after respective treatments with the various agents at the highest concentration tested during S phase. For UV-irradiated samples, collection was done after 3h of irradiation at the maximal dose. Nuclear comets were observed only for AR, CHL and UV treatments; WM and CP treatments, however, failed to induce nuclear comets (Fig. 6.3). Genotoxicity of AR as evidenced by comet assay has been reported in various cell lines such as HaCa T keratinocytes (Udensi et al., 2011), human colon cancer cells (Stevens et al., 2010), human hepatic cancer cells (Yoo et al., 2009), Jurkat T lymphoma cells (Yedjou and Sutton, 2008), human leukemia cells

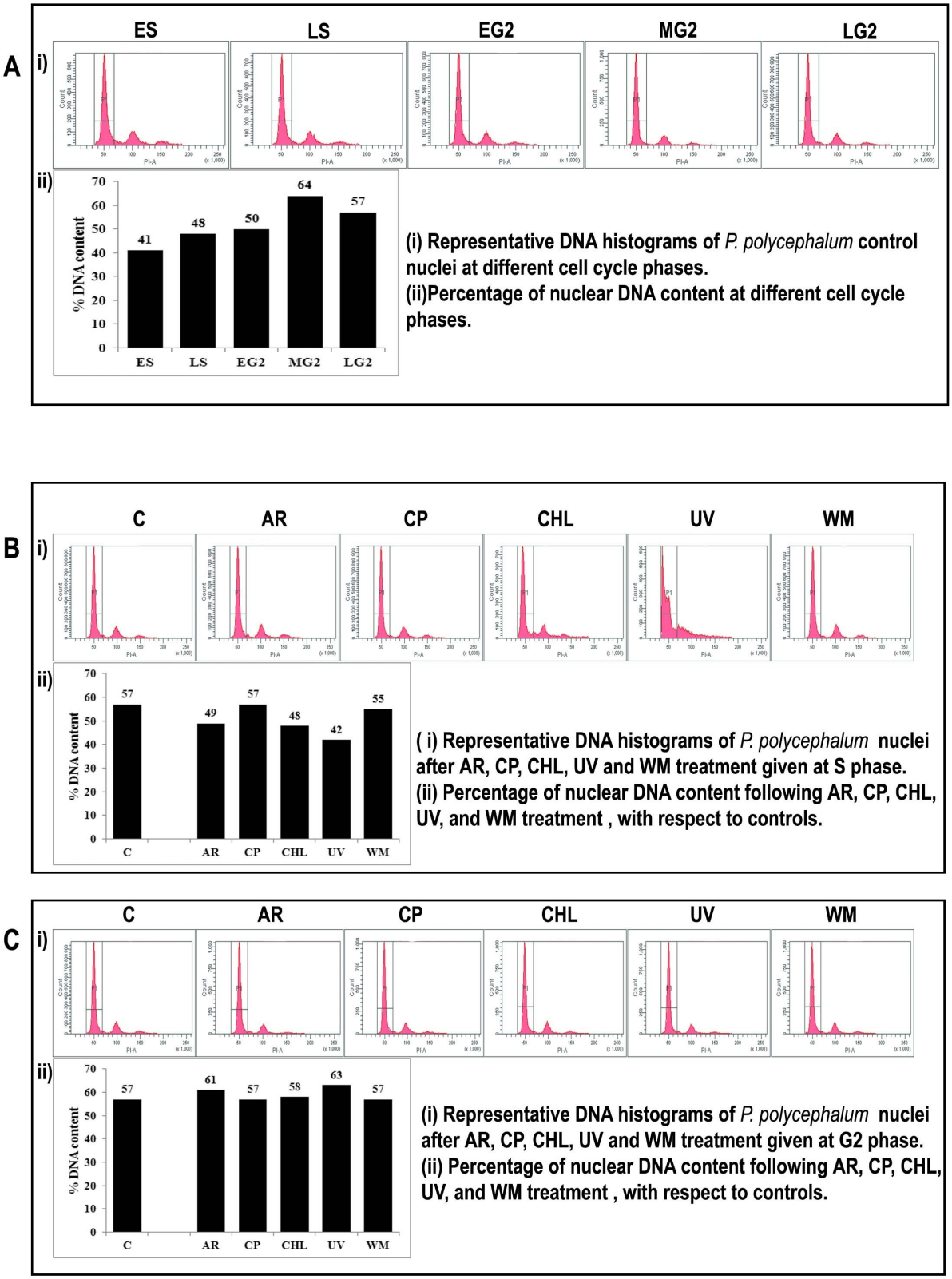

Fig. 6.2. Nuclear DNA estimation by FACS

(Yedjou and Tchounwou, 2007), human melanocytes and dendritic cells (Graham-Evans et al., 2004). UV and CHL induced genotoxicity in cell lines has also been reported earlier (Cipollini et al., 2006; Kawaguchi et al., 2010; Mughal et al., 2010).

6.4 Genomic DNA integrity check

G2 abrogation in cycling cells is usually accompanied by an inevitable mitotic catasptrophe and or apoptotic induction (Vakifahmetoglu et al., 2008; Chen et al., 2011; Chen et al., 2012). Hence, the integrity of the DNA isolated from UV/ WM treated - G2 abrogated and control macroplasmodial samples was checked on agarose gels. A ladder-like pattern was distinctly observed below the intact genomic band with a background of DNA smear below about 3 kb extending down all along the lane. Though discrete bands observed were suggestive of DNA fragmentation akin to the hallmark DNA-laddering that is associated with apoptosis caused by internucleosomal DNA cleavage, the banding, however, was not found to occur at a regular difference of 200 bp between them. Fragments covering a range of 200 bp to 2 kb were obtained (Fig. 6.4). The intensity of the fragments was found to be higher in UV-irradiated and G2 abrogated samples. The low-level smearing in the control samples may be explained away by the fact that in the multinucleate system a small percentage of damaged and or polyploid nuclei are turned-over. Upto 40 % of such pycnotic nuclei have been reported in UV-irradiated *Physarum* macroplasmodial cultures (Devi and Guttes, 1972).

DNA is prone to breakage at certain sensitive sites due to external factors such as nicking by phenol, salt concentration of the buffer used for DNA solubilization etc. Hence, to eliminate artifacts caused by these factors, DNA was isolated by procedures with and without phenol extraction, dissolved in buffers with different salt concentrations. The fragmentation pattern remained unchanged with different methods of DNA isolation or when DNA was dissolved in buffers containing

different salt concentrations. In control sample DNA fragments were less intense. It is relevant to note here that *in vitro* fragmentation of mitochondrial DNA related to macroplasmodial senescence has been reported in *Physarum* (Abe et al., 2000). The possibility of similar processes occurring in aged nuclei in the macroplasmodia needs to be ascertained by further investigations. Nuclei undergoing necrotic and /or apoptotic death within the same syncitium has been reported (Barinaga, 1998) which could possibly explain the pattern observed by us - a ladder like banding with a background smear of degraded DNA.

6.5 SDS-PAGE Protein profiles

The treatment schedules of various agents and the time of sample collection have been shown in 'Experimental Design' (Chapter 5). Samples were harvested when the control plasmodia or the drug treated advanced plasmodia was at middle pre-prophase. Protein profiles from untreated control cellular lysates showed variation concomitant with cell cycle progression through S phase to late G2 and M phase in controls (Fig. 6.5.A). Notably, three polypeptides showed cell cycle related variations. While 53 kDa band was found to be conspicuous at S phase, 57 kDa and 60 kDa bands became prominent at late G2, and middle pre-prophase respectively. A progressive decline of the 53 kDa levels with the appearance of 57 and 60 kDa bands during late G2 – M transition was evident on closer scrutiny (Fig. 6.5.A). Variations in protein profiles in response to the AR (Fig. 6.5.B & C), CP (6.5.D – H), CHL (Fig. 6.5.I & J) and WM treatments (Fig. 6.5.K - N) in S and G2 phases have been summarized in Table 6.1.

AR, CHL and UV treated samples showed similar profiles with respect to 53 kDa polypeptide in that this band was found to be the most prominent one compared to the 57 and 60 kDa bands both in the cellular and the nuclear lysates. In CP treated samples, those treated with 250µM at early S-phase showing advancement in cell

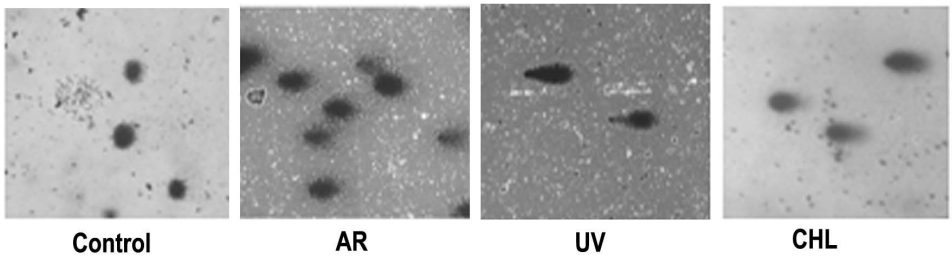

Fig. 6.3. Nuclear comets induced by DNA damaging agents

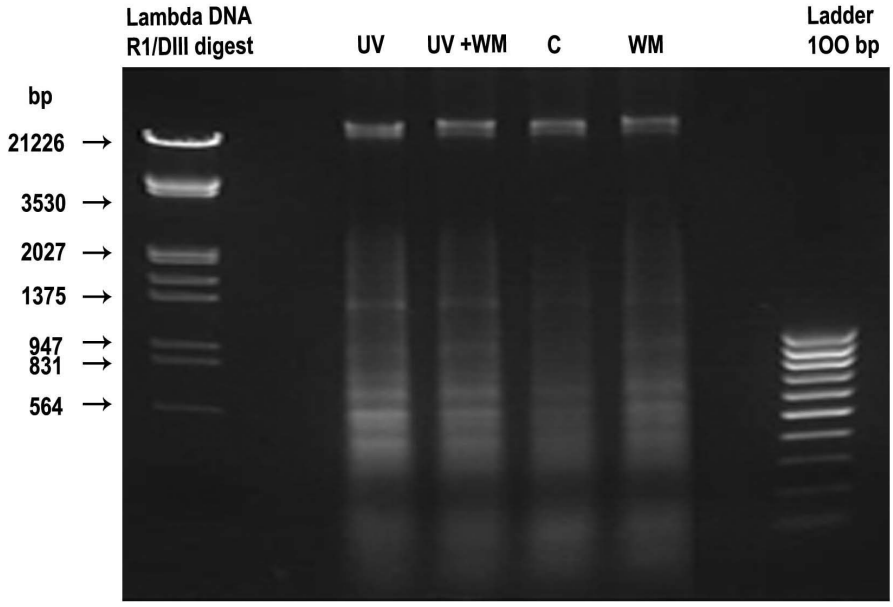

Fig. 6.4. Agarose gel (1.2%) electrophoresis of *Physarum* genomic DNA from G2 phase

cycle by 1h, exhibited a prominent band at 60 kDa compared to a prominent 57 kDa band in control. Interestingly, in samples treated with 500µM which exhibited a cell cycle delay of less than 1h, the predominant band was found at the 57 kDa position instead of 60 kDa band in control. In G2 phase treated samples and those which received combination treatments with UV showing cell cycle delays greater than 1h, 53 kDa band was relatively predominant compared to the other two bands. Contrastingly, all the three above-mentioned polypeptides were found to be drastically reduced or nearly absent in WM treated samples. This perhaps may be a consequence of decreased expression or instability. In combination treatment with UV, however, the 53 kDa band was found to be prominent. In all the drug treated and UV treated samples which showed delays in cell cycle progression, it was observed that the 57 kDa polypeptide was present for delays less than 1h. Samples exhibiting delays higher than 1h in magnitude also displayed the presence of 53 kDa polypeptide (Figs. 6.5.B, D - G, I & L). In other words, greater the delay lower was the molecular weight of the predominant polypeptide. Such apparent shifts in a narrow molecular weight range may likely result from post-translational modifications already well-established for key proteins associated with cell cycle regulation (Alberts et al., 2002). For example, *Physarum* p34-Cdc2 (Cho and Sauer, 1994), p53 and p63 (the forerunner homologue of the p53 family), involved in inducing cell cycle arrest, also reportedly show an upward mobility shift due to phosphorylation (Little and Jochemsen, 2002; Crum and McKeon, 2010).

In nuclear samples exposed to AR, CHL and UV (given alone or in combination with CP or WM), 53 kDa polypeptide was found to be more intense compared to its faint presence in the control samples and those treated with CP and WM. Strikingly, in G2 abrogated, WM treated samples, despite UV exposure, the intensity of this band was observed to be reduced to the level found in control. In view of the aforementioned report on caffeine-induced G2 abrogation in *Physarum* (Jayasree and Nair, 1991), an analysis of caffeine-induced G2 abrogated nuclear

sample revealed a striking similarity in protein profiles (Fig. 6.5.N & O). It has already been established that G2 abrogation by both WM and caffeine is brought about by inhibiting ATM/ATR (Wang and Lu, 2007), the apical kinases in the signal transduction pathway regulating cell cycle checkpoints. In G2 abrogated nuclear samples, a marked drop in the intensity of the 53 kDa band to very low, barely visible levels almost mimics the behaviour of the canonical p53 (Fig. 6.5.N). Although many of the aspects of the polypeptide strongly resemble the canonical (vertebrate) p53 (Kruse and Gu, 2009), the *Physarum* homologue has been reported to be larger, of 75 kDa, similar to p53 related plant proteins (Loidl and Loidl, 1996). In addition, western blot analysis data (this study, discussed below) also rules out the possibility of the 53 kDa polypeptide to be a homologue of vertebrate p53. Interestingly, in lower eukaryotes such as yeast, the tumor supressor p53 homologue is yet to be identified (Kuntz and O'Connell, 2009). In control nuclear sample collected at S phase the 53 kDa band was faint compared to its strong presence in the total cellular lysate profile. The nuclear control samples at middle pre-prophase showed a prominent band at 57 kDa, whereas total cellular lysate profile showed the presence of a 60 kDa band. On the basis of the aforementioned observations, it may be inferred that in untreated nuclear control samples, of the three polypeptides, only 57 kDa was clearly discernible while the other two 53 and 60 kDa - polypeptides were nearly absent. In samples exposed to potent DNA damaging agents such as AR, CHL and UV radiations, 53 kDa polypeptide became more conspicuous which may result from any one or more processes such as increased gene expression, protein-stabilization or nucleo-cytoplasmic shuttling.

6.6 Peptide-mapping

The 53, 57 and 60 kDa bands were subjected to peptide mapping with trypsin and chymotrypsin to confirm their distinctiveness (Figs. 6.6.A & B). Peptide maps of all the three polypeptides isolated from cellular and nuclear lysates generated an identical banding pattern with each enzyme (17.4, 13.9 and 11.5 kDa bands with

trypsin; 39.4 kDa with chymotrypsin), thereby confirming that these indeed are differentially modified forms of the same polypeptide. The 53 kDa form alone could be observed in the nuclear fractions of UV-irradiated, G2 arrested samples. The absence of this polypeptide in WM treated, G2-abrogated nuclear samples and the untreated controls further reinforce its role in G2 checkpoint activation leading to G2 arrest.

6.7 Western blot

The forestasted results of protein profile analysis clearly establish that 53 kDa polypeptide show properties similar to the canonical (vertebrate) p53 with respect to its stabilization and increase in the nuclear fraction in response to DNA damaging agents. Hence, its immunostainability with human p53 monoclonal antibodies was checked. Immunostaining of *Physarum* UV-irradiated lysates with anti-p53 antibody was carried out simultaneously with protein lysates human cells. Lysates from cultured human lymphocytes treated with 200μM H_2O_2 to induce p53 served as positive controls. *Physarum* proteins did not generate any signal on the western blot (Fig. 6.7.A). To check whether the positional shift shown by 53 kDa polypeptide in SDS-gel is due to phosphorylation at Ser or Tyr residues, immunostaining with antiphosphoserine and antiphosphotyrosine antibodies was also carried out. A signal was obtained only at 110 kDa position in the entire drug treated and UV treated categories except control (Figs. 6.7.B - E) under high stringency conditions. It may be pertinent to note that retinoblastoma, Rb protein (110 kDa) and Rb family proteins which function primarily as regulators of the mammalian cell cycle progression, suppressors of cellular growth and proliferation happen to fall within a similar range of molecular weights, from 105-130 kDa. These are known to get hyperphosphorylated or hypophosphorylated depending on the cell cycle phases (Claudio et al., 2002; Inoue et al., 1995; Macaluso et al., 2006). Absence of signals at 53, 57 or 60 kDa positions showed that these polypeptides do not get phosphorylated at Ser or Tyr residues. Hence, the positional shift observed in these polypeptides could only be explained away with the assumption that modifications

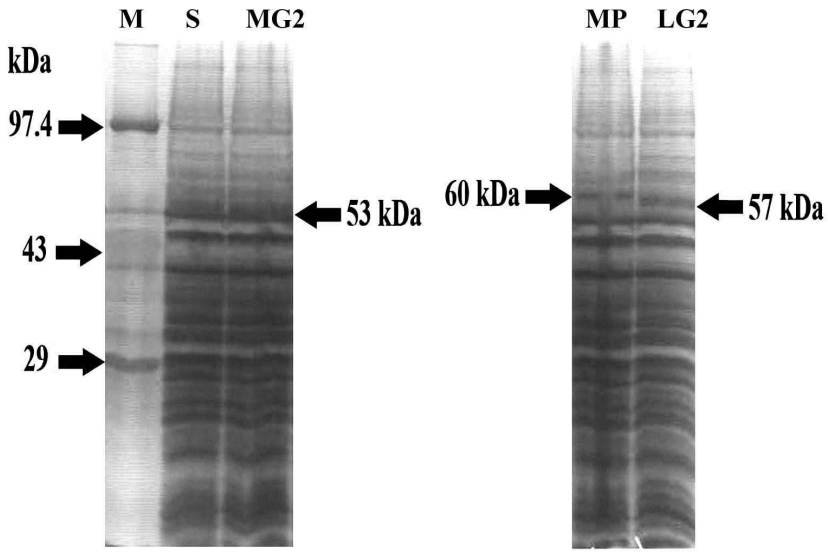

Fig. 6.5. A. Cellular lysate protein profile (12% SDS-PAGE) from untreated control samples

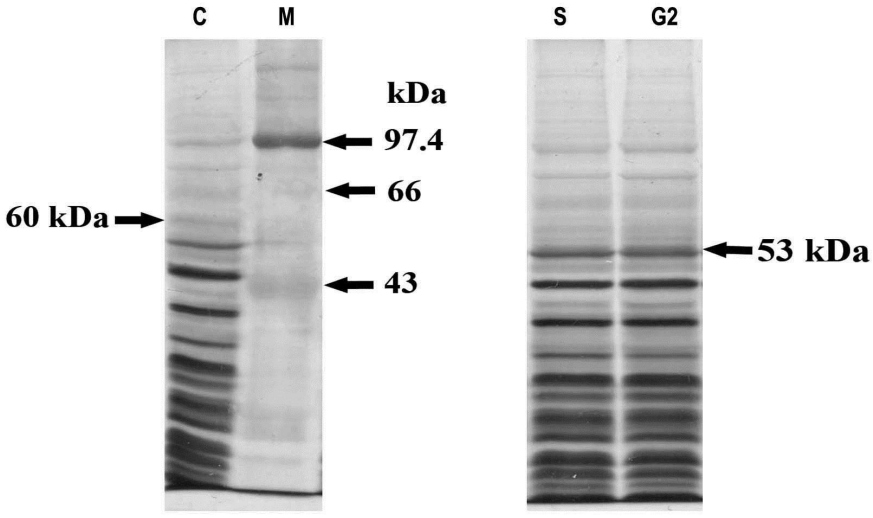

Fig. 6.5. B. Cellular lysate protein profile (12% SDS-PAGE) from AR treated samples.

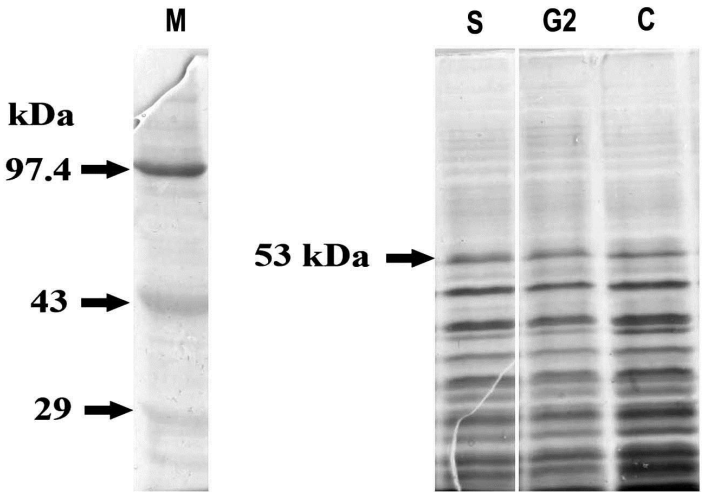

Fig. 6.5. C. Nuclear lysate protein profile (12% SDS-PAGE) from AR treated samples.

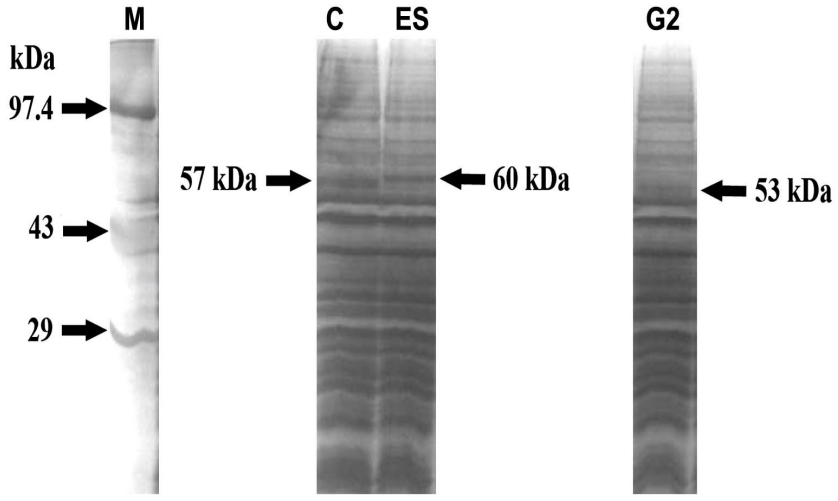

Fig 6.5. D. Cellular lysate protein profile (SDS-PAGE 12%) from 250µM CP treated samples.

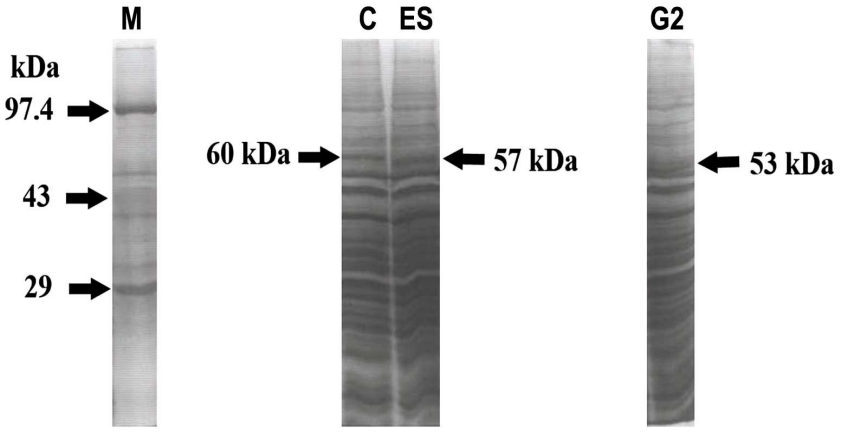

Fig 6.5. E. Cellular lysate protein profile (SDS-PAGE 12%) from 500µM CP treated samples.

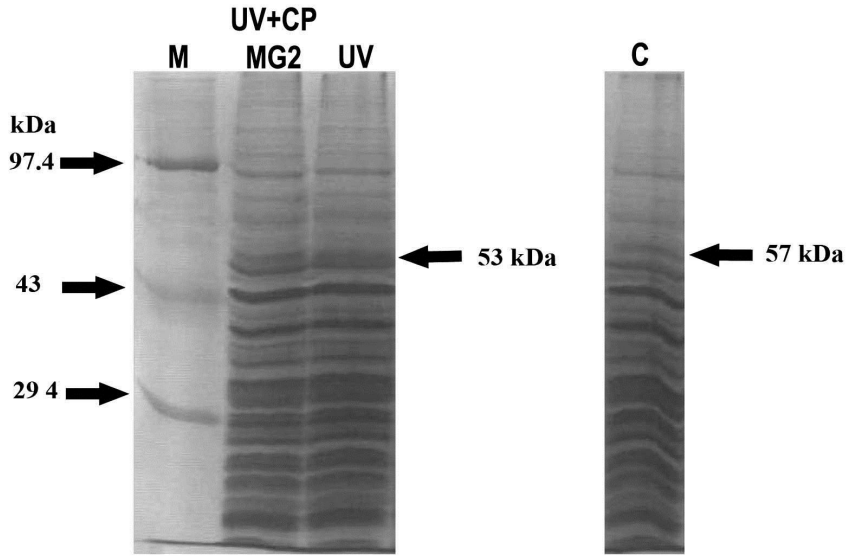

Fig. 6.5. F. Cellular lysate protein profile (SDS-PAGE 12%) from 250µM CP with UV combination treated samples.

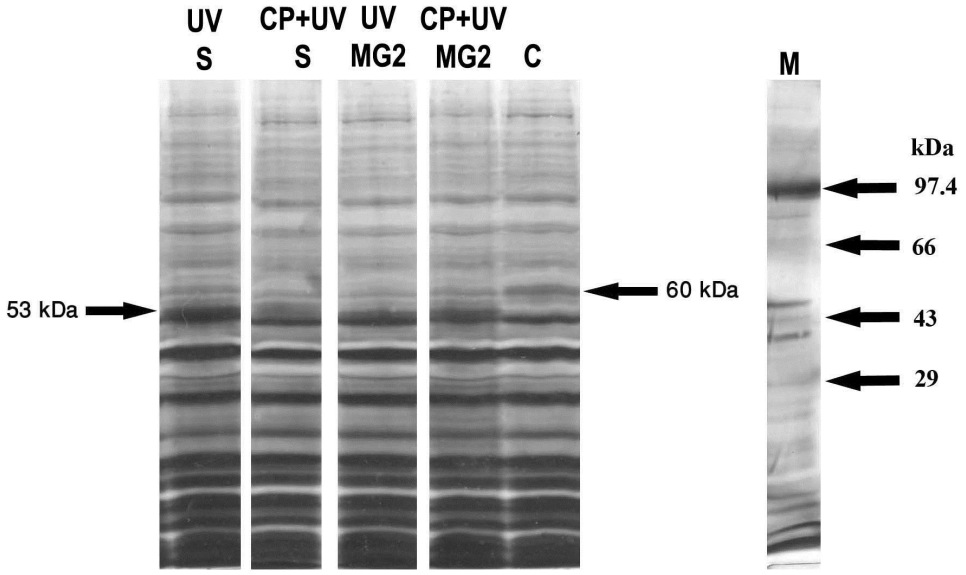

Fig. 6.5. G. Cellular lysate protein profile (SDS-PAGE 12%) from 500µM CP with UV combination treated samples.

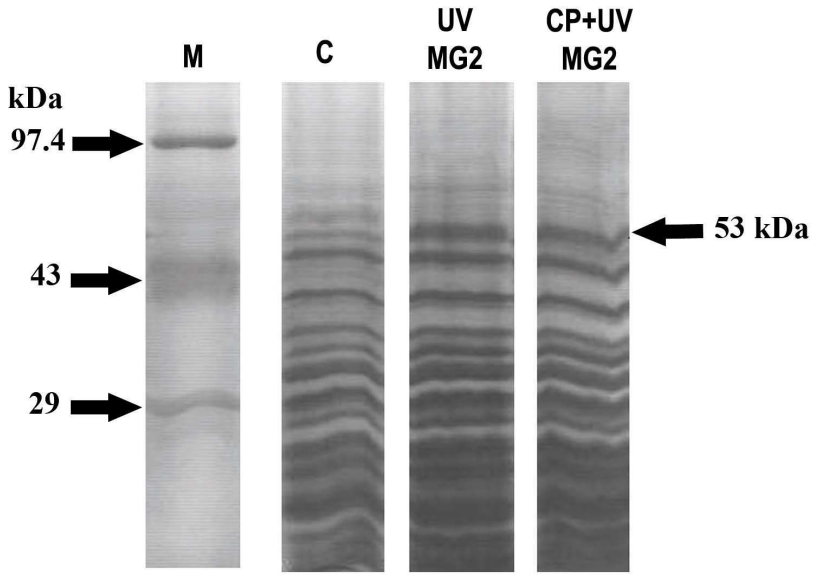

Fig 6.5. H. Nuclear lysate protein profile (SDS-PAGE 12%) from 250µM CP with UV combination treated samples.

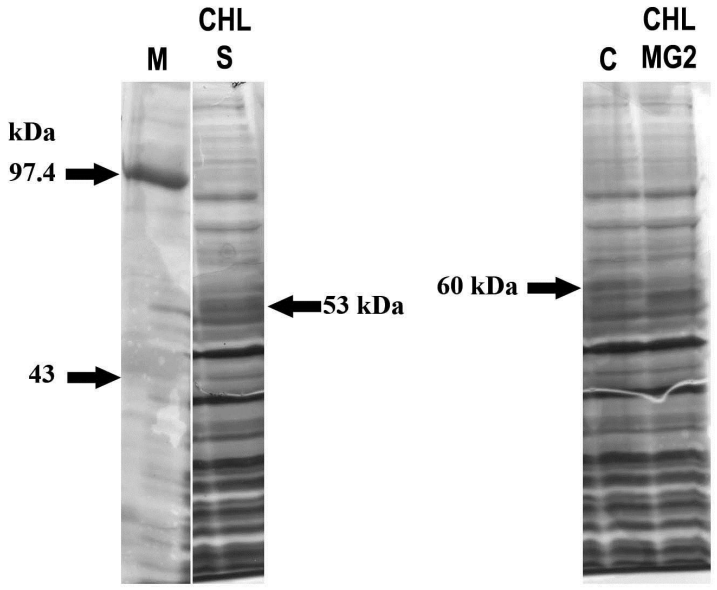

Fig 6.5. I. Cellular lysate protein profile (SDS-PAGE 12%) from 500µM CHL treated samples.

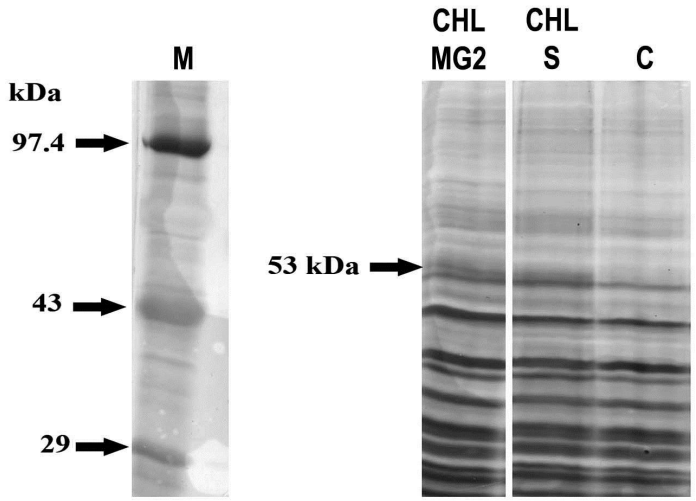

Fig 6.5. J. Nuclear lysate protein profile (SDS-PAGE 12%) from 500µM CHL treated samples.

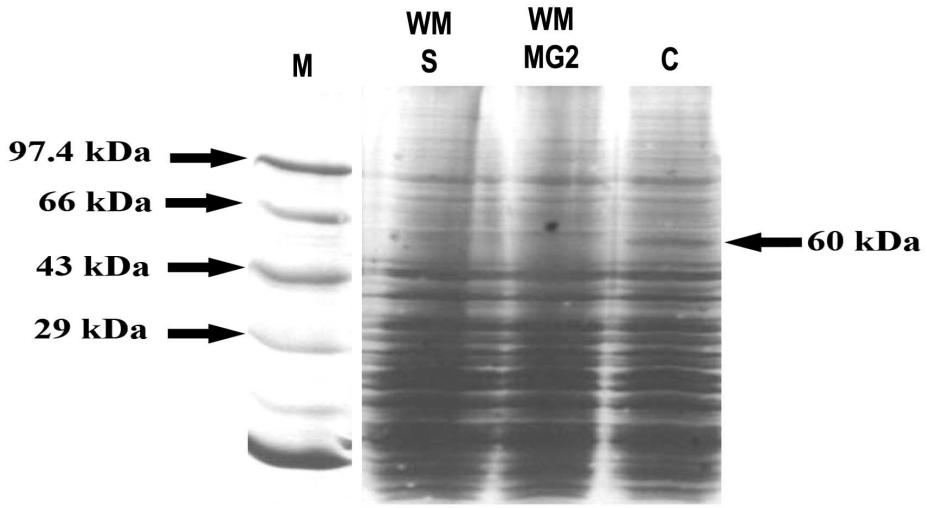

Fig 6.5. K. Cellular lysate protein profile (SDS-PAGE 10%) from WM treated samples.

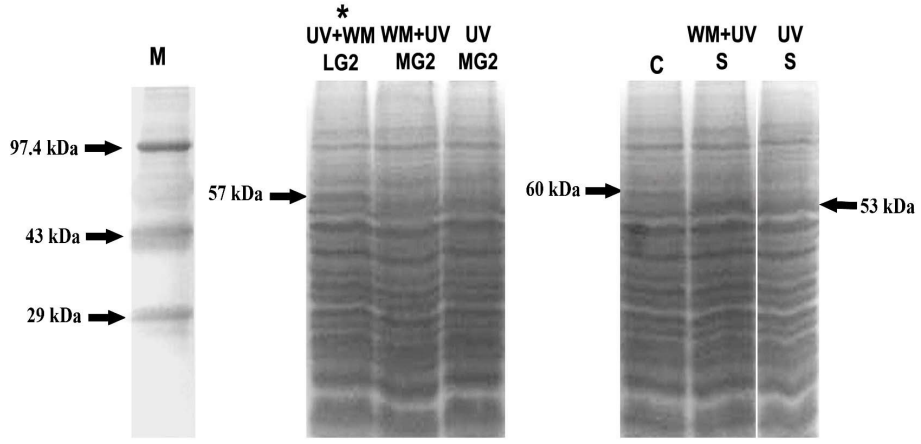

Fig 6.5. L. Cellular lysate protein profile (SDS-PAGE 10%) from WM and UV combination treated samples.

(* G2 abrogated post-treated sample)

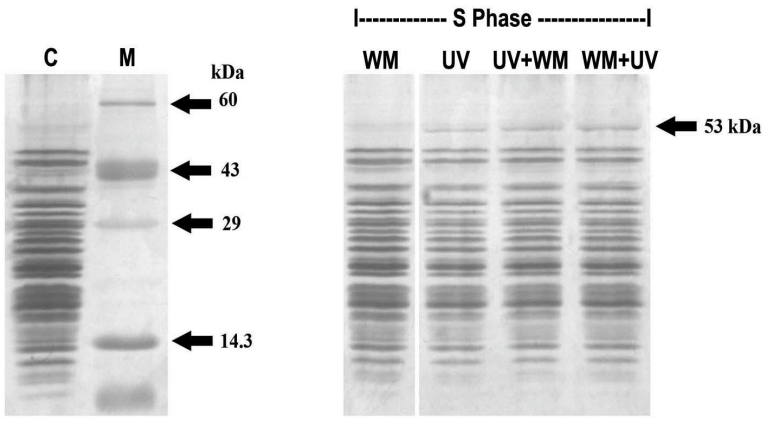

Fig 6.5. M. Nuclear lysate protein profile (15 - 20 % gradient gel) from WM and UV combination treated samples.

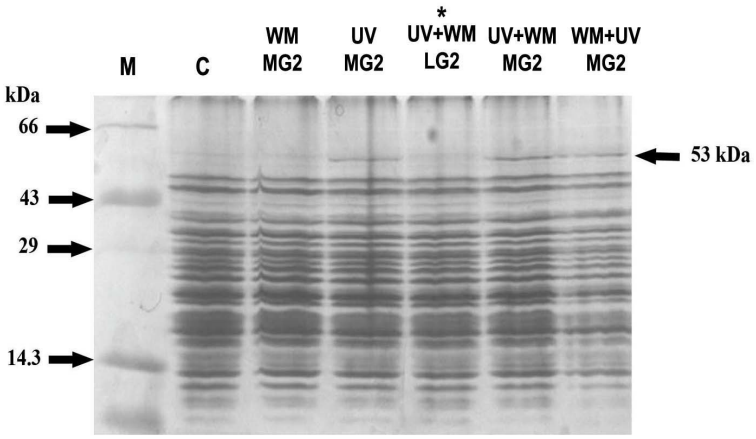

Fig 6.5. N. Nuclear lysate protein profile (15 - 20 % gradient gel) from WM and UV combination treated samples.
(* G2 abrogated post-treated sample)

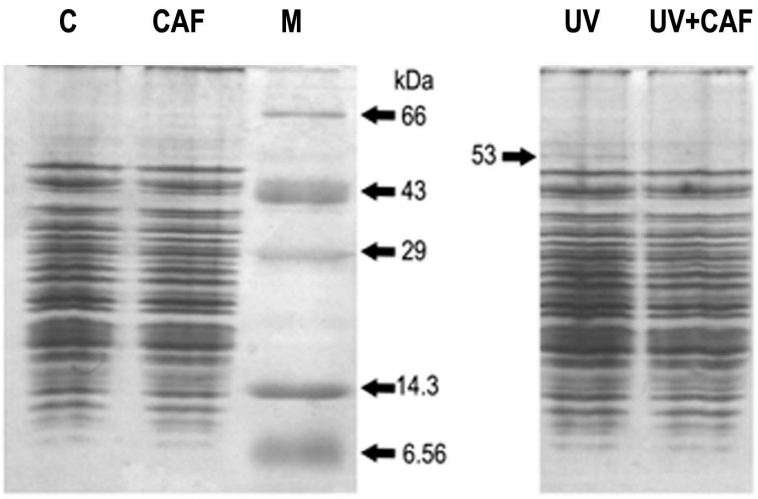

Fig 6.5. O. Nuclear lysate protein profile (15 - 20 % gradient gel) from 250µM CAF treated samples.

Table 6.1 Variations in protein profiles in response to AR, CP, WM & UV treatments

kDa	C		AR				CP			
	Cellular	Nuclear	Cellular		Nuclear		Cellular		Nuclear	
			200 µM	500 µM	200 µM	500 µM	250 µM	500 µM	250 µM	500 µM
53	S++ $G2^-$	S+ G2-	S++ G2++	S++ G2++	S++ G2++	S++ G2++	S- G2++	S- G2++	S- G2++	S- G2++
57	S+ G2++ (mid to late G2)	S- G2++	S- G2-	S- G2-	S- G2-	S- G2-	S- G2-	S+ G2-	S+ G2-	S+ G2-
60	S+ G2++ (Middle pre-prophase)	S- G2-	S- G2-	S- G2-	S- G2-	S- G2-	S++ G2-	S- G2-	S- G2-	S- G2-

kDa	CHL				WM		UV	
	Cellular		Nuclear		Cellular	Nuclear	Cellular	Nuclear
	200µM	500µM	200µM	500µM	10µM	10µM G2 abrogated		
53	S++ G2++	S++ G2++	S++ G2++	S++ G2++	S- G2-	S- G2-	S++ G2++	S++ G2++
57	S- G2-	S- G2-	S- G2-	S- G2-	S- G2-	S- G2-	S- G2-	S- G2-
60	S- G2-	S- G2-	S- G2-	S- G2-	S- G2-	S- G2-	S- G2-	S- G2-

other than phosphorylations on these residues or elsewhere on these polypeptides might indeed be responsible for the phenomenon observed as mobility shift on polyacrylamide gels.

6.8 Differential display polymerase chain reaction (DD-PCR)

Polymerase chain reaction based amplification of differentially expressed transcript pools from the samples treated with the various agents along with the respective controls was carried out. The agarose gel photographs displaying differentially expressed mRNAs as amplified cDNAs have been shown in Figure 6.8.A - E. The resultant analysis, qualitative in terms of the molecular weights of the cDNAs and quantitative in terms of the band intensities in the transcript profiles has been summarized in Table 6.8.

Differences in band intensities are represented as percentage values of Integrated Density Value (IDV) computed by AlphaEase FC software of the AlphaImager 2200 gel-documentation system using the formula:

$$\frac{\text{Sample}_{\text{Test}}\ (\text{IDV})\ \text{x}\ 100}{\text{Sample}_{\text{Control}}\ (\text{IDV})}$$

Major variations in band intensities of at least 20 % and above in expression profiles were considered. Upregulation, downregulation, near complete suppression, and induction of new mRNAs have been categorized below:

Arsenic trioxide treatment

With anchored primer oligo-dT(12)GG

1. 1348 bp band found to be almost completely suppressed (97 %)

Capsaicin treatment

With anchored primer oligo-dT(12)GG

2. A 756 bp band was found to be marginally downregulated (20 %).
3. Induction of a 191 bp band (97 %) observed.

With anchored primer oligo-dT(12)GC

4. 386 bp band was found to be downregulated marginally (25 %)

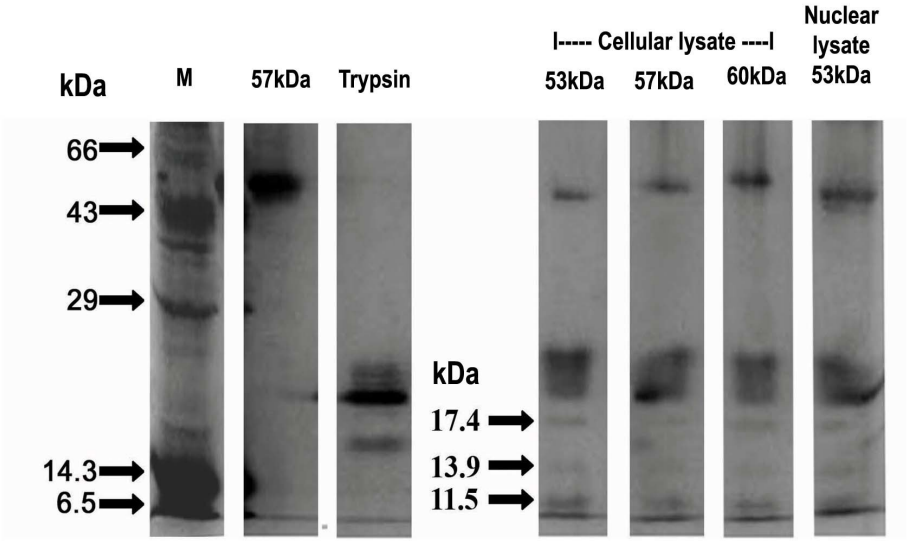

Fig. 6.6. A. Peptide Map of 60, 57 and 53kDa polypeptides following partial tryptic digestion.

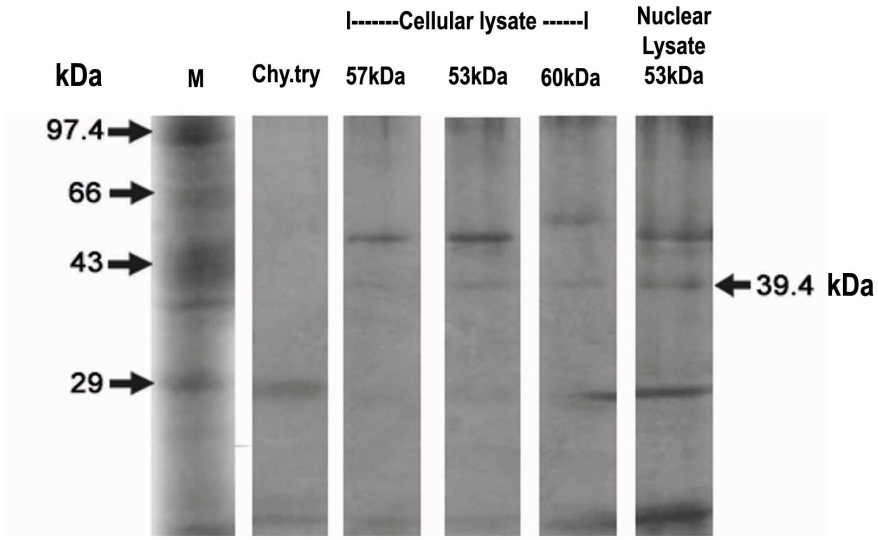

Fig 6.6. B. Peptide Map of 60, 57 and 53kDa polypeptides following partial digestion with chymotrypsin.

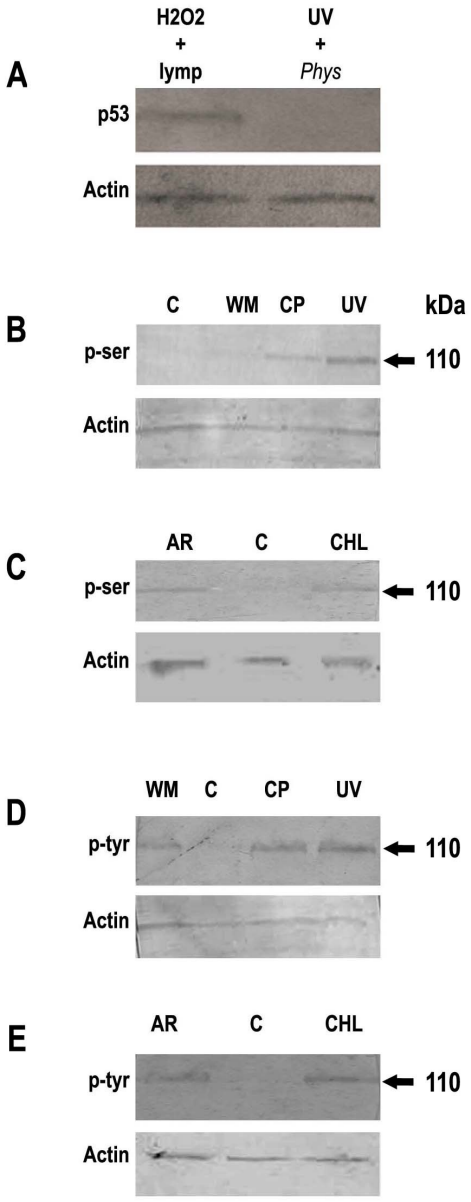

Fig. 6.7. Immunoblot of *Physarum* proteins on positively-charged nylon membrane.

5. 611 bp band showed significant inhibition (66 %)

With anchored primer oligo-dT(12)AC

6. 610 bp band showed severe inhibition (72 %)

Chlorambucil treatment

With anchored primer oligo-dT(12)CC

7. 220 bp band showed drastic downregulation (92 %)
8. 250 bp band showed almost complete downregulation (98 %)

With anchored primer oligo-dT(12)AC

9. 222 bp band was found to be drastically downregulated (89 %)
10. 980 bp band was observed to be strongly downregulated (94 %)

UV treatment

With anchored primer oligo-dT(12)AC

11. 720 bp showed a slight upregulation (30 %)

Wortmannin treatment

With anchored primer oligo-dT(12)GG

12. A 552 bp band was found to be significantly upregulated (64 %)
13. A marginal downregulation (25 %) of a 228 bp band was observed
14. 735 bp band showed significant downregulation (53 %)
15. Considerable downregulation of 756 bp (42 %) band was observed

With anchored primer oligo-dT(12)GC

16. 386 bp band was found to be drastically downregulated (89 %)
17. 611 bp band showed significant inhibition (57 %)
18. 740 bp band showed was found to be moderately downregulated (36 %)
19. 310 bp band showed significant inhibition (64 %)
20. Induction (98 %) of a 191 bp band was observed.

With anchored primer oligo-dT(12)CC

21. 720 bp band was found to be drastically downregulated (90 %)

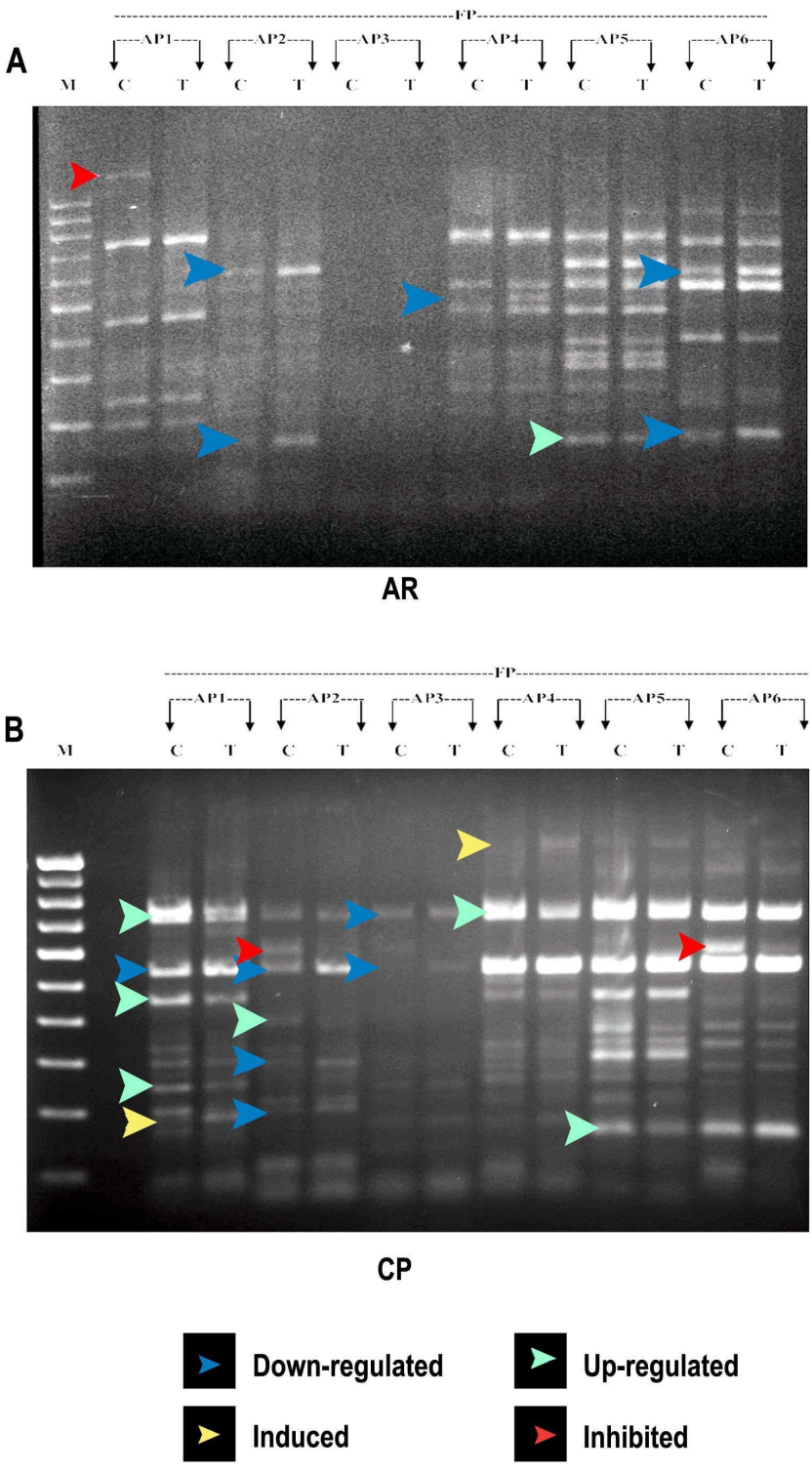

Fig. 6.8. A & B. Differential display of mRNAs from *P. polycephalum* treated with DNA damaging agents

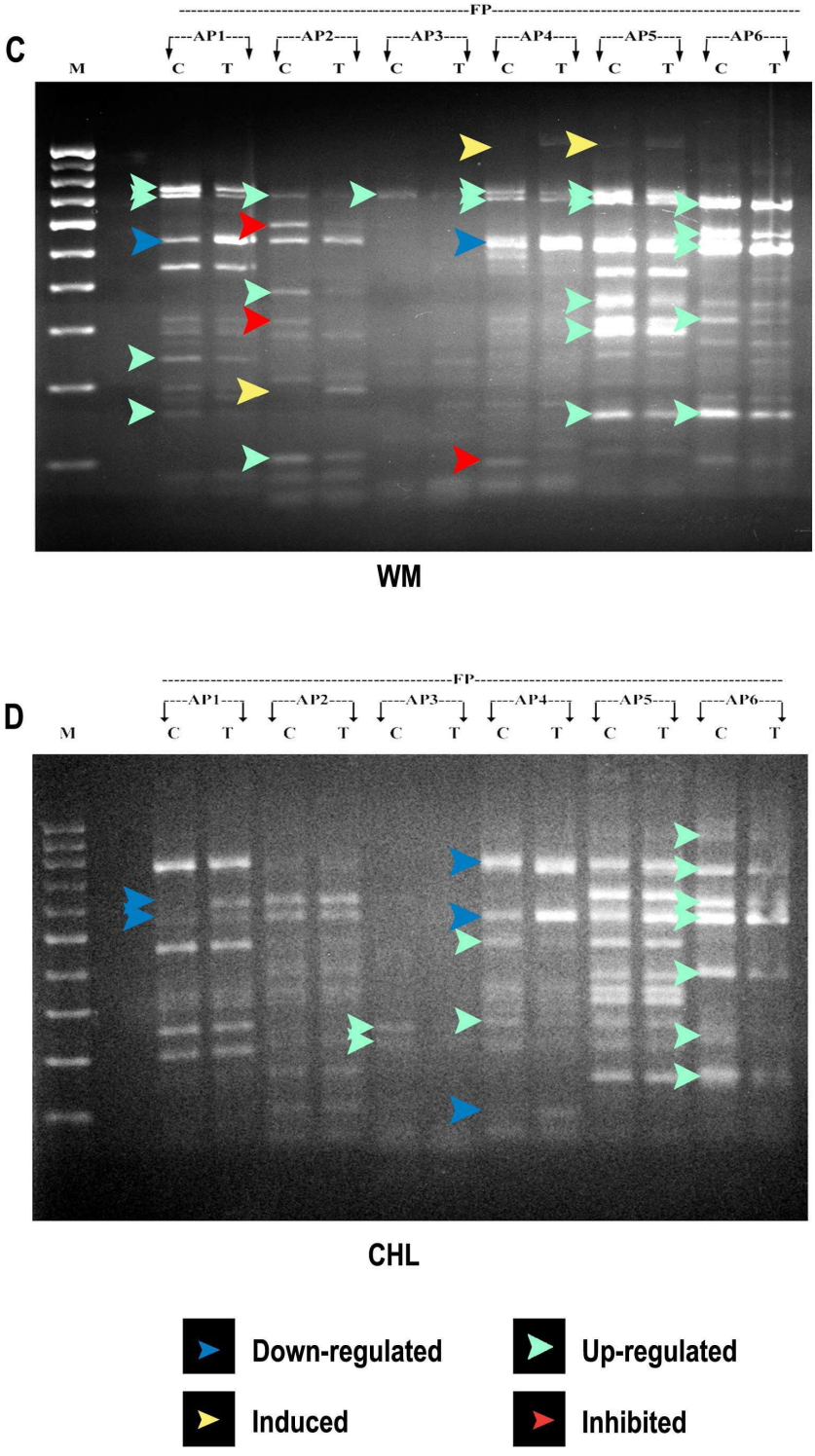

Fig. 6.8. C & D. Differential display of mRNAs from *P. polycephalum* treated with DNA damaging agents

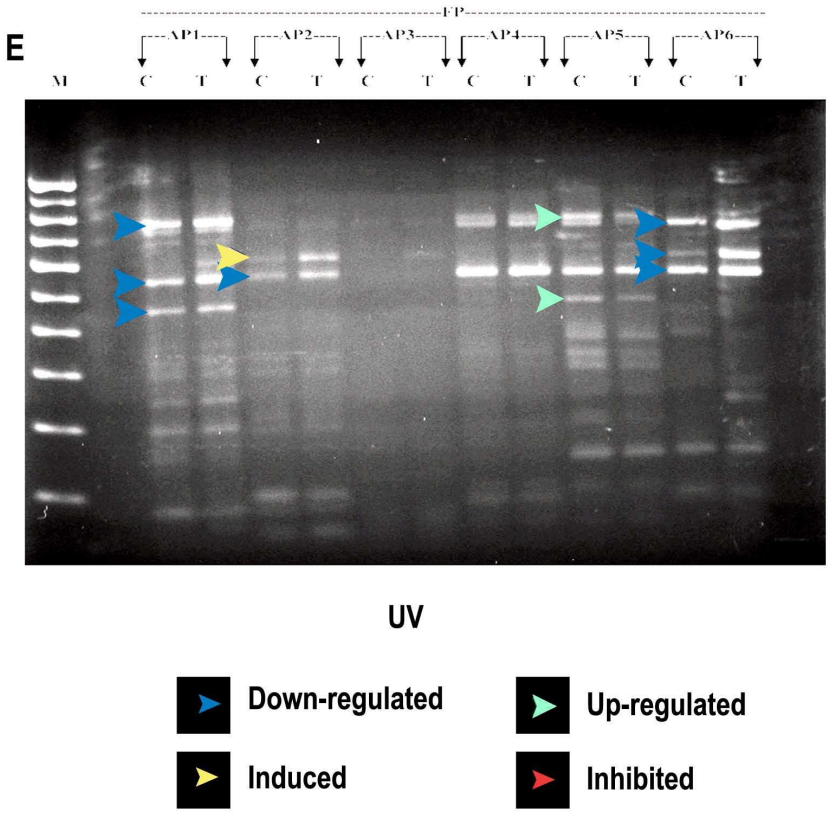

Fig. 6.8. E. Differential display of mRNAs from *P. polycephalum* treated with DNA damaging agents

Table 6.8 Transcript analysis based on DD–PCR profiles following AR, CP, WM & UV treatment

(UR – Upregulated; DR – Downregulated; IN – Inhibited; IND - Induced)

AP	bp	AR	CP	CHL	WM	UV
GG	**1348**	IN **(97%)**				
	756		DR **(20%)**		DR **(42%)**	UR (9%)
	735				DR **(53%)**	
	625			UR (11%)		
	552		UR (13%)	UR (5%)	UR **(64%)**	UR (5%)
	448		DR (13%)			UR (7%)
	228		DR (3%)		DR **(25%)**	
	191		IND **(97%)**			
	180				DR (14%)	
GC	740				DR **(36%)**	
	611	UR (8%)	IN **(66%)**		IN **(57%)**	UR (13%)
	552		UR (17%)			UR (2%)
	386		DR **(25%)**		DR **(89%)**	
	310				IN **(64%)**	
	290		UR (14%)			
	210		UR (12%)			
	191				IND **(98%)**	
	180	UR (6%)				
	100				DR (10%)	
CC	752		UR (9%)			
	720				DR **(90%)**	
	552		UR (7%)			
	250			DR **(98%)**		
	220			DR **(92%)**		
CG	**1243**		IND (9%)		IND **(29%)**	
	756		DR (14%)	UR (3%)	DR (13%)	

	720				DR (6%)	
	552	UR (5%)		UR (11%)	UR **(50%)**	
	472			DR (3%)		
	290			DR (2%)		
	110			UR (3%)		
	100				IN **(92%)**	
AG	**1243**				IND **(20%)**	
	756				DR (13%)	DR (6%)
	720				DR **(21%)**	
	478					DR (14%)
	350				DR (16%)	
	291				DR (8%)	
	180	DR (3%)	DR (10%)		DR (18%)	
AC	**980**			DR **(94%)**		
	720			DR (9%)	DR (3%)	UR **(30%)**
	610	UR (6%)	IN **(72%)**	DR 10 (%)	DR (19%)	UR (19%)
	552			DR (9%)	DR (10%)	UR (13%)
	411			DR (12%)		
	310				DR **(25%)**	
	222			DR **(89%)**		
	190	UR (9%)				
	180			DR (14%)	DR **(28%)**	

With anchored primer oligo-dT(12)CG

22. 1243 bp band was marginally upregulated (29 %)

23. 552 bp band showed a substantial increase (50 %)

24. 100 bp band was observed to be drastically inhibited (92 %)

With anchored primer oligo-dT(12)AG

25. 1243 bp band showed a marginal induction (20 %)

26. 720 bp band was observed to be slightly downregulated (21 %)

With anchored primer oligo-dT(12)AC

27. 180 bp band showed a marginal downregulation (28 %)

28. 310 bp band was observed to be slightly downregulated (25 %)

Overall, only two transcripts, apparently of same size (191 bp) were found to be newly induced following CP and WM treatment. At least five transcripts showed complete suppression, three (220, 250 & 980 bp) in CHL treated and one each in WM (100 bp) and AR (1348 bp) treated. Atleast five transcripts were found to be upregulated, four (552 & 1243 bp - two each with different primers) in WM treated and one of 720 bp in UV treated category.

Sixteen transcripts were observed to be downregulated, eleven (180, 228, 386, 611, 735, 740, 756 bp, 310 and 720 bp - two each with different primers) in WM treated, four (386, 610, 611, and 756 bp) in CP treated and one (222 bp) in CHL treated. Of the down regulated - 386, 611 and 756 bp transcripts were found to be present both in CP and WM treated samples.

6.8.A. Direct sequencing of select transcripts

A total of 28 validated DD-PCR fragments (highlighted in bold font within Table 6.8.) were subjected to direct sequencing. Thirteen transcripts were successfully sequenced and these were employed for BLASTn search to find similarities with the sequence deposits in Nucleotide collections / Expressed Sequence

Tags (EST) databanks. The results of the search have been presented at the end of this section (Fig. 6.8.A – M). The band no. 21 with the highest score of an e-value of 1e-132 showed a match with subtilisin-like protease B mRNA / *php* gene encoding Physarolisin of *P. polycephalum*. Another band no. 23 with an e-value of 2e-64 showed a match with AX4 PHD zinc finger containing protein of *Dictyostelium discoideum*, a closely related slime mould showing cellular organization. The remaining sequences showed matches to non-normalized library clones and starvation stress library of *P. polycephalum* within EST databanks.

Subtilisin-like proteases (Subtilases) represent one of the two superfamilies of serine proteases which occur in Archaea, Bacteria, fungi, yeasts, and higher eukaryotes (Siezen and Leunissen, 1997; Bryant et al., 2009). A subtilisin-like serine protease has been identified as a late replicating gene in *P. polycephalum* (Benard et al., 1992). However, the function of this remains uncharacterized (Watkins and Gray, 2008). A serine carboxyl peptidase from *Physarum*, named Physarolisin II has been characterized which is reported to be the first cold-adapted enzyme within the serine-carboxyl peptidases (Nishii et al., 2003).

A search on the sequenced transcripts using the ORF finder of NCBI revealed a number of ORF's subsequently subjected to BLASTp analysis which has also been shown at the end of this section (Fig. 6.8.A – M). The most prominent among these being a subtilisin-like protease A from *P. polycephalum* and three other proteins from the fungus, *Phytophthora infestans.*

Overall, the results of sequencing of the select clones indicate that almost all of the clones belong to the category of stress-inducible transcripts in agreement with ESTs identified in transcriptome-level studies (Barrantes et al., 2010; Glockner et al., 2008). Such a high preponderance of stress-related gene expression is indeed the expected outcome as the DNA damaging agents used in the study, directly or

indirectly generate cellular stress when administered in S or G2 phase of the cell cycle.

Reduction of nuclear DNA, induction of comets, consistent variations in some of the key proteins with the concomitant advancement and /or induction of G2 arrest in the cell cycle, clearly manifest the derailment of the the cell cycle regulatory mechanisms by the agents used in the study.

Band Name	Accession No.	BLASTn search result	e-Value	Species
2	EL578150.1	starvation stress library	7e-28	*Physarum polycephalum*

C C C C A G G G A G G T T G A G G A A A G A A T A T G C A G G C C T G G
A G G A G A A A T A A G G A A A A G T A G G T G A A T G T G G A T T G A T
C G G A T A A A A G G A A G A G T G A G G A A A T G A G G A A G G T G T
G G A A A G G T T T T T C G G T T G G T A C A T G T T G A G A G T G A G G
T T G G T T C A C A T T T C T G T T A G T C T A G T G T T T T T G C A A A C
C A T A G A A C T C T T A C A A T C T A C A G T T G T T G T T T A C G T T G
G G T A C T T G T T G C A G C A A G T T G A A A A G A T A C A A C T A A T
G T T G C T C T T C T G A T G C C G A T C T C A G T T T G C T C T G C C A G
G A T T T T G A T T T G A A A T A T C T A A C G A C G C C C C A C G T A A G
A G C A C T A T A A G A T C C G C C T T C A G C G A G A T C A A C T A T A
G T A T A A T C T T G G G A A C T T T T G C C T T G A A G T A G A A G G C
C G A G A A G T C A A A G A C T C T A T T T C G A T G G A T G T T T T G A T
C A C C G T C A A A A A A C G C T T G G C G T T A A G A G G G T C C G T C
A T T C C C C G T G C T C T A C G A A G G C A G T G T A A A C G A A A A C
A T T T T C A T C A T T T C G T T G A T G A T T G G G A T G T C A C G T G T
T C T C G G T T C A C T T T C C A C G G C G A A A G A A A A C G T C G C A
G T T A G C T G G A G G C T T T C C C T T T C C G A C T T C A T T C C G A
G T T C T T T A T C A C A C T T G T T A T T C G C T C C G T C C C G A A A A
T G G T C T C G C C T G C A G G A A G G A

Band Name	ORF Amino acid length	Accession No.	BLASTp search result	Species	e-Value
2	43	NP_001041368.1	uncharacterized protein	*Rattus norvegicus*	5.5

M K S E R E S L Q L T A T F S F A V E S E P R T R D I P I I
N E M M K M F S F T L P S *

Fig. 6.8. A. Band 2 - cDNA sequence & ORF

Band Name	Accession No.	BLASTn search result	e-Value	Species
3	EL571997.1	starvation stress library	5e-135	*Physarum polycephalum*

C C T T G G G C G G A T C T C T T T T C T G C G C A T A C T A A G G T G C
A A T G T T T G G C T T G G G C A T G G G C G A A A T C A C A C A C C G C
T G C A C A A C G A A T A T T A C G A C T T T C C C G A C T C C G A G A T T
C C G A C A G G C G T T T C C A T A T T C G C C A C G A T T G T C G C A C
T T A T T T T G G G C C C C A A T C A G C C G G A T G C T G C T G C A C A
A C A A A A T A A T G C G A A A C T G G T A G T A A A T T C A T T G T A G
G T T A G T G T A T T T C T A C C

Band Name	ORF Amino acid length	Accession No.	BLASTp search result	Species	e-Value
3	73	ZP_02143762.1	amidohydrolase family protein	*Phaeobacter gallaeciensis* BS107	1e-05

L G R I S F L R I L R C N V W L G H G R N H T P L H N E Y
Y D F P D S E I P T G V S I F A T I V A L I L G P N Q P D A
A A Q Q N N A K L V V N S L *

Fig. 6.8. B. Band 3 - cDNA sequence & ORF

Band Name	Accession No.	BLASTn search result	e-Value	Species
4	EL577699.1	starvation stress library	6e-26	*Physarum polycephalum*

G G A A C T T T T G G C T T T G T C T G G G T T T A G A A A A A T C A G A
C G A G A A A A A A T T C A G G C T A A G A A A A T G G G A T T T T G T A
T T T A A A G G G G G A A C T T T G G T T T C C C T A A C T T T C C G G
G G G C C A C C T A T A C T C T T C T T A C A A G G G T A T T T T G G T C
C G A A T T G C C T T C A A A A A A C C C C C C C T T C C T C T G C C A C A A
A C C A G T C C C C C C C C A T T T A G G G A A T T C T T T A C A A A T T G T
C C C C C A A T C C T T G G T G C G T A A T C C C C T C C C C C T T T G G
G G G C G A T A T C A A T A A A A A G T T T T A G G T G T C T C A A A T C C
A A C C C C C G C C C C T T G A A A A A A A A T T T A G C T T G T T A G C A C
A C C A G C G G G G G G G C T C C T G C C C C C C C C C C A T T C C T T C G G
A A T T G G G C G G T T T A G G T T T C C C C T C C T T T C C T G G C C C
A G G G T T T A T A A T A T A A C A T G G T C C T C

Band Name	ORF Amino acid length	Accession No.	BLASTp search result	Species	e-Value
4	90	unknown	unknown	unknown	Unknown

N F W L C L G L E K S D E K K F R L R K W D F V F K G G T
V S L T F R G P P I L F L Q G Y F G P N C L Q K P P L P L P
Q T S P P H L G N S L Q I V P Q S L V R N P L P L W G R Y Q

Fig. 6.8. C. Band 4 - cDNA sequence & ORF

Band Name	Accession No.	BLASTn search result	e-Value	Species
6	EL571997.1	starvation stress library	2e-27	*Physarum polycephalum*

A G T C C G G A C G G T C T T G G A T T G T T A T T C G G C G C C C G C G
A C T T C C T T T C G C T T T T T T T T T T T C T T T T C C C C C C C C C C C C
C C C C T T T T T T T T T T T T T T T T T T T T T T T T T T T T C C C C C C C C C C
T T T T T T T T T T T T T T T T T T T T T T T T T T T T T T T C T T G C C C C C C C C C C
T T T T T T T T T T T T T T T T T T T T T T T T T T T T T T T T G G G C C C C C T G T T A
T T T T T T T T T T T T T T T T T G T T T A G A T T G C A C C C C T C T A C G T C T
T A T A A G C C C T C C C T G A A A C G G G C C C T G A G A C C T C G C A
G T G C T T G T G A A G A C T C C A G G T C C G A G C T G C T T A A C G C
C C C C G C C C A A T G C C T T G A C C G C A G T C T G C A A C A C C G C T
A G C C A G A C T G A T T G A G G A A A T A G G A T T G T C G A A A A A A
A C C A G T G A C A A C T T G G A A T G A T A A G A T A T A G A G G C G G
G G G G G G G G G G G T G T G A G G A T T T G A G T G A G G T A G G A T C
T G G T G A G A A C C C A A A C C G A A C T A A G T A T T A C T T G C G A T
A A C G T G A T T G T A G A T T G T T G T A T T T T T T T G T A G C C G G C G
C A T C A C T C G C A C T A C G A C A T C T G G G C G A A G A C G A G T G
A G A C T G

Band Name	ORF Amino acid length	Accession No.	BLASTp search result	Species	e-Value
6	118	EIW83898.1	hypothetical protein	*Coniophora puteana*	2.8

V R T V L D C Y S A P A T S F R F F F S F P P P P P L F F F
F F F F F P P P F F F F F F F F S C P P P F F F F F F F F L G
P L L F F F F L F R L H P S T S Y K P S L K R A L R P R S A
C E D S R S E L L N A P A N A L T A V C N T A S Q T D *

Fig. 6.8. D. Band 6 - cDNA sequence & ORF

Band Name	Accession No.	BLASTn search result	e-Value	Species
12	EL571997.1	starvation stress library	2e-122	*Physarum polycephalum*

A T T G G A G G G G C T A G A A A A A A A A A A A G A G G G A C G
G G G A C T G C C A A T G A A A A A T G A A A A A T G A A G C C A G G G
T G C T G T A A G T A A A A A A T A A A A A A A A A A T A G C C G C C A C C
C C C A A T G G C A T G A A A G C T C T C C T T C C C C A A T T A C T T G
G C G C A C T C T C C G C A G A C A A A T C C T G G C A A G G A A A A A G T
T G C T T C T C T C A A C G C C T T C A T T A A C C T C G C C A A G A T T G
C A C C C C T C T A C G T C A A C C A C G C C C T C C C T G A A A T C A T
C C C T G A G A T C T C T C T C A G T G C A T G T G G G A C T C C A A G T C C
G A G G T G C A A A A G G C C G C C A C C A A T G C C T T G A C C G C T G
T C T G C A A C A C C G C T A T C C A C G C C C A T T G A C C C C G C C T
C C A T C G C C T C A T T T C T A C A A A T T A C T C C T T T T A A A G A G
G G A T T T T T T T T T T T T T T T T C G G A G C C C G A A C G T C A A T A G
T T T T T A T T T T T T T T A G A T C C G C T G G T C C C T C A A T A A A T C
G T T T G G T G A G G A G A G G G T C G G C C T T T A G T

Band Name	ORF Amino acid length	Accession No.	BLASTp search result	Species	e-Value
12	80	XP_002906761.1	elongation factor 3, putative	*Phytophthora infestans*	3e-14

M K A L L P Q L L G A L S A D K S W Q G K V A S L N A F I
N L A K I A P L Y V N H A L P E I I P E I S Q C M W D S K S
E V Q K A A T N A L T A V C N T A I H A H *

Fig. 6.8. E. Band 12 - cDNA sequence & ORF

Band Name	Accession No.	BLASTn search result	e-Value	Species
14	EC758413.1	Non-normalized library clone	2e-85	*Physarum polycephalum*

G C C A C C G A T T G T T T A T C T C T G G C T A A G C A T A G A T C A G
A C A G G T T A A A C A G A A A G G T T T A A G A A A A T T G G A T T T T
G C C A T C T T A A A G G G G G A A A C T T T G G T T G G C C C A A C T T T
C A G G G G G G C A G A A A A G A G T C T T C T T A C A T G G A A T T T T G
G A C C G A A T T G G C T T C A A A A A C C G C C C A C T C C T C G G C C
C G A A A C C A T T C C C C C C C C A T T T A G G G A A G C C T T A A A A
T A T A T T C C C C A A A C C A T T G G G C G A A A A C C C C T C T C C
C T G G G G G G G G C A A T A G C A A A A A A C A G T T T T A G G G G G A T C
A A A T C C A A C T C C T G C C C A T T G G A A A A A A A C T A G C T T G
T T A A C A C C C C C G C T G T G G G C T C C T G C C C C C C C C A T T C
C T T C G A A A T T G G G C G G T A T A G G T T T C C C C C T A T C C C C
G G G C C C A G G A A A A A A A A A A A A A A A A A A A A A A A A A A G G T A A
A A C G A A G A A A A G G G G G G A A G G G G G A G C C C C A G G T T G G
T A A A T A A T G A A T T A T C C A G G G G C G G G G G A A C G G G T G C
C C C C C A C A C C C C C C T T T G C T T T T T T T T T T T T T T T T G G G G
G G C C C C C C C C C A C C G G T T T T T T T T T T C T C C T A G A G T A C
T C C C C T A A A A A G

M G G A G A H S G G V N K L V F F Q W A G V G F D P P K
T V F A I A P P G R G V F A Q W F G E Y I L R L P *

Fig. 6.8. F. Band 14 - cDNA sequence & ORF

Band Name	Accession No.	BLASTn search result	e-Value	Species
15	EC756915.1	Non-normalized library	1e-44	*Physarum polycephalum*

A A G C G G T C C G A T C T T C A C G G A T G A G T G G T G C C T C C T A
C A C A T C T G G A G T T G A G A A C C T A G G T T C A T T C C T C C T C
G C C T G A G C T G G A T C C G A T A C A C T A A A A C T G G A A A T C C
C G G C T T C T C A T G A T G G A T A G A G G T A A A A A A T C C G A T G A
T G T G A C T C C T T C A T T G C C T C C A A T T C T C A A G G T G G T G T
G G A C A G C T T T G A G G T T G A T G A T A T G T T T A A C G C A C G C
T T T C A G A G T G G A G T C G C T G C C A G A C T T G G A A G A G C C T
A G G A T G C C C C A G G G A A A G G T A G C A T A A G C A T G A G C T A
T T T G C A A G T A T G G A A C A A A C T C A T T T C A T T G A C A C T G
G A C A T T G A C T A T A T C A A G T C A A T C T T A A A G G A A A G A A
G T T G T A T A T T T T T G G T C T A C T G T C T C G A A G T A G G A C C C
A A A A A A A G C C G T T G G C T C T G G A A A A T G C A G C C A A A T C
A C A C T C G G C A G T T G A A G C T A C G T A T G C G T C A A C G A T G
C C A A T C A C T G G G G C C C A G G A A T T G G T G C C C T T C C A A
A A T C C C T G T T C G C T T T T T T T T T T T T T T A T A T C G A G A C G A
C T G C C C T T G A C G T G T G C T A G A C C T C T T C T A C G C A G T C
G G G T A G C T C G C A G T T G C A T A G C G A T T T A C C T G T T C G G
C G T C G C T C C C T G C T C T G T C A G A T A C T G A A G A T C A A C G
C G T C A C G A T A A T G T C T A A C T G G A C G A A G A A T G C T C T C

M Q L R A T R L R R R G L A H V K G S R L D I K K K K A N
R D F G R G T N S W A P V I G I V D A Y V A S T A E C D L
A A F S R A N G F F W V L L R D S R P K I Y N F F P L R L T
*

Fig. 6.8. G. Band 15 - cDNA sequence & ORF

Band Name	Accession No.	BLASTn search result	e-Value	Species
16	EL571997.1	starvation stress library	2e-127	*Physarum polycephalum*

A A A T G G G C T T T G A A A A A A A A G T A T A T G A G C G T G C C G A
A G A C G A A G A G A T T G A C C G T G C T G C C A A G A G T G C T T G T
C A G G T A T C T T A G A C G A A T A G A C G G C A C C C C C A A T G G C
A T G A A A G C T C T C C T T C C C C A A T T A C T T G G C G C A C T C T C
C G C A G A C A A A T C C T G G C A A G G A A A A G T T G C T T C T C T C
A A C G C C T T C A T T A A C C T C G C C A A G A T T G C A C C C C T C T A
C A G C A A C C A C G C C C T C C C T G A A A T C A T C C C T G A G A T C
T C T C A G T G C A T G T G G G A C T C C A A G T C C G A G G G T G C A A A
AG G C C G C C A C C A A T G C C T T G A C C G C T G T C T G C A A C A C
C G C T A T C C A C G C C C A T T G A C C C C G C C T C C A C G C C C C A
T T T C C A C A A A T T A C T C C T T T T A A A G A G G G A T T T T T T T T
T T T T T T T T C C C C C C C C C C C C C C C C C T T T T T T T T T T T T T T
T T T T T T T T T C C C C C C C C G C C

Band Name	ORF Amino acid length	Accession No.	BLASTp search result	Species	e-Value
16	109	XP_002906761.1	elongation factor 3	*Phytophthora infestans*	2e-12

M S V P K T K R L T V L P R V L V R Y L R R I D G T P N G
M K A L L P Q L L G A L S A D K S W Q G K V A S L N A F I

N A K I A P L Y S N H A L P E I I P E I S Q C M W D S K S E
V Q K A A T N A L T A V C N T A I H A H *

Fig. 6.8. H. Band 16 - cDNA sequence & ORF

Band Name	Accession No.	BLASTn search result	e-Value	Species
17	EL578150.1	starvation stress library	8e-154	*Physarum polycephalum*

C G C C C G T G T A T C A T C T G C T A T A C G A T G G A C T T C T C C G
G C A G C C A C A T G C C A T T G C T T G T G A C G G A T G T T C A G C A
G C G T C C G T G A G G T C G A G C A C G G G T C C T G C G G A A A C A
A A T G G A A A T A T T C A A A A T T C A C G G G C A C A C T G C C G A G
C G A A G G G G G A C T A A T C G G A C T T C T T C G C A A C A C C T A G C
G T C T T T T G A A A A A G A A C A G A G G A A C T T T C A A G A A A G A
G T C T A T G T G C T A C G C G G G C T A C G A C A A C G C G G C G A A A
A A T G A C G A G C T A C T A C T T A T G T T G A A A A C T C T G A A G G
A G G A T C T T A G T T T G A T T T G C C A T G C C G T C G T G G T T T G A
T C T T T A T A G T G A C G A C T C A A G T A A G A G C A C T A T A A G A
G C G G C A A T A G G A G A G A G C G A C T A T A G T A G A G G C T T T G
C A A C A C C C G C C G T G A A G A A G A A G G A T G A G A A G T C C A A
A G G C T C T A T T T C T A T G G A G A T C T T C A C G A T T G T C A A A A
A A C A C G A G A C A A A A A G A G G G T C C G T C A T T C C C C T G C T
C T A C G A A G G C A C T G C A C C C G A A A C A T T T C C T C A T T T C
G T T G A T G A T C G G A T T T C A C G T G T G C T A G G T C A C T T C C
C C T G C G A T G G A T A C G T C A C A A T T A G T G T A G G T T T C A C
C T G T C C G G C G T C A T C C C T G C T C T G T A T C C A C T T G T G A T
G A G A T T C G T C C C A A A G T A G C T G C C C C A G G A A G G A

Band Name	ORF Amino acid	Accession No.	BLASTp search result	Species	e-Value

	length				
17	116	EHI46716.1	RsmD family RNA methyltransferase	*Rhodococcus opacus*	0.24

M P S W F D L Y S D D S S K S T I R A A I G E S D Y S R G
F A T P A V K K K D E K S K G S I S M E I F T I V K K H E T
K R G S V I P L L Y E G T A P E T F P H F V D D R I S R V L
G H F P C D G Y V T I S V G F T C P A S S L L C I H L *

Fig. 6.8. I. Band 17 - cDNA sequence & ORF

Band Name	**Accession No.**	**BLASTn search result**	**e-Value**	**Species**
18	EL578150.1	starvation stress library	7e-123	*Physarum polycephalum*

A G G G G G T A T G G T T A A G A A G T G G C A G G G T C T G G A C G C
C A T G G A G G A G A A A C T G C C A C T G C A A G T G A C G G A T G T T
T A G C A G C G T A C T A G A G G T C G C G C A C G G G T C C T G C G G A
A A C C A C T G A A A A A A T T C A A A A T T C A C G G G C A C A C T G C
C G A G C G A A C G G G A C T A A T C G G A C T T C T T T T T T T G C C T
C G C G T C T T T T G A A A A A G A A G A G A G G A T C T T T C A A G A A
A G A G T C T T T G T G C T A C G C A T G C T A C G A C A A C G A G G G G
A A A G A T C A C G T G C T A A T A C T T A T G T T G A A A A C T C T G A A
G G A G G A T C T T A G T T T G A T T T G C C A T G C C G T T T G A T T T G
A T C T T T A T A G T G A C G A C T C A T G T A A G A G C A C T A T A A G A
G C G G C C A T A G G A G A T A G C A A C T T A G T T A G A A G C T T T G
C A T T A T C C G C C T T G A A G A C G A A G C A T G A G A A T T C C A
T A G G C T C T A T C T C G A T A G T G A T C C T C A C C A T T G T C A A A
A A A C A C G T G A C G A A A A G A G G G A C C G T C A T T C C C C T G C
T C T A C G A A G G C A C T G C A C A C G A A A C A T T T C A T C C C T C
G C T G A C T A C T G G A T T T C A C G T G T G C T A G T T C A C T A C C
C C G G T G A T A T A T A C C T C A C A G T T A C T T T T C G A T T T A C C
T G T C C G A T T T C A T C C C T G C T C T T T A T C C C C T T G T T G T T
C G A T T C G T C A C C A A A A T G G C C T G G C C G G A C G A A G G A T
T

Band Name	ORF Amino acid length	Accession No.	BLASTp search result	Species	e-Value
18	57	ABR17502.1	unknown	*Picea sitchensis*	0.60

M T V P L F V T C F L T M V I T I E I E P M E F S C F V F K
A D N A K L L T K L L S P M A A L I V L L H E S S L *

Fig. 6.8. J. Band 18 - cDNA sequence & ORF

Band Name	Accession No.	BLASTn search result	e-Value	Species
21	DQ407661.1	subtilisin-like protease B mRNA	1e-132	*Physarum polycephalum*

B A A C A T T T T G A A T T T T G A G T G C A G A G T G G A T C C T G G G
C G A G C A A C C A C G A A C A G C G A A G C A G C G G G G G A T T C C
T T C T C A A C T G C G C T G G C T C C G G C G C A A C A A A A A G G G A
A A T C G A G G C T T C T T G T G A T G G A T G G A A G T A A G A A T C A
G A G G A T G A G A C T C C T T C G C T G C C T C C A T A G C T C A A G G
A A A T G A G G A C A A C A G G C A G G T T G A T A A T A G G T T C A G T
G C A A G C A T C A A G A T T G A A G T C G C T G G A A G A C T G G A T A
A A A A C T A G G A T C A A T T T G G C T G C G G G G G C A T T T G C A T
G A G C G A T T T G C A A G T C C G A A G C G G T C T C A A C T C C C C A
T C C G T G G C C A C T G G C A T C A T C A A G G T C A T C C A A A G G G
T T T T A G T T C G A C C A T T T T G G T C T A C T T T C T G G A A G T A G
G A C G C T G G A A A G T C G T T G G C T C T G G A A A A T G C A G G A G
G A T C G G A C T C G C A C A G A T G A A G C T A C G T A T G C G T C A A
C G A T G C C A A T C A C T G G G G C C C A G G A A T T C G T C A C C T C
G A C A T C C A T T C G C T T A T C A A A T A T G T A C G T G A C G A G A
G C T A C G G A G A T C T C G A T A C C T G T A C G T A C T A T C T A G G
T T G A A C A G G T G A G C A G G T C A T T A C A C C G C C A C C T T G T
T G T T G A T G G T G A T G G A G G A G G A G A C A C C C A A G G T G T C
A T T A T T C A T G T T A T T T G A A G G C G A G T

Band Name	ORF Amino acid length	Accession No.	BLASTp search result	Species	e-Value
21	120	ABD72568.1	subtilisin-like protease A	*Physarum polycephalum*	1e-29

L D D L D D A S G H G W G V E T A S D L Q I A H A N A P A A K L I L V F I Q
S S S D F N L D A C T E P I I N L P V V L I S L S Y G G S E G V S S S D S Y F H
P S Q E A S I S L F V A P E P A Q L R R N P P L L R C S W L L A Q D P L C T Q
N S K C

Fig. 6.8. K. Band 21 - cDNA sequence & ORF

Band Name	Accession No.	BLASTn search result	e-Value	Species
23	XM_634951.1	AX4 PHD zinc finger-containing protein	2e-64	Dictyostelium discoideum

A A A A A G C A A T T A G G G G G T G T G T G A A C A G T G G A T C G A G
G A G G G T G A A C A A C A A C T G A G T A A C C G A A A T A A C T A C C
C T A A C A A C A A T T A C A A G A A T A A G A T A A C C A G A A T A A C A
A T T A C T A C A A C A A T A A T A G T G G G T A C C A G G G T G C G C C
T T A T C C G A G C G C T T T T G C G A C T A A T T A C T C G G C G T T T G
G G A A C A A C C G A G G C A G G T T G A T A A A A A T T T T G A T G T A
A T T T A T T A G A T T T T A G G C G C T G A A A A A A T A A A A A A A A A
A A A T G A A A A C A A G G A G T G C G G G G G G C A T C T G T G T G A G C
G A T G T G G G A C T C C T A A G A G G T G C T G C C T C C C C C T C T T
A G T T T C T G A T G T C A T C C T A T G A G T A G A C T T C A T T T T T T T
T G T T C T T C A G T T T C G C C T C A T T A A G A A T G T G G A C C T T G
C G C T T C C C G T T G A T G A T G A A A T A T G A G T C C A A A T C A G
A C T C G A C A T C T G T T G C T A C G T A T C C T T C A C T T A T C T C A
A T C A C C G G G C C C C G G C A G T G T G T G A A T C A A T G T T G C G
G A G G A A A A T T A C T T G T G T A T C C A T G C A A A A A A A A A A A
A A A A A A A A A A T G

Band Name	ORF Amino acid length	Accession No.	BLASTp search result	Species	e-Value
23	94	XP_003787876.1	PREDICTED: zinc finger protein 334	*Otolemur garnettii*	3.4

M K S T H R M T S E T K R G R Q H L L G V P H R S H R C P
R T P C F H F F F L F F Q R L K S N K L H Q N F Y Q P A S V
V P K R R V I S R K S A R I R R T L V P T I I V V V I V I L V I
L F L *

Fig. 6.8. L. Band 23 - cDNA sequence & ORF

Band Name	Accession No.	BLASTn search result	e-Value	Species
26	EL578150.1	starvation stress library	5e-106	*Physarum polycephalum*

G C G G C G T A T T T G T T C A C G T G C A G G T C T G A C G A C G T T G
T G C A G G A C A A G C G A C T A G C T T G T G C C G G A T G T T C A G C
A G C G T A A G T G A G G T C G C G C A C G G G A C C T G C T T A A A C A
A A T G G A A A T A T T C A A A A T T C A C G G G C A G C T G C T C A G C
G A A G G G G A C T A T T C G G A C T T C T T C G C T T T G T T T C G C G
T C T T T T G A A A A A G A A C A G A G G A A C T T T C A A G A T A G A G
C T T T A A G T G C T A C G C G G G C T A C T T C T A C G C G G G G G A A
A A T G A C G T G C C T A T A C T T A T G T T G C A A A C T C T G A A G G
A G G A T C T T A G T T T G A T T T G C C A T G C C G T C G T G G T T T G A
T C T T T A T A G C G A C G A C G C A A G T A A G A G C A C T A T A A G A
G C G T C A A T A G G A G A T A T C G A C T T T G G T A G T G G C T T T G
C A T T T C C C G C C T T G A A G A A G A A G G G C T G A G A A T T C C A A
A G G C T C T A T C T C T A T G G A G A C C C T C A C C A T T G T C A A A A
G A C G C T A G A C G T T G C G A G G G A C C G T C A T T C C C C T G C T
C T A C G A A G G C A C T G C A A A C G A A A C A T T T C C A C C C T C G
T T G A C G A C T G A G A T T T C A C G T G T G C T A G T T C A C T T C C A
C T G C T A T G T A T A C C T T G C A A T T A G T G T A C C A T T C A C C T

G T C C G G C G T C A T C C C T G C T C T T T C A G A C C T T G G T G T T
C A A T T C G T C C G G T A A T G G T C T C C G C C C G C G A A G G A A

Band Name	ORF Amino acid length	Accession No.	BLASTp search result	Species	e-Value
26	75	ZP_10569504.1	ring-hydroxylating dioxygenase, large terminal subunit	*Variovorax sp*	5.7

M F S S V S E V A H G T C L N K W K Y S K F T G S C S A K
G T I R T S S L C F A S F E K E Q R N F Q D R A L S A T R A
T S T R G K M T C L Y L C C K L *

Fig. 6.8. M. Band 26 - cDNA sequence & ORF

7. CONCLUSION AND FUTURE PERSPECTIVES

The highlights of investigations on the cell cycle modulating effects of select agents known to have a direct or indirect damaging effect on cellular DNA are being concluded in this section. The response of the naturally synchronous cultures of true slime mold, *Physarum polycephalum* to these agents have been dissected out on the cellular level in terms of delays in overall duration of cell cycle, variation in nuclear DNA content, and genotoxicity evaluation. At the molecular level, integrity of isolated genomic DNA, protein profiling, peptide-mapping, western blot analysis of cellular and nuclear lysates and transcript profiling by differential display of mRNA from the control and treated systems have thrown up interesting results.

7.1 Cell cycle modulatory effects

***Arsenic trioxide*:** Sensitivity to arsenic trioxide in terms of mitotic delay was found to be greater in G2 at lower concentrations than in S phase. Sensitivity starts at 5µM concentration and remains constant upto 50µM. *From 100µM onwards the sensitivity to arsenic trioxide further increased in a dose dependent manner.* In terms of magnitude, however, *mitotic delays were maximal during S phase at higher concentrations.* Lower concentrations upto 50µM had no effect on cell cycle progression. The slow S phase progression observed in *Physarum* could be attributable to the inactivation of Cdc25A homologue which normally activates the CDKs in S and G2 phases. Mitotic delay observed with arsenic trioxide treatment in G2 phase is also in agreement with reports of arsenite-induced inhibition of CDK-cyclin complexes resulting in G1 and G2-M arrest. *This is strongly suggestive of the link between arsenic induced ROS generated DNA damage and G2 checkpoint activation in Physarum*

***Capsaicin*:** Capsaicin was found to exert phase-specific and concentration dependent cell effects. *Early S-phase treatment with lower concentrations elicited a shortening effect on the total cell cycle duration which peaked at 250µM with an*

advancement of 1h in the G2-M transition. This effect was also observed when capsaicin was administered prior to UV-irradiation. At 500µM, however, this effect was reversed resulting in a marginal delay of about 40 min in a 9h cycle. *G2 phase sensitivity to capsaicin, however, was different in that both 250 and 500µM concentrations and combination treatments with UV elicited significant G2 arrests. Here the shortened cell cycle induced by capsaicin only during S phase and at low (250µM) concentration alone is indeed striking.* A causal link with particular threshold levels of free-radical generation by capsaicin regulating checkpoint pathways cannot be ruled out.

***Chlorambucil*:** *Sensitivity to this compound was found to be more in S phase compared to G2 phase. Significant delay was observed from 100µM onwards.*

***Wortmannin*:** At 10µM, Wortmannin treatment elicited cell cycle phase specific effects in S and G2 phase where a cell cycle delays of 2.5h and 45 min respectively in comparison with untreated control. *The UV-sensitizing effect of WM was clearly evident in S phase eliciting additional delays than brought about by UV alone.* This could be explained by the reported inhibitory effect of wortmannin on PIKK family proteins which are needed for sensing and transducing DNA damage signals for the checkpoint activation. In such a situation, failure of DNA repair in S phase would lead to G2 checkpoint activation and G2 arrest to facilitate repair. Interestingly, *the phenomenon of 'G2 checkpoint abrogation' was clearly evident in post-treated category where UV-irradiation carried out 20 min prior to metaphase is followed by WM treatment.*

7.2 Variation in Nuclear DNA content

The DNA content, as expected, was found to increase in control samples collected at early to late S phase. However, the increase was observed to continue into G2. This is in agreement with the pattern of replication of ribosomal DNA genes in *Physarum* which exist as large palindromic extra-chromosomal elements. Their

replication is confined to the last two-thirds of S phase and all of the G2 phase. A small decrement of about 5 % observed in nuclear DNA of control samples collected at very late G2 close to G2-M transition is in agreement with the reported reduced PI uptake due to commencement of chromatin condensation at this time in cell cycle. The S phase treated samples other than wortmannin and capsaicin showed a decrease in their nuclear DNA. *Interestingly, the magnitude of cell cycle delay induced by the agents during S phase treatment, exhibited a strong correlation with the nuclear DNA content. This should prove to be an inexpensive parameter which could be useful to infer the phase of cell cycle affected by respective treatments, thereby obviating the need for isotopic or non-isotopic labelling of DNA for estimation purposes.* This relationship holds true for G2 phase as well.

7.3 Genotoxicity evaluation

Only treatments with DNA damaging agents eliciting comparatively higher cell cycle delays - UV-irradiation, chlorambucil and arsenic trioxide – were found to induce nuclear comets. *Again, the extent of G2 arrest / cell cycle delay induced is indicative of the genotoxic potential of the DNA damaging agent as per this study.*

7.4 Integrity check on Genomic DNA

The ladder-like DNA pattern observed on agarose gels obtained from G2 abrogated and controls appeared to be interesting in that it showed a mixed type indicative of both specific and non-specific DNA fragmentation: a background smear along with discrete bands akin to DNA laddering associated with apoptosis caused by internucleosomal DNA cleavage. However the banding was not found to occur at a regular interval of 200 bp, the hallmark of apoptotic. Although a low-level of smearing in the control samples were observed, the DNA fragmentation was higher in UV-irradiated and G2 abrogated samples. Given the fact that in this multinucleate

acellular system a small percentage of damaged and/or polyploid nuclei are turned-over, the phenomenon is worth further probing.

7.5 SDS-PAGE Protein profiling:

In the protein profiles, remarkably three polypeptides showed cell cycle related variations. *While 53 kDa was conspicuous at S phase, 57 kDa and 60 kDa bands became prominent at late G2, and middle pre-prophase respectively. A progressive decline of the 53 kDa levels with the appearance of 57 and 60 kDa bands during late G2 – M transition was evident.* In all the treated samples which showed delays in cell cycle progression, it was observed that *the 57 kDa polypeptide was present for delays less than 1h and in samples exhibiting delays higher than 1h in magnitude displayed the presence of 53 kDa polypeptide. Greater the delay lesser the molecular weight of the predominant polypeptide. A shift in 53 kDa polypeptde to higher molecular weights of 57 and 60 kDa was observed to be essential for mitotic progression of cell cycle.* Such apparent shifts in a narrow molecular weight range may likely result from post-translational modifications. *Moreover, 53 kDa polypeptide was found to be involved in G2 abrogation where a marked drop in the intensity of the 53 kDa nuclear band to barely visible levels as that for control samples are seen.* But in UV-treated nuclear samples the intensity of this was found to be high.

7.6 Peptide mapping

Peptide mapping with trypsin and chymotrypsin carried out to confirm the distinctiveness of the above mentioned polypeptides revealed that these indeed are differentially modified forms of the same polypeptide.

7.7 Western blot

Western blot with anti-p53 antibody did not pick up the signal with *Physarum* proteins. Immunostaining carried out with anti-phosphoserine and anti-

phosphotyrosine antibodies, to check whether positional shift shown by 53 kDa polypeptide in SDS-gel is due to phosphorylation at serine or tyrosine residues, gave a signal only at 110 kDa position ruling out the occurrence of post-translational modifications of these polypeptides other than phosphorylations at serine or tyrosine residues.

7.8 Transcript profiling by DD-PCR

The differential display of transcripts from *Physarum* cultures subjected to various DNA damaging agents showed distinctive variations. Direct sequencing of a few select bands indicate that almost all of the bands belong to the category of stress-inducible transcripts in agreement with ESTs identified based on nucleotide and protein level searches. This indeed gives a molecular-level reflection of variations induced by agents used in the study.

FUTURE PERSPECTIVES

The overall results of the study throws open a number of future explorations at the cellular and molecular level. Since the vertebrate p53 homologue has been elusive in lower eukaryotes such as yeast and other fungi, it may be worthwhile to further investigate the role of the cell cycle related 53 kDa polypeptide found in the present study. Detailed cellular localization studies inclusive of its phosphorylation status in response to treatments with a wide array of cell cycle perturbers / potential drugs should prove beneficial in unravelling molecular mechanisms underlying cell cycle regulation. More importantly, since it has been found to be involved in G2 abrogation, identifying the gene at the structural and functional level should be rewarding. Given the fact that a great majority of these cell cycle regulatory genes are highly conserved evolutionarily from yeast to man, the importance of such

investigations can never be overemphasized. Since G2 abrogation has been hailed as a novel strategy to sensitise cancer cells towards apoptotic death, the amenability of the model system to G2 abrogation as shown by this study further demonstrates the utility of *Physarum cultures* for screening prospective G2 abrogators natural and synthetic. This is also true for comet-assay based screening for potential genotoxic agents. The results of transcript profiling carried out in this study also unequivocally attest the potential of the system to identify key molecular players involved in cell cycle regulation.

REFERENCES

Abe T., Takano H., Sasaki N., Mori K and Kawano S. In vitro DNA fragmentation of mitochondrial DNA caused by single-stranded breakage related to macroplasmodial senescence of the true slime mold, *Physarum polycephalum*. *Curr Genet.* 37, 125-35 (2000)

Abraham R.T. Cell cycle checkpoint signaling through the ATM and ATR kinases. *Genes Dev.* 15, 2177–2196 (2001)

Adlakha RC., Shipley GL., Zhao J, Jones KB., Wright DA., Rao PN and Sauer HW. Amphibian oocyte maturation induced by extracts of *Physarum polycephalum* in mitosis. *J Cell Biol.* 106, 1445–1452 (1988)

Alberts B., Johnson A., Lewis J., Raff M., Roberts K and Walter P. Molecular Biology of the Cell. New York: Garland Science. 4th edition. (2002)

Aldrich and Daniel. Cell Biology of *Physarum* and Didymium, part 1. Edited by Academic Press. (1982)

Aleem E. The Effect of Loss of P27 and Cdk2 on Cell Cycle Progression in Response to Ultraviolet Irradiation in Mouse Embryo Fibroblasts. *J Am Sci*. 8, 373-382 (2012)

Alexopoulos JC. Morphology, Taxonomy and Phylogeny. In Cell Biology of *Physarum* and Didymium. Aldrich HC and Daniel JW (eds). New York: Academic Press. 1, 3-23 (1982)

Alscher RG., Donahue JL and Cramer CL. Reactive oxygen species and antioxidants: relationships in green cells. *Physiol Plant.* 100, 224–233 (1997)

Anderson HJ., Andersen RJ and Roberge RM. Inhibitors of the G2 DNA damage checkpoint their potential for cancer therapy. *Prog Cell Cycle Res*. 5, 423-430 (2003)

Aravindan T, John T and Nair VR. Cordycepin susceptibility of actinomycin-insensitive postirradiation mitotic cycle in plasmodia of *Physarum polycephalum*. Schw. *Ind J Exp Biol.* 30, 861–864 (1992).

Ausubel FM. Analysis of proteins. Short Protocols in Molecular Biology. Wiley USA. 10.1 – 10.86 (1995)

Bai H., Li H., Zhang W., Matkowskyj KA., Liao J., Srivastava SK and Yang GY. Inhibition of Chronic Pancreatitis and Pancreatic Intraepithelial Neoplasia (PanIN) by Capsaicin in LSL-KrasG12D/Pdx1-Cre Mice. *Carcinogenesis*. 32, 1689-1696 (2011)

Balajee AS and Bohr VA. Genomic heterogeneity of nucleotide excision repair. *Gene*. 250, 15–30, (2000)

Barinaga, M. Is Apoptosis key in Alzheimer's disease? *Science*. 281, 1303-1304 (1998)

Barrantes I., Glockner G., Meyer S and Marwan W. Transcriptomic changes arising during light-induced sporulation in *Physarum polycephalum*. *BMC genomics*. 11, 115 (2010)

Bartkova J., Tommiska J., Oplustilova L., Aaltonen K., Tamminen A., Heikkinen T., Mistrik M., Aittomaki K., Carl B., Heikkila P., Lukas J., Nevanlinna H and Bartek J. Aberrations of the MRE11–RAD50–NBS1 DNA damage sensor complex in human breast cancer: MRE11 as a candidate familial cancer-predisposing gene. *Mol Oncol.* 2, 2 9 6 – 3 1 6 (2008)

Batchelor E., Loewer A., Mock C and Lahav G . Stimulus-dependent dynamics of p53 in single cells. *Mol Syst Biol.* 7, 488 (2011)

Bateman F. Azathioprine and chlorambucil: mechanism of action and use indermatology in Dermatology Chapter of the ACVSc Science Week Proceedings, Gold Coast, 2-3 (2010)

Benard M., Pallotta D and Pierron G. Structure and identity of a late-replicating and transcriptionally active gene. *Exp Cell Res.* 201, 506-13 (1992)

Bensimon A ., Aebersold R and Shiloh Y. Beyond ATM: The protein kinase landscape of the DNA damage response. *FEBS Lett.* 585, 1625–1639 (2011)

Beucher A., Birraux J., Tchouandong L., Barton O., Shibata A., Conrad S., Goodarzi AA., Krempler A., Jeggo PA and Lobrich M. ATM and Artemis promote

homologous recombination of radiation induced DNA double-strand breaks in G2. *EMBO*. 28, 3413–3427 (2009)

Bhattacharyya S., Sandy A and Groden J. Unwinding Protein Complexes in ALTernative Telomere Maintenance. *J Cell Biochem.* 109, 7–15 (2010)

Bhutani M., Pathak AK., Nair AS., Kunnumakkara AB., Guha S., Sethi G and Aggarwal BB. Capsaicin is a novel blocker of constitutive and interleukin-6-inducible STAT3 activation. *Clin Cancer Res.* 13, 3024-32 (2007)

Blaes N., Elbaz M., Heitz F., Caussé E., Glock Y., Puel J and Bayard, F. Differential display fingerprints: new approach to characterize smooth muscle cells and human coronary atherectomy tissues. *Pathol Biol.* 55, 328-335 (2007)

Boldogh I., Milligan D., Lee MS., Bassett H., Lloyd RS and McCullough AK. hMYH cell cycle-dependent expression, subcellular localization and association with replication foci: evidence suggesting replication-coupled repair of adenine: 8-oxoguanine mispairs. *Nucleic Acids Re*s. 29, 2802-2809 (2001)

Boldogh I., Roy G., Lee MS., Bacsi A., Hazra TK., Bhakat KK., Dasa GC and Mitra S. Reduced DNA double strand breaks in chlorambucil resistant cells are related to high DNA-PKcs activity and low oxidative stress. *Toxicology*. 193, 137–152 (2003)

Bonner JT. Brainless behavior: A myxomycete chooses a balanced diet. *Proc Natl Acad Sci U S A.* 107, 5267-8 (2010)

Bosch TCG and Lohmann JU. Non radioactive differential display of messenger RNA. In The Nucleic Acid Protocols Handbook. Rapley R (ed). New Jersey Humana press. 645-651 (2000)

Boschi E and Vergara M. A protocol for nonradioactive differential display tested on carrot auxin-resistant mutants. *Plant Mol Biol Reporter*. 16, 1-8 (1998)

Boutros R., Lobjois V and Ducommun B. CDC25 phosphatases in cancer cells:key players? Good targets?. *Nat Rev Cancer*. 7, 495-507 (2007)

Bradbury DA., Newton R., Zhu YM., El-Haroun H., Corbett L and Knox AJ. Cyclooxygenase-2 induction by bradykinin in human pulmonary artery smooth muscle cells is mediated by the cyclic AMP response element through a novel autocrine loop involving endogenous prostaglandin E2, E-prostanoid 2 (EP2), and EP4 receptors. *J Biol Chem*. 278, 49954-49964 (2003)

Bröker LE., Kruyt FAE and Giaccone G. Cell death independent of caspases: a review. *Clin Cancer Res.* 11, 3155-3162 (2005)

Bryant M., Schardl C., Hesse U and Scott, B. Evolution of a subtilisin-like protease gene family in the grass endophytic fungus Epichloe festucae. *BMC Evol Biol.* 9, 168 (2009)

Bucher N and Britten CD. G2 checkpoint abrogation and checkpoint kinase-1 targeting in the treatment of cancer. *Br J Cancer.* 98, 523–8 (2008)

Bundschuh R., Altmuller J., Becker C., Nurnberg P and Gott J. Complete characterization of the edited transcriptome of the mitochondrion of *Physarum polycephalum* using deep sequencing of RNA. *Nucleic Acids Res*. 39, 6044-6055 (2011)

Burland T. Isolation of nuclear DNA from *Physarum*. http://bicmra.usuhs.mil/*Physarum*/Protocols/burland/PpNucDNA.html (1993)

Burland TG and Dee J. Isolation of cell cycle mutants of *Physarum polycephalum*. *Mol Gen Genet.* 179, 43-8 (1980)

Caldecott KW. Single-strand break repair and genetic disease. *Nat Rev Genet.* 9, 619–631 (2008)

Cann KL and Dellaire G. Heterochromatin and the DNA damage response:the need to relax. *Biochem Cell Biol.* 89, 45–60 (2011)

Chanda S., Bashir M., Babbar S., Koganti A and Bley K. In vitro hepatic and skin metabolism of capsaicin. *Drug Metab Dispos.* 36, 670–675 (2008)

Chang HC., Chen ST., Chien SY., Kuo SJ., Tsai HT and Chen DR. Capsaicin may induce breast cancer cell death through apoptosis-inducing factor

involving mitochondrial dysfunction. *Hum Exp Toxicol*. 30, 1657-1665 (2011)

Charlton M., Merry B and Goyns M. Differential display analysis can reveal patterns of gene expression in immortalised hepatoma cells which are similar to those observed in young adult but not old adult liver cells. *Cancer Lett*. 143, 45-50 (1999)

Chen D., Yang Z., Wang Y., Zhu G and Wang X. Capsaicin induces cycle arrest by inhibiting cyclin-dependent-kinase in bladder carcinoma cells. *Int J Urol.* 19, 662-8 (2012)

Chen T., Stephens PA., Middleton FK and Curtin NJ. Targeting the S and G2 checkpoint to treat cancer. *Drug Discov Today.* 17, 194-202 (2011)

Cheng Q and Chen J. Mechanism of p53 stabilization by ATM after DNA damage. *Cell Cycle*. 9, 472–478 (2010)

Cheok CF., Bachrati CZ., Chan KL., Ralf C., Wu L and Hickson ID. Roles of the Bloom's syndrome helicase in the maintenance of genome stability. *Biochem Soc Trans*. 33, 1456–1459 (2005)

Chernikova SB., Lindquist KL and Elkind MM. Cell cycle-dependent effects of wortmannin on radiation survival and mutation. *Radiat Res.* 155, 826–831 (2001)

Chittka A., Volff J and Wizenman, A. Identification of genes differentially expressed in dorsal and ventral chick midbrain during early Development. *BMC Dev Biol*. 9, 29 (2009)

Cho J and Sauer H. A non-cycling mitotic cyclin in the naturally synchronous cell cycle of *Physarum polycephalum*. *Eur J Cell Biol.* 65, 94-102 (1994)

Christodoulopoulos G., Malapetsa A., Schipper H., Golub E., Radding C and Panasci LC. Chlorambucil induction of HsRad51 in B-cell chronic lymphocytic leukemia. *Clin Cancer Res.* 5, 2178–2184 (1999)

Chu WK and Hickson ID. RecQ helicases: multifunctional genome caretakers. *Nat Rev Cancer*. 9, 644–654 (2009)

Ciccia A and Elledge SJ. The DNA Damage Response:Making it Safe to Play with Knives. *Mol Cell.* 40, 179-204 (2010)

Cipollini M., He J., Rossi P., Baronti F., Micheli A., Rossi AMn and Barale R. Can individual repair kinetics of UVC-induced DNA damage in human lymphocytes be assessed through the comet assay?. *Mutat Res.* 601, 150-61 (2006)

Claudio PP., Tonini T and Giordano A. The retinoblastoma family: twins or distant cousins. *Genome Biol.* 3, 3012 (2002)

Costanzo V., Paull T., Gottesman M and Gautier J. Mre11 Assembles Linear DNA Fragments into DNA Damage Signaling Complexes. *PLoS Bio*. 2, 0600-0609 (2004)

Courdavault S., Baudouin C., Charveron M., Canguilhemb B., Faviera A., Cadeta J and Douki T. Repair of the three main types of bipyrimidine DNA photoproducts in human keratinocytes exposed to UVB and UVA radiations. *DNA Repair*. 4, 836–844 (2005)

Crum CP and McKeon FD. p63 in epithelial survival, germ cell surveillance, and neoplasia. *Annu Rev Pathol.* 5, 349-71 (2010)

Daniel JW and Baldwin HH. Methods of culture for plasmodial myxomycetes; in Methods in cell physiology. Prescott D M (ed). Academic Press New York. 1, 9–41 (1964)

de Lima-Bessa KM., Armelini MG., Chigançcas V., Jacysyn JF., Amarante-Mendes GP., Sarasin A and Menck CF. CPDs and 6–4PPs play different roles in UV-induced cell death in normal and NER-deficient human cells. *DNA Repair*. 7, 303–312 (2008)

Deckbar D., Jeggo PA and Löbrich M. Understanding the limitations of radiation-induced cell cycle Checkpoints. *Crit Rev Biochem Mol Biol.* 46, 271–283 (2011)

Deinl I., Spielvogel H., Garcia-Herdugo G., Exenberger R., Thoni G and Sachsenmaier W. Combined effects of X-rays and caffeine on the timing of mitosis and the regulation of salvage pathway enzymes in *Physarum*

polycephalum. 9th European *Physarum* Conference, University of Leicester, England (1990)

Dejmek J., Iglehart JD and Lazaro JB. DNA-dependent protein kinase (DNA-PK)-dependent cisplatin-induced loss of nucleolar facilitator of chromatin transcription (FACT) and regulation of cisplatin sensitivity by DNA-PK and FACT. *Mol Cancer Res.* 7, 581-591 (2009)

Derry S., Lloyd R., Moore RA and McQuay HJ. Topical capsaicin for chronic neuropathic pain in adults. *Cochrane Database Syst Rev*. 4, 1-35 (2009)

Devi VR and Guttes E. Macromolecular syntheses and mitosis in uv-irradiated plasmodia of *Physarum polycephalum*. *Radiat Res.* 51, 410-30 (1972)

Didier C., Cavelier C., Quaranta M., Demur C and Ducommun B. Evaluation of Polo-like kinase 1 inhibition on the G2/M checkpoint in acute myelocytic leukaemia. *Eur J Pharmacol* . 591, 102–5 (2008)

Draetta G., Piwnica-Worms H., Morrison D., Druker B., Roberts T and Beach D. Human cdc2 protein kinase is a major cell-cycle regulated tyrosine kinase substrate. *Nature.* 336, 738–744 (1988)

Ducommun B and Wright W. Variation of tubulin half-life during the cell cycle in the synchronous plasmodia of *Physarum polycephalum*. *Eur J Cell Biol.* 50, 48–55 (1989)

Ducommun B., Tollon Y., Gares M., Beach D and Wright M. Cell cycle regulation of $p34^{cdc2}$ kinase activity in *Physarum polycephalum*. *J Cell Sci.* 96, 683–689 (1990)

Ekstrand MI., Falkenberg M., Rantanen A., Park CB., Gaspari M., Hultenby K., Rustin P., Gustafsson CM and arsson NG. Mitochondrial transcription factor A regulates mtDNA copy number in mammals. *Hum Mol Genet.* 13, 935–944 (2004)

Fekairi S., Scaglione S., Chahwan C., Taylor ER., Tissier A., Coulon S., Dong MQ., Ruse C., Yates JR and Russell P. Human SLX4 is a Holliday junction resolvase subunit that binds multiple DNA repair/recombination endonucleases. *Cell*. 138, 78–89 (2009)

Fisher AEO., Hochegger H., Takeda S and Caldecott KW. Poly(ADP-ribose) polymerase 1 accelerates single-strand break repair in concert with poly(ADP-ribose) glycohydrolase. *Mol Cell Biol.* 27, 5597–5605 (2007)

Flora SJS. Arsenic induced oxidative stress and its reversibility. *Free Radic Biol Med.* 51, 257-81 (2011)

Foster CJ and Lozano G. Loss of p19ARF enhances the defects of Mdm2 overexpression in the mammary gland. *Oncogene.* 35, 25-31 (2002)

Freeman JL and Rayburn AL. Metamorphosis in *Xenopus laevis* is not associated with large-scale nuclear DNA content variation. *J Exp Biol.* 207, 4473-4477. (2004)

Frucht-Pery, J., Feldman ST and Brown SI. The use of capsaicin in herpes zoster ophthalmicus neuralgia. *Acta Ophthalmol Scand*. 75, 311-313 (1997)

Fry J and Matthews HR. Flow cytometry of the differentiation of *Physarum polycephalum* myxamoebae to cysts. *Exp Cell Res.* 168, 173 – 181 (1987)

Fu X., Yucer N., Liu S., Li M., Yi P., Mu JJ., Yang T., Chu J., Jung SY., O'Malley BW., Gu W., Qin J., Wang Y. RFWD3–Mdm2 ubiquitin ligase complex positively regulates p53 stability in response to DNA damage. *Proc Natl Acad Sci. U.S.A.* 107, 4579–4584 (2010)

Giannattasio M., Lazzaro F., Longhese MP., Plevani P and Muzi-Falconi M. Physical and functional interactions between nucleotide excision repair and DNA damage checkpoint. *EMBO J.* 23, 429–438 (2004)

Glockner G., Golderer G., Werner-Felmayer G., Meyer S and Marwan W. A first glimpse at the transcriptome of *Physarum polycephalum*. *BMC genomic.* 9, 6 (2008)

Goodarzi AA and Block WD., Lees-Miller SP. The role of ATM and ATR in DNA damage-induced cell cycle control. *Prog Cell Cycle Res.* 5, 393–411 (2003)

Graham-Evans B., Cohly HH., Yu H and Tchounwou PB. Arsenic-induced genotoxic and cytotoxic effects in human keratinocytes, melanocytes and dendritic cells. *Int J Environ Res Public Health.* 1, 83-9 (2004)

Green CM., Erdjument-Bromage H., Tempst P and Lowndes NF. A novel Rad24 checkpoint protein complex closely related to replication factor C. *Curr Biol.* 10, 39–42 (2000)

Greiner AN and Meltzer EO. Overview of the Treatment of Allergic Rhinitis and Nonallergic Rhinopathy. *Proc Am Thorac Soc.* 8, 121-131 (2011)

Guttes E., Guttes S and Rusch HP. Morphological observations on growth and differentation of *Physarum polycephalum* grown in pure culture. *Dev Biol.* 3, 588-614 (1961)

Guttes E and Guttes S. Mitotic synchrony in the plasmodia of *Physarum polycephalum* and mitotic synchronization by coalescence of microplasmodia. In Methods in cell physiology. D M Prescott (ed.) New York: Academic Press. 1, 43–54 (1964)

Haindl M and Holler E. Use of the giant multinucleate plasmodium of *Physarum polycephalum* to study RNA interference in the myxomycete. *Anal Biochem.* 342, 194-199 (2005)

Halliwell B. Oxidative stress and cancer: have we moved forward?. *Biochem J*. 401, 1-11 (2007)

Hames BD. One-dimensional polyacrylamide gel electrophoresis. Gel Electrophoresis of Proteins. New York: IRL Press. 1-147 (1990)

Han YH., Kim SZ., Kim SH and Park WH. Arsenic trioxide inhibits growth of As4.1 juxtaglomerular cells via cell cycle arrest and caspase-independent apoptosis. *Am J Physiol Renal Physiol.* 293, 511-20 (2007)

Hanasoge S and Ljungman M. H2AX phosphorylation after UV irradiation is triggered by DNA repair intermediates and is mediated by the ATR kinase. *Carcinogenesis*. 28, 2298-2304 (2007)

Hardman N. Molecular organization of the *Physarum* genome. The molecular Biology of *Physarum polycephalum*. Dove FW, Dee J, Hatano S, Haugli FB, Wohlfarth-Bottermann KE(ed) . Plenum, London. 106, 39-66 (1986)

Harper JW and Elledge SJ. The DNA damage response: ten years after. *Mol Cell.* 28, 739-45 (2007)

Hebbar V., Damera G and Sachdev G. Differential expression of MUC genes in endometrial and cervical tissues and tumors. *BMC cancer*. 5, 124 (2005)

Hei TK., Liu SU. X and Waldren C. Mutagenicity of arsenic in mammalian cells: role of reactive oxygen species. *Proc Natl Acad Sci U S A.* 95, 8103–8107 (1998)

Helleday T., Lo J., van Gent DC, and Engelward BP. DNA double-strand break repair: from mechanistic understanding to cancer treatment. *DNA Repair*. 6, 923–935 (2007)

Holleran JL., Fourcade J., Egorin MJ., Eiseman JL., Parise RA., Musser SM., White KD., Covey JM., Forrest GL and Pan SS. In vitro metabolism of the phosphatidylinositol 3-kinase inhibitor, wortmannin, by carbonyl reductase. *Drug Metab Dispos*. 32, 490–496 (2004)

Hu H and Gatti RA. MicroRNAs: new players in the DNA damage response. *J Mol Cell Biol*. 3, 151–158 (2011)

Huang SP., Chen JC., Wu CC., Chen CT., Tang NY., Ho YT., Lo C., Lin JP., Chung JG and Lin JG. Capsaicin-induced apoptosis in human hepatoma HepG2 cells. *Anticancer Res.* 29, 165-74 (2009)

Huh HC., Lee SY., Lee SK., Park NH and Han IS. Capsaicin induces apoptosis of cisplatin-resistant stomach cancer cells by causing degradation of cisplatin-inducible Aurora-A protein. *Nutr Cancer*. 63, 1095-103 (2011)

Huttermann A and Chet I. Activity of some enzymes in *Physarum polycephalum*. *Arch Mikrobiol.* 74, 90-100 (1970)

Indirabai WPS and Nair VR. Synthesis of actinomycin insensitive RNA during the first post-irradiation mitotic cycle in the synchronously mitotic plasmodia of *Physarum polycephalum*. *J Biosci.* 16, 9–19 (1991)

Inoue A., Torigoe T., Sogahata K., Kamiguchi K., Takahashi S., Sawada Y., Saijo M., Taya Y., Ishii S and Sato N. 70-kDa heat shock cognate protein interacts directly with the N-terminal region of the retinoblastoma gene product pRb. *J Biol Chem.* 270, 22571-6 (1995)

Ip SC., Rass U., Blanco MG., Flynn HR., Skehel JM and West SC. Identification of Holliday junction resolvases from humans and yeast. *Nature*. 45, 357–361 (2008)

Ip SW., Lan SH., Huang AC., Yang JS., Chen YY., Huang HY., Lin ZP., Hsu YM., Yang M.D and Chiu CF. Capsaicin induces apoptosis in SCC-4 human tongue cancer cells through mitochondria-dependent and-independent pathways. *Environ Toxicol.* 27, 332-41 (2010)

Isosaki M., Nakayama H., Kyotani Y., Zhao J., Tomita S., Satoh H and Yoshizumi M. Prevention of the wortmannin-induced inhibition of phosphoinositide 3-kinase by sulfhydryl reducing agents. *Pharmacol Rep*. 63, 733-739 (2011)

Ito K., Nakazato T., Yamato K., Miyakawa Y., Yamada T., Hozumi N., Segawa K., Ikeda Y and Kizaki M. Induction of apoptosis in leukemic cells by homovanillic acid derivative, capsaicin, through oxidative stress: implication of phosphorylation of p53 at Ser-15 residue by reactive oxygen species. *Cancer Res.* 64, 1071–1078 (2004)

Itoh K., Izumi A., Mori T., Dohmae N., Yui R., Maeda-Sano K., Shirai Y., Kanaoka MM., Kuroiwa T and Higashiyama T. DNA packaging proteins Glom and Glom2 coordinately organize the mitochondrial nucleoid of *Physarum polycephalum*. *Mitochondrion*. 11, 575-586 (2011)

Jacobson DN., Johnke RM and Adelman MR. Studies on motility in *Physarum polycephalum*. In Cell Motility. Goldman R., Pollard T and Rosebaum J (eds). Cold Spring harbour conference on Cell proliferation. Vol B, 749-770 (1976)

Jagger J. (ed). Introduction to research in ultraviolet photobiology. New Jersey: Prentice Hall. (1967)

Jang JJ., Kim SH and Yun TK. Inhibitory effect of capsaicin on mouse lung tumour development. *In Vivo.* 33, 49–54 (1989)

Jayasree PR and Nair VR. Reduction of ultraviolet-induced mitotic delay by caffeine in G2-phase irradiated Plasmodia of *Physarum polycephalum*. *J Biosci.* 16, 1–7 (1991)

Jayasree PR and Nair VR. Reduction of UV-induced mitotic delay by caffeine in BUdR-substituted Plasmodia of *Physarum polycephalum* . *Ind J Expl Biol.* 31, 101–105 (1993)

Jayasree PR., Kumar P and Nair R. The plasmodia of *Physarum polycephalum*, an elegant system to demonstrate the importance of genome integrity in traversing the G2/M checkpoint of the cell cycle. *Curr Sci.* 78, 1127-1130 (2000)

Jones J and Adamatzky A. Towards *Physarum* binary adders. *Biosystems.* 101, 51-58 (2010)

Kang HJ., Soh Y., Kim MS., Lee EJ and Surh YJ. Roles of JNK-1 and p38 in selective induction of apoptosis by capsaicin in ras-transformed human breast epithelial cells. *Int J Cancer*. 103, 475–482 (2003)

Kanki T., Ohgaki K., Gaspari M., Gustafsson CM., Fukuoh A., Sasaki N., Hamasaki N and Kang D. Architectural role of mitochondrial transcription factor a in maintenance of human mitochondrial DNA. *Mol Cell Biol.* 24, 9823–9834 (2004)

Kastan MB. DNA Damage Responses: Mechanisms and Roles in Human Disease. *Mol Cancer Res.* 6, 517-524 (2008)

Kawabe T. G2 checkpoint abrogators as anticancer drugs. *Mol Cancer Ther*. 3, 513–519 (2004)

Kawaguchi S., Nakamura T., Yamamoto A., Honda G and Sasaki YF. 2010. Is the comet assay a sensitive procedure for detecting genotoxicity?. *J Nucleic Acids.* (2010)

Kim SH., Jang YW., Hwang P., Kim HJ., Han GY and Kim CW. The reno-protective effect of a phosphoinositide 3-kinase inhibitor wortmannin on streptozotocin-induced proteinuric renal disease rats. *Exp Mol Med*. 44, 45–51 (2012)

Kitchin KT and Conolly R. Arsenic-induced carcinogenesis-oxidative stress as a possible mode of action and future research needs for more biologically based risk assessment. *Chem Res Toxicol*. 23, 327–335 (2010)

Kitchin KT and Wallace K. Evidence against the nuclear in situ binding of arsenicals–oxidative stress theory of arsenic carcinogenesis. *Toxicol Environ Chem.* 232, 252-257 (2008)

Kligerman AD and Tennant AH. Insights into the carcinogenic mode of action of arsenic. *Toxicol Appl Pharmacol.* 222, 281–288 (2007)

Kligerman AD., Malik SI and Campbell JA. Cytogenetic insights into DNA damage and repair of lesions induced by a monomethylated trivalent arsenical. *Mutat Res.* 695, 2–8 (2010)

Kohama K and Nakamura A. *Physarum* Cell Culture. *Encyclopedaia of life sciences.* John Wiley & Sons, Ltd. www.els.net. 1-3 (2001)

Kojima C., Ramirez DC., Tokar EJ., Himeno S., Drobná Z., Stýblo M., Mason RP and Waalkes MP. Requirement of arsenic biomethylation for oxidative DNA damage. *J Natl Cancer Inst*. 101, 1670–1681 (2009)

Kruse JP and Gu W. Modes of p53 regulation. *Cell*. 137, 609-622 (2009)

Kubbies M and Pierron G. Mitotic cell cycle control in *Physarum*. Unprecedented insights via flow-cytometry. *Exp Cell Res.* 149, 57-67 (1983)

Kumar PRM and Nair VR. Effect of heat shock on the different phases of the mitotic cycle in *Physarum polycephalum*. *Curr Sci.* 59, 615–616 (1990)

Kumar PRM and Nair VR. Synergistic effect of heat shock and UV-irradiation on mitosis and protein synthesis in G2-phase plasmodia of *Physarum polycephalum* Schw: Reduction in UV-induced mitotic delay in preheat-shocked system. *Indian J Exp Biol.* 29, 305–309 (1991)

Kumar PRM and Nair VR. A comparative study of mitotic delay and inhibition of transcription in cells exposed to U V and heat-shock: the possible use of mitotic delay duration as a parameter for assaying extent of damage and recovery. *Curr Sci.* 62, 314–316 (1992)

Kumar PRM and Nair VR. Synergistic effect of griseofulvin and ultraviolet-irradiation on mitotic cycle durations in the plasmodia of *Physarum polycephalum*. *Biomed Lett.* 48, 137–143 (1993)

Kumari PAV and Nair VR. Preferential synthesis of low-molecular weight RNA in UV-irradiated plasmodia of *Physarum polycephalum*. *Radial Res.* 88, 37–46 (1981)

Kumari PAV and Nair VR. Transcription in ultraviolet-irradiated plasmodia of *Physarum polycephalum*. *J Biosci.* 5, 365–375 (1983)

Kumari PAV and Nair VR. Mitotic delays and macromolecular synthesis in G2 phase-irradiated Plasmodia of *Physarum polycephalum*. *Exp Cell Res.* 151, 104–111 (1984)

Kuntz K and O'Connell MJ. The G2 DNA damage checkpoint: could this ancient regulator be the Achilles heel of cancer?. *Cancer Biol Ther.* 8,1433-9 (2009)

Laemmli UK. Cleavage of structural proteins during the assembly of the head of bacteriophage T4. *Nature.* 227, 680-685 (1970)

Laffler TG and Tyson JJ. The *Physarum* cell cycle. In The molecular biology of *Physarum polycephalum*. WF Dove., J Dee., S Hatano., F B Haugli and K-E Wohlfarth-Bottermann (eds). New York: Plenum Press. 79–109 (1986)

Langerak P and Russell P. Regulatory networks integrating cell cycle control with DNA damage checkpoints and double-strand break repair. *Phil Trans R Soc B.* 366, 3562–3571 (2011)

Lee YS., Kang YS., Lee JS., Nicolova S and Kim JA. Involvement of NADPH oxidase-mediated generation of reactive oxygen species in the apototic cell death by capsaicin in HepG2 human hepatoma cells. *Free Radic Res.* 38, 405–412 (2004)

Lehmann G M. and McCabe M J. Arsenite Slows S Phase Progression via Inhibition of cdc25A Dual Specificity Phosphatase Gene Transcription. *Am J Physiol Renal Physiol.* 293, F511-20 (2007)

Leist M and Jäättela M. Four deaths and a funeral: from caspases to alternative mechanisms. *Nat Rev Mol Cell Biol*. 2, 589–98 (2001)

Lewin B. Cell cycle and growth regulation. In Genes VIII. Pearson Prentice Hall. 843- 873 (2004)

Lin WC., Lin FT and Nevins JR. Selective induction of E2F1 in response to DNA damage, mediated by ATM-dependent phosphorylation. *Genes Dev.* 15, 1833–1844 (2001)

Little NA and Jochemsen AG. p63. *Int J Biochem Cell Biol.* 34, 6-9 (2002)

Liu G., Zhang Y., Bode AM., Ma WY and Dong Z. Phosphorylation of 4E-BP1 is mediated by the p38/MSK1 pathway in response to UVB irradiation. *J Biol Chem*. 277, 8810–8816 (2002)

Liu S X., Athar M., Lippai I., Waldren C and Hei T. K. Induction of oxyradicals by arsenic: implication for mechanism of genotoxicity. *Proc Natl Acad Sci. U S A.* 98, 1643–1648 (2001)

Liu Y., Jiang N., Wu J., Dai W and Rosenblum JS. Polo-like kinases inhibited by wortmannin. Labeling site and downstream effects. *J Biol Chem.* 282, 2505-11 (2007)

Llabres M., Agust´ı S., Alonso-Laita P and Herndl G J. Synechococcus and Prochlorococcus cell death induced by UV radiation and the penetration of lethal UVR in the Mediterranean Sea. *Mar Ecol Prog Ser.* 399, 27–37 (2010)

Loidl A and Loidl P. Oncogene-and tumor-suppressor gene-related proteins in plants and fungi. *Crit Rev Oncog.* 7, 49-64 (1996)

Lorca T., Bernis C., Vigneron S., Burgess A., Brioudes E., Labbé JC and Castro A. Constant regulation of both the MPF amplification loop and the Greatwall-PP2A pathway is required for metaphase II arrest and correct entry into the first embryonic cell cycle. *J Cell Sci.* 123, 2281-2291 (2010)

Lu KH., Lee HJ., Huang ML., Lai SC., Ho YL., Chi CW Chang YS. Synergistic Apoptosis-Inducing Antileukemic Effects of Arsenic Trioxide and Mucuna macrocarpa Stem Extract in Human Leukemic Cells via a Reactive Oxygen Species-Dependent Mechanism. *Evid Based Complement Alternat Med.* 2012, 1-14 (2012)

Lubin D and Jensen EH. Effects of clouds and stratospheric ozone depletion on ultraviolet radiation trends. *Nature.* 377, 710–713 (1995)

Luehrsen KR., Marr LL., van der Knaap E and Cumberledge S. Analysis of differential display RT-PCR products using fluorescent primers and GENESCAN software. *BioTechniques*. 22, 168-174 (1997)

Luncsford PJ., Chang DY., Shi G., Bernstein J., Madabushi A., Patterson DN., Lu AL and Toth EA. A structural hinge in eukaryotic MutY homologues mediates catalytic activity and Rad9-Rad1- Hus1 checkpoint complex interactions. *J Mol Biol.* 403, 351-70 (2010)

Macaluso M., Montanari M and Giordano, A. Rb family proteins as modulators of gene expression and new aspects regarding the interaction with chromatin remodeling enzymes. *Oncogene.* 25, 5263-5267 (2006)

Mahaney BL., Meek K and Lees-Miller SP. Repair of ionizing radiation-induced DNA double-strand breaks by non-homologous end-joining. *Biochem J.* 417, 639–650 (2009)

Mahimainathan L., Ghosh-Choudhury N., Venkatesan BA., Danda RS and Choudhury GG. 2005. EGF stimulates mesangial cell mitogenesis via PI3-kinase-mediated MAPK-dependent and AKT kinase-independent manner: involvement of c-fos and p27Kip1. *Am J Physiol Renal Physiol.* 289, F72-82 (2005)

Mailand N., Bekker-Jensen S., Bartek J and Lukas J. Destruction of Claspin by SCFbetaTrCP restrains Chk1 activation and facilitates recovery from genotoxic stress. *Mol Cell*. 23, 307–318 (2006)

Maity R., Sharma J and Jana NR. Capsaicin induces apoptosis through ubiquitin–proteasome system dysfunction. *J Cell Biochem.* 109, 933-942 (2010)

Marshall G., Ferreccio C., Yuan Y, Bates M N., Steinmaus C, Selvin S, Liaw J and Smith A H. Fifty-year study of lung and bladder cancer mortality in Chile related to arsenic in drinking water. *J Natl Cancer Inst*. 99, 920–928 (2007)

Martin GW and Alexopoulos CJ. The Myxomycetes. Iowa City: Univ. Iowa Press. 19 (1969)

Martinez V., Vucic EA., Adonis M., Gil L and Lam WL. Arsenic biotransformation as a cancer promoting factor by inducing DNA damage and disruption of repair mechanisms. *Mol Biol Int.* 2011, 1-11 (2011)

Marwan W. Amoeba-inspired network design. *Science's STKE*. 327, 419 (2010)

Mazon G., Mimitou EP and SymingtonL S. SnapShot: Homologous recombination in DNA double-strand break repair. *Cell.* 142, 648.e1-648.e2 (2010)

Mazzini G., Giordano P., Riccardi A and Montecucco C.M. A flow cytometric study of the propidium iodide staining kinetics of human leukocytes and its relationship with chromatin structure. *Cytometry.* 3, 443-448 (1983)

McCollum G., Keng PC and McCabe Jr M.J. Arsenite delays progression through each cell cycle phase and induces apoptosis following G2/M arrest in U937 myeloid leukemia cells. *J Pharmacol Exp Ther.* 313, 877-887 (2005)

Mccormick JJ., Mark C and Rusch HP. DNA repair after ultraviolet irradiation in synchronous plasmodia of *Physarum polycephalum*. *Biochim Biophys Acta* . 287, 246–255 (1972)

McKenzie RL., Bjorn LO., Bais A and Ilyasd M. Changes in biologically active ultraviolet radiation reaching the Earth's surface. *Photochem Photobio Sci*. 2, 5–15 (2003)

Meghvansi MK., Siddiqui S., Khan MH., Gupta VK., Vairale MG., Gogoi HK and Singh L. Nagachilli: a potential source of capsaicinoids with broad-spectrumethnopharmacological applications. *J Ethnopharmacol.* 132, 1-14 (2010)

Mifflin RC., Saada JI., Mari JF., Adegboyega PA., Valentich JD and Powell DW. Regulation of COX-2 expression in human intestinal fibroblasts: Mechanisms of IL-1- Mediated induction. *Am J Physiol Cell Physiol*. 282, C824-34 (2002)

Mimitou EP and Symington LS. DNA end resection: many nucleases make light work. *DNA Repair*. 8, 983-995 (2009)

Min JK., Han KY., Kim EC., Kim YM and Lee SW. Capsaicin inhibits in vitro and in vivo angiogenesis. *Cancer Res.* 64, 644–651 (2004)

Mirzayans R., Pollock S., Scott A., Enns L., Andrais B and Murray D. Relationship between the radiosensitizing effect of wortmannin, DNA double-strand break rejoining, and p21WAF1 induction in human normal and tumor-derived cells. *Mol Carcinog*. 39, 164-172 (2004)

Moon DO., Kang CH., Kang SH., Choi YH., Hyun JW., Chang WY., Kang HK., Koh YS., Maeng YH., Kim YR and Kim GY. Capsaicin sensitizes TRAIL-induced apoptosis through Sp1-mediated DR5 up-regulation: involvement of Ca(2+) influx. *Toxicol Appl Pharmacol.* 259, 87-95 (2011)

Mu JJ., Wang Y., Luo H., Leng M., Zhang J., Yang T., Besusso D., Jung SY and Qin J. A proteomic analysis of ataxia telangiectasia-mutated (ATM)/ATM-Rad3-related (ATR) substrates identifies the ubiquitin-proteasome system as a regulator for DNA damage checkpoints. *J Biol Chem.* 282, 17330–4 (2007)

Mughal A., Vikram A., Ramarao P and Jena G. Micronucleus and comet assay in the peripheral blood of juvenile rat: establishment of assay feasibility, time of sampling and the induction of DNA damage. *Mutat Res*. 700, 86-94 (2010)

Munoz IM., Hain K., Declais AC., Gardiner M., Toh GW., Sanchez-Pulido L., Heuckmann JM., Toth R., Macartney T and Eppink B. Coordination of structure-specific nucleases by human SLX4/BTBD12 is required for DNA repair. *Mol Cell*. 35, 116–127 (2009)

Murray A W and Hunt T. The cell cycle. New York: Oxford University Press (1993)

Murray AW and Kirschner MW. Dominoes and clocks: The union of two views of the cell cycle. *Science*. 246, 614–621 (1989)

Nadin SB., Vargas–Roig LM and Ciocca DR. A silver staining method for single-cell gel assay. *J Histochem Cytochem.* 49, 1183-1188 (2001)

Nair RV. Periodic events and cell cycle regulation in the plasmodia of *Physarum polycephalum*. *J Biosci.* 20, 105-139 (1995)

Nakada S., Chen GI., Gingras AC and Durocher D. PP4 is a gamma H2AX phosphatase required for recovery from the DNA damage checkpoint. *EMBO Rep.* 9, 1019–1026 (2008)

NIH news release. www.genome.gov/dmd/img.cfm?node=photos/plants & id=79127

Niida H and Nakanishi M. DNA damage checkpoints in mammals. *Mutagenesis.* 21, 3–9 (2006)

Nishii W., Kuriyama H and Takahashi K. The *Physarum polycephalum* php gene encodes a unique cold-adapted serine-carboxyl peptidase, physarolisin II. *FEBS Lett.* 546, 340-4 (2003)

O'Connell MJ., Walworth NC and Carr AM. The G2-phase DNA-damage checkpoint. *Trends Cell Biol.* 10, 296–303 (2000)

Oyagbemi AA., Saba AB and Azeez OI. Capsaicin: a novel chemopreventive molecule and its underlying molecular mechanisms of action. *Indian J Cancer*. 47, 53-8 (2010)

Park JS., Park SJ., Peng X., Wang M., Yu M and Lee SH. Involvement of DNA-dependent protein kinase in UV-induced replication arrest. *J Biol Chem*. 274, 32520-32527 (1999)

Parsons JL., Preston BD., O'Connor TR and Dianov GL. DNA polymerase δ-dependent repair of DNA single strand breaks containing 3′-end proximal lesions. *Nucleic Acids Res*. 35, 1054–1063 (2007)

Polo SE and Jackson SP. Dynamics of DNA damage response,proteins at DNA breaks: a focus, on protein modifications. *Genes Dev*. 25, 409–433 (2011)

Polo SE., Kaidi A., Baskcomb L., Galanty Y and Jackson SP. Regulation of DNA-damage responses and cell-cycle progression by the chromatin remodelling factor CHD4. *EMBO J*. 29, 3130–3139 (2010)

Powley IR., Kondrashov A., Young LA., Dobbyn HC., Hill K., Cannell IG., Stoneley M., Kong YW., Cotes JA., Smith GC., Wek R., Hayes C., Gant TW., Spriggs KA., Bushell M and Willis AE. Translational reprogramming following UVB irradiation is mediated by DNA-PKcs and allows selective recruitment to the polysomes of mRNAs encoding DNA repair enzymes. *Genes Dev*. 23, 1207–1220 (2009)

Pramanik KC., Boreddy SR and Srivastava SK. Role of mitochondrial electron transport chain complexes in capsaicin mediated oxidative stress leading to apoptosis in pancreatic cancer cells. *PLoS One*. 6: e20151 (2011)

Qin XJ., Hudson LG., Liu W., Timmins GS and Liu KJ. Low concentration of arsenite exacerbates UVR-induced DNA strand breaks by inhibiting PARP-1 activity. *Toxicol Appl Pharmacol*. 232, 41–50 (2008)

Qu X., Zou Z., Sun Q., Luby-Phelps K., Cheng P., Hogan R.N., Gilpin C., Levine and B. Autophagy gene-dependent clearance of apoptotic cells during embryonic development. *Cell*. 128, 931-946 (2007)

Rai R., Peng G., Li K and Lin SY. DNA damage response: the players, the network and the role in tumor suppression. *Cancer Genom Proteom*. 4, 99-106 (2007)

Rastogi RP., Richa Kumar A., Tyagi MB and Sinha RP. Molecular mechanisms of ultraviolet radiation-induced DNA damage and repair. *J Nucleic Acids*. 2010, 1-32 (2010)

Ravanat JL., Douki T and Cadet J. Direct and indirect effects of UV radiation on DNA and its components. *J Photochem Photobiol.* 63, 88–102 (2001)

Reinhardt HC and Yaffe MB. Kinases that control the cell cycle in response to DNA damage: Chk1, Chk2, and MK2. *Curr Opin Cell Biol.* 21, 245-55 (2009)

Reyes-Escogido ML., Gonzalez-Mondragon EG and Vazquez-Tzompantzi E. Chemical and pharmacological aspects of capsaicin. *Molecules*. 16, 1253-70 (2011)

Richards BL, Whittle SL and Buchbinder R. Neuromodulators for pain management in rheumatoid arthritis. *Cochrane Database Syst Rev*. 1, (2012)

Roberts JJ. Inactivation of the DNA template in HeLa cells treated with chlorambucil. *Int J Cancer.* 16, 91-102 (1975)

Rodriguez-Rochaa H., Garcia-Garciaa A., Panayiotidisb M I and Francoa Rodrigo. DNA damage and autophagy. *Mutat Res*. 711, 158–166 (2011)

Roschier M., Kuusisto E and Salminen A. A differential display protocol to identify differentially expressed mRNAs in potassium-deprived cerebellar granule cells. *Brain Res Prot.* 5, 121-131 (2000)

Rosenberg IM. Peptide Mapping and Microsequencing. Protein Analysis and Purification Benchtop techniques. Boston: Birkhauser. 183-206 (1996)

Rosenzweig KE., Youmell MB., Palayoor ST andPrice, B.D. Radiosensitization of human tumor cells by the phosphatidylinositol3-kinase inhibitors wortmannin and LY294002 correlates with inhibition of DNA-dependent protein kinase and prolonged G2-M delay. *Clin Cancer Res.* 3, 1149-56 (1997)

Rossman T G. Mechanism of arsenic carcinogenesis: an integrated approach. *Mutat Res*. 533, 37–65 (2003)

Sachsenmaier W., Dönges KH., Rupff H and Czihuk G. Advanced initiation of synchronous mitoses in *Physarum polycephalum* following UV-irradiation; *Z. Naturforsch.* 25, 866–871 (1970)

Sanchez AM., Malagarie-Cazenave S., Olea N., Vara D., Chiloeches A and Diaz-Laviada I. Apoptosis induced by capsaicin in prostate PC-3 cells involves ceramide accumulation, neutral sphingomyelinase and JNK activation. *Apoptosis.* 12, 2013–2024 (2007)

Sánchez AM., Martínez-Botas J., Malagarie-Cazenave S., Olea N., Vara D., Lasunción M.A and Díaz-Laviada I. Induction of the endoplasmic reticulum stress protein GADD153/CHOP by capsaicin in prostate PC-3 cells: a microarray study. *Biochem Biophys Res Commun*. 372, 785–791 (2008)

Sarkaria JN., Tibbetts RS., Busby EC., Kennedy AP., Hill DE and Abraham RT. Inhibition of phosphoinositide 3-kinase related kinases by the radiosensitizing agent wortmannin. *Cancer Res.* 58, 4375–4382 (1998)

Sauer H W. Developmental Biology of *Physarum*. Cambridge: Cambridge University Press. 162-163 (1982)

Schreiber V., Dantzer F., Ame JC and de Murcia G. Poly(ADP-ribose): novel functions for an old molecule. *Nat Rev Mol Cell Biol.* 7, 517–528 (2006)

Selvam JN., Kumaravadivel N., Gopikrishnan A., Kumar B.K., Ravikesavan R and Boopathi MN. Identification of a novel drought tolerance gene in Gossypium hirsutum L. cv KC3. *Commun Biometry Crop Sci.* 4, 9-13 (2009)

Shi H., Shi X and Liu KJ. Oxidative mechanism of arsenic toxicity and carcinogenesis. *Mol Cell Biochem*. 255, 67-78 (2004)

Shirakawa T., Gunji YP and Miyake Y. An associative learning experiment using the plasmodium of *Physarum polycephalum*. *Nano Communication Networks*. 2, 99-10 (2011)

Shreeram S., Demidov ON., Hee WK., Yamaguchi H., Onishi N., Kek C., Timofeev ON., Dudgeon C., Fornace AJ., Anderson CW., Minami Y., Appella E and Bulavin DV. Wip1 phosphatase modulates ATM dependent signaling pathways. *Mol Cell*. 23, 757–764 (2006)

Shtivelman E., Sussman J and Stokoe, D. A role for PI 3-kinase and PKB activity in the G2/M phase of the cell cycle. *Curr Biol.* 12, 919-924 (2002)

Sidhu JS., Ponce RA., Vredevoogd MA., Yu X., Gribble E., Hong SW., Schneider E and Faustman EM. Cell cycle inhibition by sodium arsenite in primary embryonic rat midbrain neuroepithelial cells. *Toxicol Sci.* 89, 475-484 (2006)

Siezen RJ and Leunissen JAM. Subtilases: the superfamily of subtilisin-like serine proteases. *Protein Sci.* 6, 501–523 (1997)

Simeonova P P and Luster M I. Mechanisms of arsenic carcinogenicity: genetic or epigenetic mechanisms?. *J Environ Pathol Toxicol Oncol.* 19, 281–286 (2000)

Singh KP and DuMond JW. Genetic and epigenetic changes induced by chronic low dose exposure to arsenic of mouse testicular Leydig cells. *Int J Oncol.* 30, 253–260 (2007)

Singh KP., Kumari R., Treas J and DuMond JW. Chronic exposure to arsenic causes increased cell survival, DNA damage, and increased expression of mitochondrial transcription factor A (mtTFA) in human prostate epithelial cells. *Chem Res Toxicol.* 24, 340–349 (2011)

Singh NP., McCoy MT., Tice RR and Schneider EL. A simple technique for quantitation of low levels of DNA damage in individual cells. *Exp Cell Res.* 175, 184 - 191 (1988)

Sinha RP., Rastogi RP., Ambasht NK and Hader DP. Life of wetland cyanobacteria under enhancing solar UV-B radiation. *Proc Nat Acad Sci India*. 78, 53–65 (2008)

Solomon KR. Effects of ozone depletion and UV-B radiation on humans and the environment. *Atmos Ocean.* 46, 185–202 (2008)

Song JI and Grandis JR. STAT signaling in head and neck cancer. *Oncogene.* 19, 2489–2495 (2000)

Stein RC. Prospects for phosphoinositide 3- kinase inhibition as a cancer treatment. *Endocrine Related Cancer*. 8, 237-248 (2001)

Stevens, J.J., Graham, B., Walker, A.M., Tchounwou, P.B and Rogers, C. The effects of arsenic trioxide on DNA synthesis and genotoxicity in human colon cancer cells. *Int J Environ Res Publ health*. 7, 2018-2032 (2010)

Su TT. Cellular responses to DNA damage: one signal, multiple choices. *Annu Rev Genet*. 40, 187-208 (2006)

Suresh D and Srinivasan K. Tissue distribution and elimination of capsaicin, piperine and curcumin following oral intake in rats. *Indian J Meds Res.* 131, 682-691 (2010)

Surh YJ. More than spice: capsaicin in hot chili peppers makes tumor cells commit suicide. *J Natl Cancer Inst*. 94, 1263–1265 (2002)

Svendsen JM and Harper JW. GEN1/Yen1 and the SLX4 complex: solutions to the problem of Holliday junction resolution. *Genes Dev.* 24, 521–536 (2010)

Sykora P and Snow ET. Modulation of DNA polymerase beta-dependent base excision repair in cultured human cells after low dose exposure to arsenite. *Toxicol Appl Pharmacol.* 228, 385–394 (2008)

Symington LS and Gautier J. Double-strand break end resection and repair pathway choice. *Annu Rev Genet*. 45, 247-71 (2011)

Talà A., De Stefano M., Bucci C and Alifano P. Reverse transcriptase-PCR differential display analysis of meningococcal transcripts during infection of human cells: up-regulation of priA and its role in intracellular replication. *BMC Microbiol*. 8, 131 (2008)

Thiriet C and Hayes JJ. Assembly into chromatin and subtype-specific transcriptionaleffects of exogenous linker histones directly introduced into a living *Physarum* cell. *J Cell Sci.* 114, 965 – 973 (2001)

Thoennissen N., O'Kelly J., Lu D., Iwanski G., La D., Abbassi S., Leiter A., Karlan B., Mehta R and Koeffler H. Capsaicin causes cell-cycle arrest and apoptosis in ER-positive and-negative breast cancer cells by modulating the EGFR/HER-2 pathway. *Oncogene*. 29, 285-296 (2009)

Tjeertes JV., Miller KM and Jackson SP. Screen for DNA-damage-responsive histone modifications identifies H3K9Ac and H3K56Ac in human cells. *EMBO J.* 1878-89 (2009)

Tomita M., Suzuki N., Matsumoto Y., Hirano K., Umeda N and Sakai K. Sensitization by wortmannin of heat- or X-ray induced cell death in cultured Chinese hamster V79 cells. *J Radiat Res.* 41, 93-102 (2000)

Tsou MF., Lu HF., Chen SC., Wu LT., Chen YS., Kuo HM., Lin SS and Chung JG. Involvement of Bax, Bcl-2, Ca2+ and caspase-3 in capsaicin-induced apoptosis of human leukemia HL-60 cells. *Anticancer Res.* 26, 1965-71 (2006)

Tsuda S and Jones J. The emergence of synchronization behavior in *Physarum polycephalum* and its particle approximation. *Biosystems.* 103, 331-341 (2011)

Udensi UK., Graham-Evans BE., Rogers C and Isokpehi RD. Cytotoxicity patterns of arsenic trioxide exposure on HaCaT keratinocytes. *Clin Cosmet Investig Dermatol.* 4, 183–190 (2011)

Vaissière T and Herceg Z. Histone code in the cross-talk during DNA damage signalling. *Cell Res.* 20, 113–115 (2010)

Vakifahmetoglu H., Olsson M and Zhivotovsky B. Death through a tragedy: mitotic catastrophe. *Cell Death Differ.* 15, 1153-62 (2008)

van den Heuvel S. Cell-cycle regulation. WormBook (ed). The *C. elegans* Research Community, WormBook. (2005)

Venkatesan RN., Treuting PM., Fuller ED., Goldsby RE., Norwood TH., Gooley TA., Ladiges WC., Preston BD and Loeb LA. Mutation at the polymerase active site of mouse DNA polymerase δ increases genomic instability and accelerates tumorigenesis. *Mol Cell Biol.* 27, 7669–7682 (2007)

Venu T., Vishwanadham D., Jayasree PR., Kumar PR M. Ethanolic extract of *Bacopa monniera* (Brahmi) induces shortening of cell-cycle durations in naturally synchronous *Physarum polycephalum*. *Curr Sci.* 85, 245 (2003)

Verma RS and Babu A. Tissue culture techniques and chromosome preparation. Human chromosomes - Principle and techniques. New Delhi - McGraw-Hill Inc. 6-63 (1995).

Wang L and Lu L. Pathway-Specific Effect of Caffeine on Protection against UV Irradiation–Induced Apoptosis in Corneal Epithelial Cells. *Invest Ophthalmol Vis Sci.* 48,652-60 (2007)

Watanabe S., Tero A., Takamatsu A and Nakagaki T. Traffic optimization in railroad networks using an algorithm mimicking an amoeba-like organism, *Physarum* plasmodium. *Bio Systems.* 105, 225-32 (2011)

Watkins RF and Gray MW. Sampling gene diversity across the supergroup Amoebozoa: large EST data sets from *Acanthamoeba castellanii*,

Hartmannella vermiformis, Physarum polycephalum, Hyperamoeba dachnaya and *Hyperamoeba sp*. *Protist.* 159,269-81 (2008)

Whitelaw CA., Ruperti B and Roberts JA. Differential display: Analysis of gene expression during plant cell separation processes. *Mol Biotechnol.* 21, 251-258 (2002)

Wipf P and Halter RJ. Chemistry and biology of wortmannin. *Org Biomol Chem.* 3, 2053–2061 (2005)

Wu CC., Lin JP., Yang JS., Chou ST., Chen SC., Lin YT., Lin HL and Chung JG. Capsaicin induced cell cycle arrest and apoptosis in human esophagus epidermoid carcinoma CE 81T/VGH cells through the elevation of intracellular reactive oxygen species and Ca^{2+} productions and caspase-3 activation. *Mutat Res.* 601, 71-82 (2006)

Xia Y., Yang Q., Gong X., Ye F and Liou YC. Dose-dependent mutual regulation between Wip1 and p53 following UVC irradiation. *Int J Biochem Cell Biol*. 43, 535-44 (2011)

Yan W., Shao Z., Li F., Niu L., Shi Y., Teng M and Li X. Structural basis of γH2AXrecognition by humanPTIP BRCT5-BRCT6 domains in the DNA damage response pathway. *FEBS Lett.* 585, 3874–3879 (2011)

Yang CM., Chien CS., Hsi LD., Luo SF and Wang CC. Interlenken-1 B-induced COX-2 expression is mediated through activation of p42/44 and p38 MAPKS, and NF-kappa B Pathway in canine tracheal smooth muscle cells. *Cell Signal.* 14, 899-911 (2002)

Yang X., Wood PA and Hrushesky WJ M. Mammalian TIMELESS Is Required for ATM-dependent CHK2 Activation and G2/M Checkpoint Control. *J Biol Chem.* 285, 3030–3034 (2010)

Yedjou C and La'Mont Sutton PT. Genotoxic mechanisms of arsenic trioxide in human jurkat T-lymphoma cells. *Met Ions Biol Med.* 10, 495-499 (2008)

Yedjou CG and Tchounwou PB. In-vitro cytotoxic and genotoxic effects of arsenic trioxide on human leukemia (HL-60) cells using the MTT and alkaline single cell gel electrophoresis (Comet) assays. *Mol Cell Biochem.* 301, 123-30 (2007)

Ying S., Myers K., Bottomley S., Helleday T and Bryant HE. BRCA2-dependent homologous recombination is required for repair of Arsenite-induced replication lesions in mammalian cells. *Nucleic Acids Res.* 37, 5105–5113 (2009)

Yoo DR., Chong SA and Nam MJ. Proteome profiling of arsenic trioxide-treated human hepatic cancer cells. *Cancer Genom Proteom*. 6, 269-274 (2009)

Zeeshan M and Prasad S. Differential response of growth, photosynthesis, antioxidant enzymes and lipid peroxidation to UV-B radiation in three cyanobacteria. *S Afr J Bot*. 75, 466-474 (2009)

Zhang Q., Raghunath PN., Xue L., Majewski M., Carpentieri DF and Odum N. Multilevel dysregulation of STAT3 activation in anaplastic lymphoma kinase-positive T/null-cell lymphoma. *J Immunol*. 168, 466-74 (2002)

Zhang Y., Cho YY., Petersen BL., Bode AM., Zhu F and Dong Z. Ataxia telangiectasia mutated proteins, MAPKs, and RSK2 are involved in the phosphorylation of STAT3. *J Biol Chem*. 278, 12650–12659 (2003)

Zhong JL., Yang L., Lü F., Xiao H., Xu R., Wang L., Zhu F and Zhang Y. UVA, UVB and UVC induce differential response signaling pathways converged on the eIF2α phosphorylation. *Photochem Photobiol.* 87, 1092-104 (2011)

Zhou BB and Elledge SJ. The DNA damage response: putting checkpoints in perspective. *Nature.* 408, 433-439 (2000)

APPENDIX

Minimum salts solution (MSS)

Components	Grams per litre
Citric acid monohydrate	33.65
Ferrous sulphate	0.50
Magnesium sulphate	5
Calcium chloride (dihydrate)	5
Manganese chloride (tetrahydrate)	5
Zinc sulphate (heptahydrate)	0.28

Semi defined growth media (SDM)

Components	Grams per litre
Tryptone	10
Yeast extract	1.5
Dextrose monohydrate	11
Potassium dihydrogen phosphate	2

Add 120 ml MSS to the media, adjust the the pH to 4.6 with 30 % potassium hydroxide and make upto 1 litre. Before use, add 10ml hemin solution (0.05 % in 0.1 N sodium hydroxide) per litre.

Buffer A

0.25 M Sucrose

10 mM Calcium chloride

10 mM Tris-Cl (pH 7.2)

0.2 % Triton X-100

Buffer B

1M Sucrose

10 mM Calcium chloride

10 mM Tris-Cl (pH 7.2)

0.2 % Triton X-100

Washing solution

150 mM Sodium chloride

10 mM Tris-Hcl (pH 8)

Phosphate buffered saline (pH 7.4)

Components	**Grams per litre**
Sodium chloride	8
Potassium chloride	0.2
Disodium hydrogen phosphate	1.44
Potassium dihydrogen phosphate	0.24

Lysis Buffer

100mM EDTA

20mM Tris- Cl (pH 8)

0.5 % SDS

Just before use, add 1/20th vol. Proteinase K stock (2mg/ml in water)

TE (pH 8)

10 mM Tris-Cl

1mM EDTA

Physarum polycephalum strain McArdle unknown sequence

GenBank: EU371923.1

FASTA Graphics

Go to:

LOCUS EU371923 347 bp DNA linear INV 24-FEB-2008

DEFINITION Physarum polycephalum strain McArdle unknown sequence.

ACCESSION EU371923

VERSION EU371923.1 GI:168071455

KEYWORDS .
SOURCE Physarum polycephalum
ORGANISM Physarum polycephalum
Eukaryota; Amoebozoa; Mycetozoa; Myxogastria; Myxogastromycetidae;
Physariida; Physaraceae; Physarum.

REFERENCE 1 (bases 1 to 347)

AUTHORS Kumar,M.P.R., Jayasree,P.R. and Rabindran,R.M.

TITLE Direct Submission

JOURNAL Submitted (03-JAN-2008) Biotechnology, University of Calicut,

Calicut University P.O., Malappuram, Kerala 673 635, India

FEATURES Location/Qualifiers

source 1..347

/organism="Physarum polycephalum"
/mol_type="genomic DNA"
/strain="McArdle"
/db_xref="taxon:5791"
/PCR_primers="fwd_seq: ctcaatcagagcctgaaccac, rev_seq:
ggaaaagaaagcaggagaagc"

ORIGIN

1 ctcaatcaga gcctgaacca ctccttttcc tccccctcgt tgtttttag ctcttcgttt

61 gctgtgtaaa gtttttccca gaattcccga atcatctcca ttatgtctcc tgggttcgta

121 tccgtccatc cttctctcat atactttggt aggattcttt gtattgattt tctttttttt

181 gccttttca acattttgtc gaaaattttt ttgagcccct ccacccctcc ctttctattt

241 ccattatgaa gtttttatc tcaatcctcc tatatctatt ttttctttta ttgaccgttc

301 ttgaaatttt attctccatt tcttttgctt ctcctgcttt cttttcc

//